# The role of cholesterol in the uptake and pathogenesis of *Mycobacterium avium* subspecies *paratuberculosis* in human monocytes

Dayle Keown

A thesis submitted in accordance with the requirements of the University of Canterbury for the degree of Master of Science (Cellular and Molecular Biology)

At the University of Canterbury, Christchurch,
New Zealand

June 2010

UC
UNIVERSITY OF CANTERBURY
Te Whare Wānanga o Waitaha
CHRISTCHURCH NEW ZEALAND

UNIVERSITY of OTAGO
SAPERE AUDE
Te Whare Wānanga o Otāg

# Abstract

Crohn's disease (CD) is a chronic inflammatory bowel disease, primarily affecting the young, which causes marked morbidity and reduced quality of life. Currently there is no cure for CD, and the causes of this disease are poorly understood.

In ruminants, Johne's disease (JD) is characterised by chronic intestinal inflammation similar to CD and is caused by the pathogen *Mycobacterium avium* subspecies *paratuberculosis* (MAP), which invades and replicates within the phagocytes of infected animals, leading to chronic disease. There is increasing molecular and microbiological evidence of Map bacteria in CD patients. However, little is known regarding the role of Map in the aetiology of CD.

This thesis demonstrated that a human isolate of Map traffics through THP-1 human monocytes via a similar path to that taken by pathogenic mycobacteria. Flow cytometry demonstrated that Map are phagocytosed via a cholesterol-dependant mechanism, potentially mediated by a cell wall constituent. Once internalised, live Map reside in cholesterol-rich areas of the cell. These compartments exhibit reduced acidity compared to the compartments containing killed-Map, and have atypical retention of markers including the late endosomal marker Rab 7 and cellular TACO protein. Both of these markers were also present on phagosomes of pathogenic mycobacteria, where they interrupt fusion of the compartment with lysosomes. This was confirmed by visualisation of these proteins on phagosomes containing *M. bovis*, a known mycobacterial pathogen.

Cholesterol depletion using simvastatin affected Map persistence in THP-1 cells at 1 and 2 weeks post infection, a finding similar to other studies with *M. tuberculosis*. Spheroplast-like forms were evident after long term culture of Map with THP-1 monocytes, visualised by light and electron microscopy. These were similar to forms observed in peripheral blood leukocytes from a CD patient.

Collectively, these results support the hypothesis that Map may be involved in the aetiology of at least a subset of CD cases.

# Acknowledgements

This thesis, as it exists today, could not have happened without the help and support of a huge group of people.

As always, the first thank you must be to Mum and Dad, I simply wouldn't be where I am today without your ongoing support and encouragement.

Thank you Jacqui, for taking me on at the very beginning, and helping me to develop the scientific skills to get the most out of this project. Your expert guidance and support has made this thesis what it is today.

Thank you Dave, for holding the fort at Canterbury, keeping me informed and on track, and providing the expertise to enable me to get the most out of my writing and microscopy.

Thank you Nina, Kenny, Elizabeth, Peter and Liane, for the stimulating conversations, keeping the lollies topped up, and for keeping me sane, long may it continue.

Thank you Kelly, for being so accommodating, and putting in the extra hours on the microscope to get the pictures done on time; and to Jeremy and Hamish, for the expert proofing and support.

Thank you everyone at the Otago School of Medicine, Christchurch. Your assistance and friendship has made this research an extremely productive and rewarding experience.

Thank you for taking the time to read this thesis, I hope you enjoy learning about this area as much as I have enjoyed researching it.

# Table of Contents

## Chapter 4. Cholesterol involvement in Map uptake and fate



## Chapter 5. Map bacterial morphology during long term survival



## Chapter 6. General discussion

# List of Figures

# Abbreviations

| | |
|---|---|
| AIEC | Adherent invasive *Escherichia coli* |
| ATCC | American type culture collection |
| BSA | Bovine serum albumin |
| CD | Crohn's Disease |
| CFU | Colony forming unit |
| CWD | Cell wall deficient |
| DIC | Differential interference contrast |
| EtOH | Ethanol |
| FBS | Foetal bovine serum |
| FITC | Fluorescein isothiocyanate |
| G.I | Gastro-intestinal |
| JD | Johne's Disease |
| *M. bovis* BCG | *Mycobacterium bovis* Bacillus Calmette-Guérin |
| Map | *Mycobacterium avium* subspecies *paratuberculosis* |
| MßCD | Methyl-β-cyclodextrin |
| MOI | Multiplicity of infection |
| OD | Optical density |
| PBS | Phosphate buffered saline |
| PI | Propidium Iodide |
| RILP | Rab 7-interacting lysosomal protein |
| RT | Room temperature |
| SEM | Standard error of the mean |
| SimV | Simvastatin |
| TEM | Transmission electron microscopy |
| TX-100 | Triton X-100 detergent |
| ZN stain | Ziehl Neelsen stain |

# Chapter 1. Introduction

## 1.1 Crohn's disease

Crohn's disease (CD) is a chronic, inflammatory bowel disease that is increasing in frequency in developed countries (Shanahan, 2002). In New Zealand, the Canterbury region has one of the highest described rates of CD in the world, with approximately 155 people of every 100,000 affected (Gearry et al., 2006). CD can occur at any age, but tends to disproportionately affect the young (Polito et al., 1996), leading to a marked morbidity and reduced quality of life. Symptoms include, but are not limited to, chronic inflammation of the gastro-intestinal (GI) tract, abdominal pain, (bloody) diarrhoea, vomiting, weight loss as well as extra-intestinal manifestations such as rashes, arthritis and ocular inflammation. Currently, there is no known cure. Treatment is limited to therapy for inflammation and corrective surgery to repair fistulae and/or remove severely diseased sections of intestine and bowel tissue (Baumgart and Sandborn, 2007).

The initiating factors for CD are currently unknown. It is thought that the inflammation found in Crohn's patients is due to an overactive, innate and adaptive immune response in genetically susceptible individuals. Enteric microflora are thought to contribute to the initiation, maintenance and/or relapse of the disease in at least a subset of cases (El-Zaatari et al., 2001; Goyette et al., 2007). Various microbes such as Adherent invasive *Escherichia. coli* (AIEC), *Stenotrophomonas maltophilia*, and *Epstein Barr virus* are implicated in the aetiology of CD (Carvalho et al., 2009; Knosel et al., 2009; Lapaquette et al., 2009), but the most well studied (and controversial) is *Mycobacterium avium* subspecies *paratuberculosis*.

## 1.2 Mycobacteria

Mycobacteria are a group of species belonging to the family Mycobacteriaceae, in the Corynebacterinae sub-group of the Actinomycete line (Guenin-Mace et al., 2009). Although most species of mycobacteria are classed as saprophytic (Chacon et al., 2004), several significant animal and human pathogens exist. The oldest and most well publicised mycobacterial diseases still cause significant morbidity and mortality.

*Mycobacterium tuberculosis* is thought to infect one third of the human population, and cause 2-3 million deaths per year from pulmonary tuberculosis (TB) (Jozefowski et al., 2008). Leprosy, also known as Hansen's disease, is caused by *Mycobacterium leprae* that persists inside non-myelinated schwann cells, causing nerve damage and skin lesions. Unlike TB, the prevalence of leprosy has been significantly reduced in recent years due to the World Health Organisation's eradication program (Worobec, 2009). Other mycobacterial species that cause human disease include *M. avium* (pulmonary infection), *M. marinum* (granulomatous skin disease) and *M. ulcerans* (Buruli ulcer) (Torrado et al., 2007; Watt, 1995; Yamazaki et al., 2006).

### 1.3 *Mycobacterium avium* subspecies *paratuberculosis*

*Mycobacterium avium* subspecies *paratuberculosis* (Map) is one of the most fastidious and slow-growing species in the genus *Mycobacterium*. Map is classified as part of the *Mycobacterium avium* complex (MAC), composed of *M. avium avium*, *M. avium silvaticum*, and *M. avium paratuberculosis*. Map is typically differentiated from other MAC species by its dependence on an iron source (mycobactin J) for culture (Lilenbaum et al., 2007; Watt, 1995), and the presence of the genetic insertion element IS900 (van der Giessen et al., 1994). Map strains include "types" isolated from different animals (e.g. 'sheep type' or 'cattle type'). These are differentiated by culture and DNA typing (Collins et al., 2002; Favila-Humara et al., 2010). However, strains isolated from bovine and ovine sources in the same region are more closely related to each other than strains from the same host species in different regions, suggesting local strain adaptation to multiple animal hosts in an area (Motiwala et al., 2003).

Map is an obligate intracellular pathogen, with a thick, lipid-rich cell wall (Figure 1.1). This high concentration of lipids confers resistance to desiccation, temperature fluctuations, acidic or alkaline conditions, chemical disinfectants, as well as many antibiotics (Lilenbaum et al., 2007). In addition, other cell wall constituents, such as mycolic acids (which make up 30-60% by dry weight) contribute to virulence (Guenin-Mace et al., 2009).


**Figure 1.1. Transmission micrograph of Map bacilli.** (A) Cross and (B) longitudinal sections of Map bacteria, showing the thick cell wall (arrows) characteristic of mycobacteria. Scale bar indicates 250 nm. Images adapted from Hines and Styer (2003).

The complexity of the mycobacterial cell wall differs greatly from that of other micro-organisms (Figure 1.2) (Collins et al., 1990), making cell division more complex and time consuming than in "normal" Gram positive or Gram negative bacteria. This leads to a longer division time and therefore a much slower growth rate than most other bacteria (Hett and Rubin, 2008).

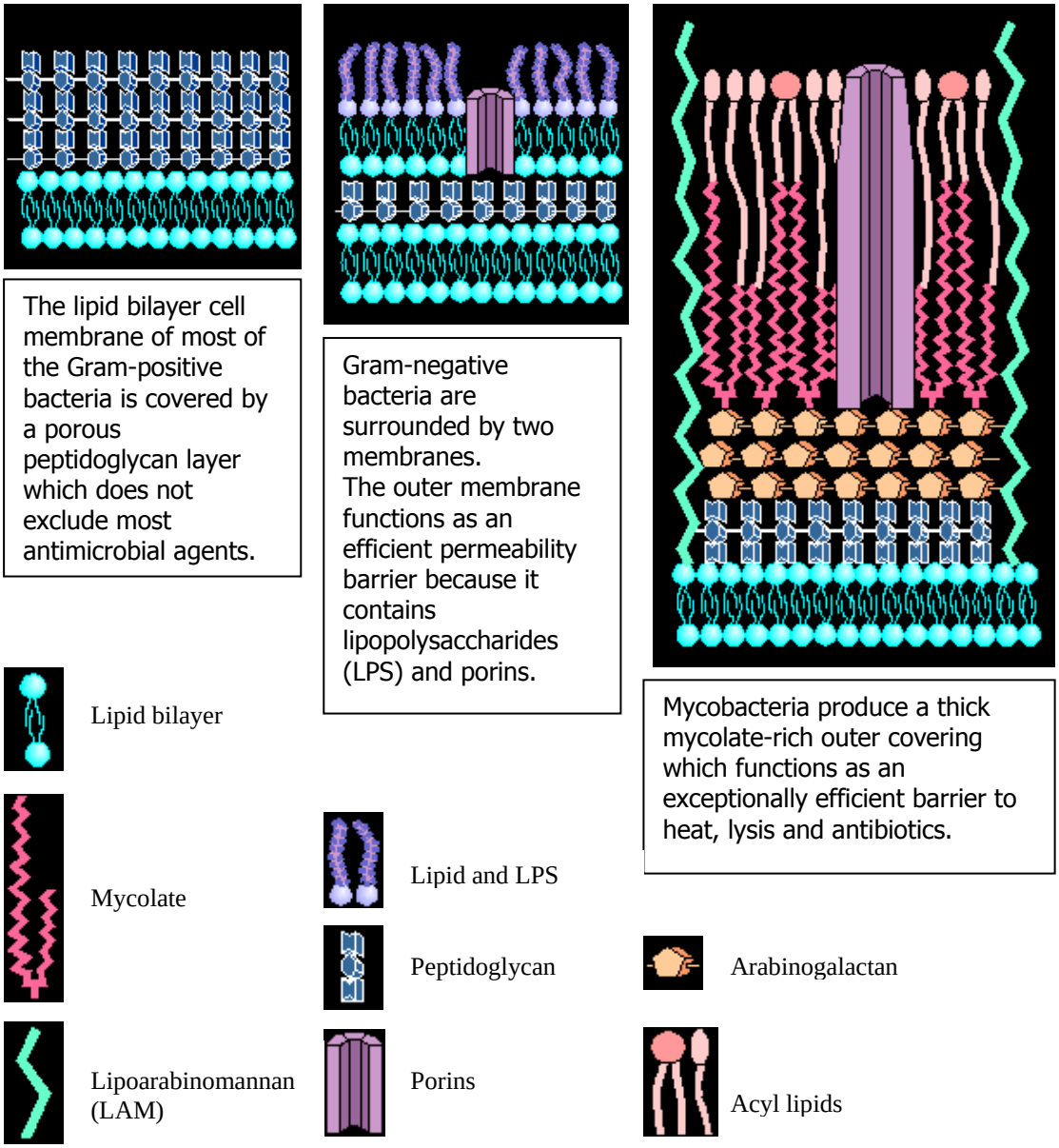


**Figure 1.2. Bacterial cell walls.** A comparison of the cell walls of three classes of micro-organisms with Gram positive (left), Gram negative (middle) and mycobacteria (right). Figure adapted from University of Cape Town website (http://web.uct.ac.za).

Because of its thick cell wall, Map is able to survive in the environment for extended periods of time. The bacillary form has been shown to survive for five months in clear water, nine months in shallow water, and 11 months in bovine faeces. Map can also survive for up to 47 months in dry soil and at -14ºC for at least one year. Some

studies suggest that Map can survive for even longer in acidic soils (Collins et al., 1990).

### 1.4 Map and Johne's disease

Map is the causative agent of Johne's disease, a chronic enteritis leading to wasting, diarrhoea and eventually death of infected animals. Johne and Frothingham initially reported Johne's disease in the late 1800's. However, it was not until 1910 that Trowt proved Map's involvement by growing Map in the laboratory and inducing disease in experimentally-infected cattle, thus successfully fulfilling Koch's postulates (reviewed in Harris and Barletta, 2001).(Harris and Barletta, 2001)

Map enters the body via the faecal-oral route, moves across the intestinal epithelium then gains access into professional phagocytes, predominantly macrophages. From here it is able to persist, replicate and contribute to the disease phenotype (Valentin-Weigand and Goethe, 1999). Ruminants are severely affected (Figure 1.3) with fecal shedding of Map, development of granulomatous lesions in the ileum and draining lymph nodes, as well as infertility characterizing this disease in these animals (Feola et al., 1999). Map infection has a severe effect on the dairy economy. In the USA, Johne's positive herds experience an annual economic loss of approximately $100 per cow due to loss of milk production and cow replacement costs (Ott et al., 1999).

**Figure 1.3. Cow with Johne's disease.** An animal with end-stage Johne's disease, exhibiting characteristic wasting. Image adapted from www.johnes.org.

## 1.5 Linking Map and Crohn's disease

In addition to causing widespread illness in bovine and other ruminant populations, Map can cause intestinal disease in a wide variety of other non-ruminant animals including at least 4 species of sub-human primates (Hines and Styer, 2003; Lilenbaum et al., 2007).

The similarities between the gross pathology and histology of Johne's disease in ruminants, and CD in humans initiated debate concerning the role of Map in CD (Goswami et al., 2000). Mucosal cobblestoning and the characteristic creeping mesenteric fat found in CD are also found in pathological specimens of Johne's diseased animals (Figure 1.4). Many researchers have suggested that this similarity is indicative of Map involvement in CD (Chamberlin et al., 2001; Chiodini, 1989; Elsaghier et al., 1992; Greenstein, 2003).

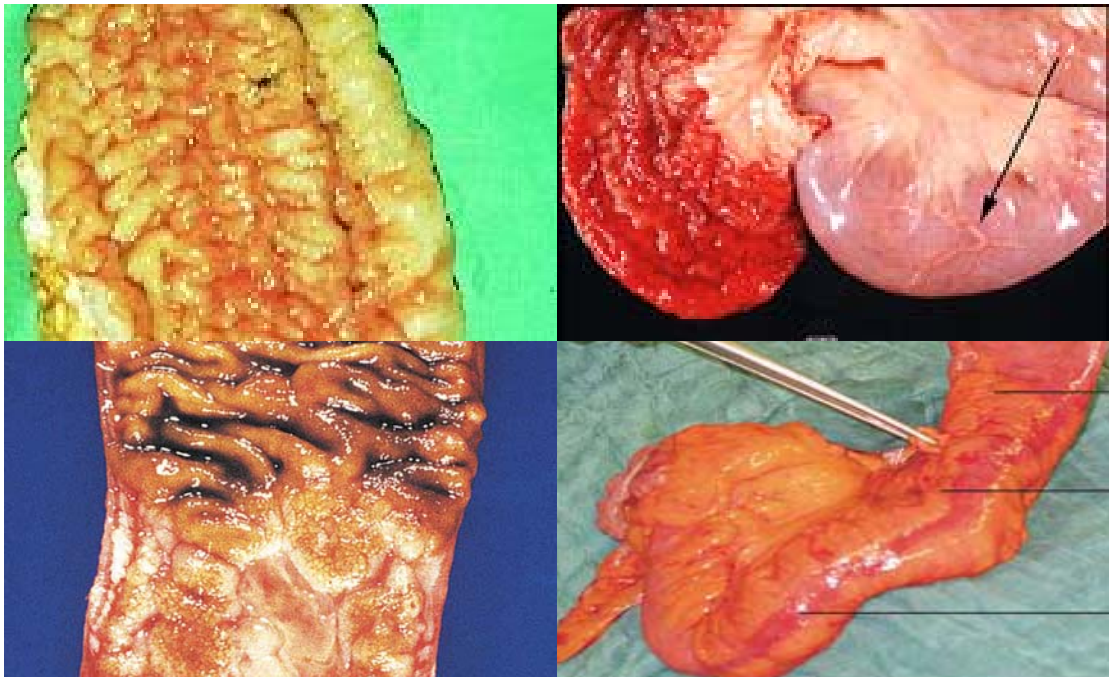

**Figure 1.4. Mucosal cobblestoning and creeping mesenteric fat characteristic of Johne's and Crohn's diseased tissue.** Mucosal cobblestoning (left) and creeping mesenteric fat (right) in tissue typical of Johne's disease (top) and Crohn's disease (bottom). Images adapted from Blowey et al., 1997 (top left), www.johnes.org (top right), Rosai, 2004 (bottom left), and Schaffler et al., 2005 (bottom right). (Blowey et al., 1997; Rosai, 2004; Schaffler et al., 2005).

Many different studies have used molecular and microbiological tools to demonstrate Map in CD patient serum, diseased tissue and breast milk (Bentley et al., 2008; Chiodini et al., 1984; Moss et al., 1992; Naser et al., 2000; Olsen et al., 2009; Sechi et al., 2004). However, there are also many studies that have found no genetic, serological or culture evidence of Map in tissue or blood samples taken from patients with CD (Cho et al., 1986; Heatley et al., 1975; Sasikala et al., 2009). This failure to consistently isolate Map from Crohn's disease patients, as well as studies that report the presence of Map in the blood of healthy individuals (Abubakar et al., 2008; Juste et al., 2008), leaves uncertainty surrounding the role of Map in CD. Despite this anomaly, several anti-mycobacterial drug trials have successfully decreased disease activity and/or increased remission in CD patients. However, the overall results from these trials have been mixed (Emery and Whittington, 2004; Gui et al., 1997).

### 1.6 Mycobacterial entry into host cells

Fundamental to mycobacterial involvement in animal and human disease is the ability for these bacteria to invade and survive within cells. Pathways of entry have been intensively characterised for many pathogens (Aderem and Underhill, 1999). However, how mycobacteria enter host cells is a subject of intensive research and debate. Considerable variation, within and among species, suggests that pathogenic mycobacteria enter cells via several different pathways (Darnelishvilli et al., 2007).

Some pathogenic bacterial species such as Fim-H *Escherichia coli* (*E. coli*) and *Bordetella pertussis* enter macrophages via pathways that fail to stimulate an oxidative burst (Baorto et al., 1997). Whether mycobacteria modify the phagocytic process in this way remains largely unknown but beads coated with mycobacterial mannose from both pathogenic and non-pathogenic mycobacterial strains bypass activation of NADPH oxidase (the respiratory burst) and exhibit attenuated fusion with lysosomes in human macrophages (Dequcker et al., 1999). This suggests that some mycobacteria may possess cell wall components that aid intracellular survival. However, it remains unclear whether mycobacteria are phagocytosed via a normal pathway, then persist by affecting phagosome-lysosome fusion once inside the cell, or whether they exploit a pathway of entry into the cell that results in them residing in a compartment that is unlikely to fuse with lysosomes (Rosenberger et al., 2000). Mycobacterial uptake into macrophages was originally thought to be mediated solely

by complement and mannose receptors (Darnelishvilli et al., 2007). More recently, however, other receptors (including the transferrin and scavenger receptors) have been shown to be equally important, suggesting mycobacterial uptake may involve several alternate pathways (Bermudez and Sangari, 2001). *M. avium* subspecies *avium* grown in macrophages uses a different mechanism to gain entry to cells than those grown on laboratory media, suggesting the development of an intracellular phenotype may affect uptake (Bermudez et al., 2004). Mycobacterial ligands implicated in uptake include cell wall proteins such as the mannans (common on mycobacterial cell walls) as well as other less well defined proteins including a 35 kDa major membrane protein reportedly involved in bacterial internalisation into bovine epithelial cells (Bannatine et al., 2003).

Evidence is also emerging of an essential role for cholesterol in the phagocytosis of pathogenic organisms, including mycobacteria. Cholesterol-enriched plasma membrane domains (lipid rafts) are thought to play a significant role in mycobacterial entry. Depletion of plasma membrane cholesterol specifically inhibits cellular uptake of *Mycobacterium bovis, M. tuberculosis* and *M. kansasii* into phagocytic cells (Kaul et al., 2004; Pandey and Sassetti, 2008). In addition, cholesterol aggregation is shown to occur at the site of mycobacterial internalisation (Gatfield and Pieters, 2000). Depletion of cellular cholesterol stimulates phagosomal maturation (de Chastellier and Thilo, 2006) and decreases survival of pathogenic mycobacteria (Pandey and Sassetti, 2008). Conversely, increased cholesterol increases susceptibility to, and severity of mycobacterial infection (Martens et al., 2008).

### 1.7 Mycobacterial survival inside phagocytic cells

Typically, a bacterium is taken up by the cell and deposited into a phagosome. This compartment sequentially fuses with early and late endosomes, and then finally lysosomes. As more lysosomes fuse with the maturing phagosome, the phagosomal pH drops dramatically, and the bacterium is killed (Beron et al., 2002; Desjardins et al., 1994b).

Many intracellular pathogens, including mycobacteria, halt the progression of the phagocytic process at the early endosomal stage. This modified compartment fails to

fuse with lysosomes (Kelley and Schorey, 2003; Sun et al., 2007), and is conducive to mycobacterial persistence and/or replication (Gomes et al., 1999).

Pathogenic mycobacteria such as *M. bovis* and *M. tuberculosis* reside in phagosomes that acquire markers of early endosomes, but fail to fuse with late endosomal and lysosmal organelles. The lack of fusion of mycobacterium containing vacuoles with end stage organelles (e.g. lysosomes) is attributed to a failure of the intermediate molecules responsible for docking and fusion of endosomes to the mycobacteria-containing compartment (Clemens et al., 2000b). Consistent with this hypothesis, *M. bovis* secretes a factor that binds a late endosomal molecule (Rab 7) integral for phagosome-lysosome fusion, switching it from an active (GTP bound) to an inactive (GDP bound) form. By impairing Rab 7 function, further maturation of the *M. bovis* phagosome is compromised (Sun et al., 2007).

Once phagocytosed, many virulent mycobacteria remain associated with cholesterol-rich membranes (de Chastellier and Thilo, 2006; Pandey and Sassetti, 2008). It has been proposed that close association with cholesterol-rich areas of the cell allow intracellular mycobacteria to acquire host cholesterol as a carbon energy source (Pandey and Sassetti, 2008) and thus permit them to remain metabolically active in their cellular microenvironment. However, other benefits of residing in a cholesterol-rich compartment have recently been documented. Cholesterol-rich membranes are more recalcitrant to fusion with lysosomes than membranes with normal levels of cholesterol (Huynh et al., 2008). In addition, cholesterol mediates the association of a protein integral for mycobacterial persistence.

The recruitment of the TACO (Tryptophan-aspartate-containing-coat) protein to the phagosomal membrane prevents phagosome maturation and/or fusion with lysosomes (Gatfield and Pieters, 2000). TACO is anchored to the mycobacterium-containing phagosomal membrane in a cholesterol-dependent manner. Increased phagosomal cholesterol has been shown to prolong its normally transient association with the early phagosome (Ferrari et al., 1999). Cellular cholesterol depletion with agents such as methyl-β-cyclodextrin (MβCD) mitigates this effect, and results in greater clearance of mycobacteria from infected cells (de Chastellier and Thilo, 2006; Deghmane et al., 2007). Thus, association with cholesterol-rich areas of the cell is

thought to prolong intracellular mycobacterial survival. To date, however, a role for cholesterol in Map infection has not been demonstrated

### 1.8 Thesis aims

The aim of this thesis was to analyse whether cell membrane-associated cholesterol has a role in the uptake and intra-cellular survival of Map in human monocytes. Specifically, Map bacteria were tracked through THP-1 monocytes using markers of early and late endosomes, and phagosomal acidity. The dependence of phagocytosis and trafficking on cholesterol was measured using depletion and co-localisation studies. Finally, the effect of cholesterol depletion on survival of Map was investigated, and long term persistence of these bacteria was assessed using light and electron microscopy.

# Chapter 2. Materials & Methods

## 2.1 Introduction

The experiments described in the results chapters of this thesis (Chapters 3 through 5) utilise a series of methods that were adapted and optimised for studying Map and THP-1 cells. The development of these methods is described in this chapter.

## 2.2 Bacterial strains and culture

Two different mycobacterial strains were used in this study. *Mycobacterium avium* subsp. *paratuberculosis* (Map) strain Dominic (ATCC 43545) was originally obtained from the intestinal tissue of a Crohn's Disease patient(Chiodini et al., 1984). Since its isolation, this strain has been used in a variety of studies as a representative human Map isolate(Greenstein et al., 2007a; Jaravata et al., 2007). *M. bovis* Bacillus Calmette Guerin (BCG) (ATCC 19210) is the cause of bovine tuberculosis but is also known to jump the species barrier and cause tuberculosis in humans(O'Reilly and Daborn, 1995). *M. bovis* reportedly survives in human leukocytes following uptake via a cholesterol-dependent pathway(Gatfield and Pieters, 2000), and was used as a positive control for these experiments. Strains were sub-cultured from stocks held at the University of Otago, Christchurch.

Mycobacterial strains were cultured in Middlebrook 7H9 media broth supplemented with OADC (oleic acid dextrose catalase; Becton Dickinson, Sparks, MD, USA), 0.05% Tween-80 (Sigma, St Louis, MO, USA) and 2 µg/ml mycobactin J (Allied Monitor, Fayette, MO, USA), as previously described(Chiodini et al., 1984; Feola et al., 1999; Shin and Collins, 2008). This medium supports the growth of human and ruminant-derived strains of Map(Shin and Collins, 2008; Sung and Collins, 1998). Cultures took 15 days to reach late-exponential growth phase (Figure 2.1) and were maintained at this level by regular passage into fresh medium.

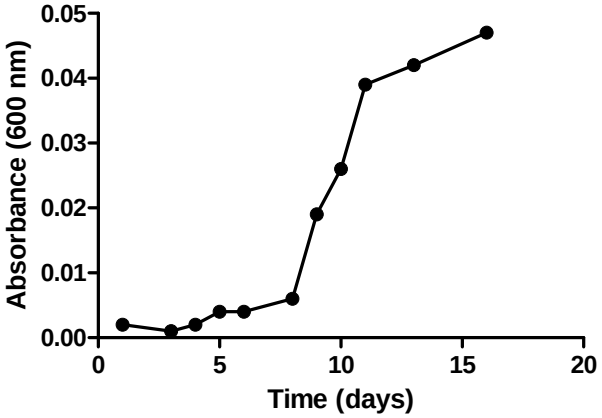


**Figure 2.1**. **Absorbance values for culture of bacillary Map.** Initial growth of Map in Middlebrook 7H9 media. Bacteria were grown to late log phase before being used for experimentation (approximately 16 days). To quantitate bacterial numbers, 100 µl of bacterial suspension in PBS was aliquoted into a 96 well plate and absorbance was measured at 600 nm. Values were blanked using bacteria-free PBS (phosphate buffered saline).

*E. coli* strain BL21 (ATCC BAA-1025) has been used in previous mycobacterial studies (Gatfield and Pieters 2000) and provided an additional control for these experiments. Each strain was maintained on blood agar plates (Fort Richard, Auckland, NZ) and transferred to Brucella broth (BD Biosciences, Sparks MD, USA) with (*H. pylori*) and without (*E. coli*) the addition of 5% foetal bovine serum (FBS; Gibco, Auckland, NZ). Broth cultures were incubated with constant rotation (100 rpm) at 37$^{o}$C in a $CO_2$ (10%) incubator.

Map, *M. bovis* BCG and *H. pylori* are classified as bio-safety level 2 (BSL-2) (ATCC), while *E. coli* strain BL21 is designated level 1 (ATCC). As such, all bacterial manipulations were conducted in a biological safety hood, and all experiments were conducted under BSL-2/PC2 conditions.

### 2.2.1 Enumeration of bacteria

Map and *M. bovis* growth were quantified using a standardised spectrophotometric method (D Glubb, submitted). One hundred microlitres of bacterial solution (in PBS) was read at 600 nm to give the optical density (OD) (Figure 2.2). For experimental procedures, the OD of Map and *M. bovis* suspensions was enumerated and the solution diluted to give a working concentration of approximately 100 million bacteria/ml.

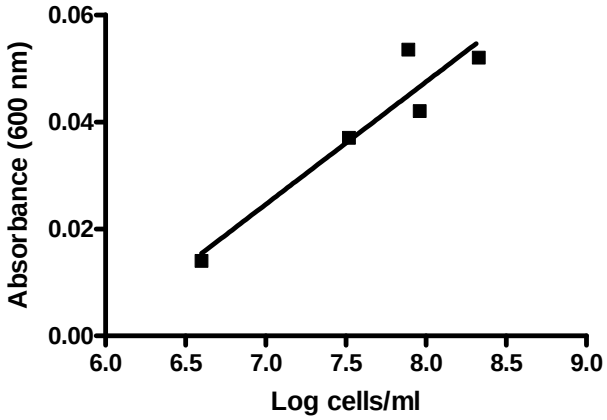


**Figure 2.2. Enumeration of Map and *M. bovis* bacteria.** The graph relates optical density of a 100 µl bacterial solution to bacterial CFUs/ml. Data from unpublished work of D. Glubb.

*E. coli* strain BL21 was enumerated by direct counting of a dilution series using a haemocytometer.

### 2.2.2 Bacterial labelling

Visualising bacteria for flow cytometry and fluorescent microscopy requires a label that is non-toxic, and not washed out during incubations with cells. Additionally, the label must demonstrate negligible interaction with the processes being studied, or with bacterial or cellular constituents such as ligands or receptors.

Fluorescein isothiocyanate (FITC) is a functionalised derivative of fluorescein that is reactive towards nucleophiles such as the amine and sulfhydryl groups on proteins

with which it forms covalent bonds(Hermanson, 2008). FITC permanently labels both bacteria (Pikaar et al., 1995) and mycobacteria (Kudo et al., 2004; Schuller et al., 2001) with minimal effects on bacterial survival and bacteria-cell interactions. It is also applicable to fluorescence microscopy and flow cytometry(Baorto et al., 1997; Marques et al., 2001), exciting with blue light, and fluorescing green (488 and 530 nm respectively).

Labelling the bacteria for these experiments required a FITC concentration that was high enough to give a reliable signal by both flow cytometry and fluorescent microscopy for at least 48 hours post treatment, and to ensure that even a single bacterium inside a cell could be clearly identified. To achieve this, 1 ml aliquots of bacteria were pelleted by centrifugation (10,000 rpm, 5 min) and the supernatant removed. The bacteria were then resuspended in 200 µl of 100 µg/ml FITC solution for 1 h at 37$^{o}$C in the dark. Following labelling, the bacteria were washed three times with PBS (10,000 rpm, 5 min), before being resuspended in PBS (Figure 2.3).

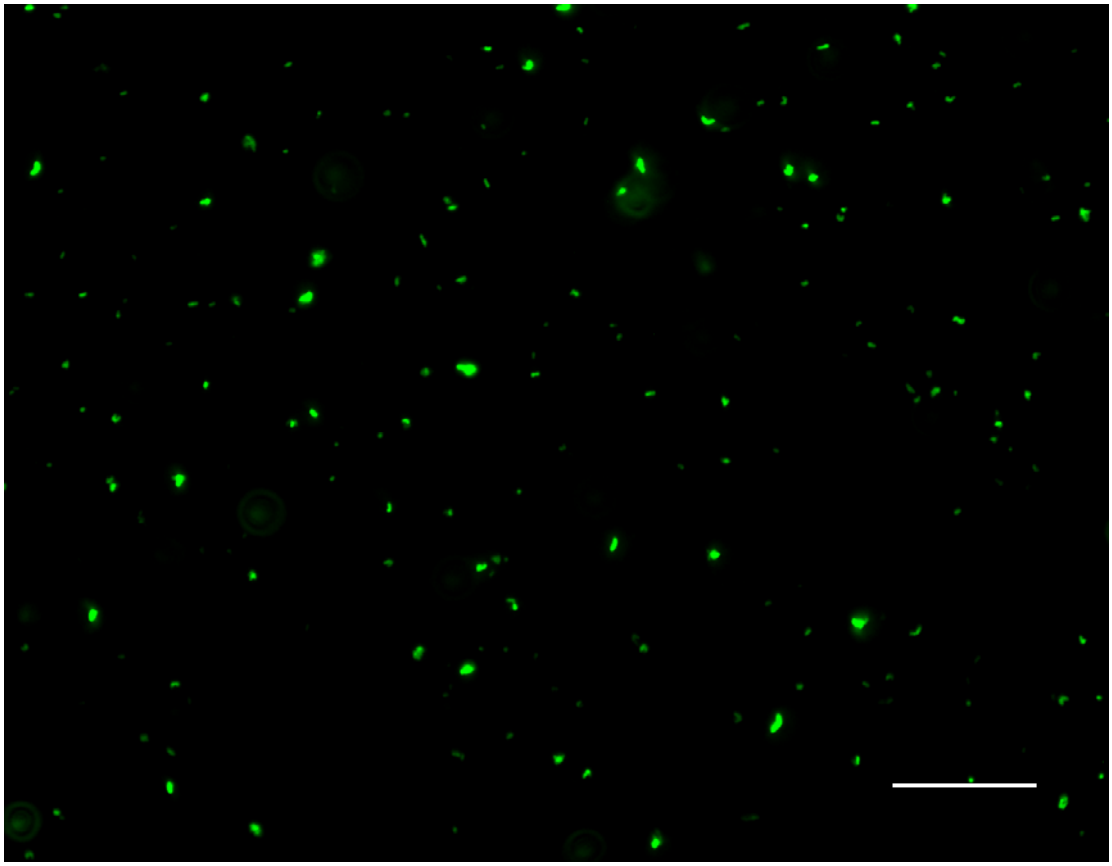

**Figure 2.3. FITC-labelled Map.** Map bacteria were labelled with 100 µg/ml FITC. Green fluorescence was imaged using blue light excitation. Scale bar indicates 10µm.

To ensure that labelling Map with 100 µg/ml FITC had no significant effect on bacterial viability, labelled and unlabelled Map were serially diluted and plated on Middlebrook 7H9 agar. Colonies were counted after 6 weeks. Results showed no observable effect on Map viability (Figure 2.4). Confirming this observation, in a related study, *M. bovis* labelled with a similar concentration of FITC did not show reduced viability(Schuller et al., 2001).

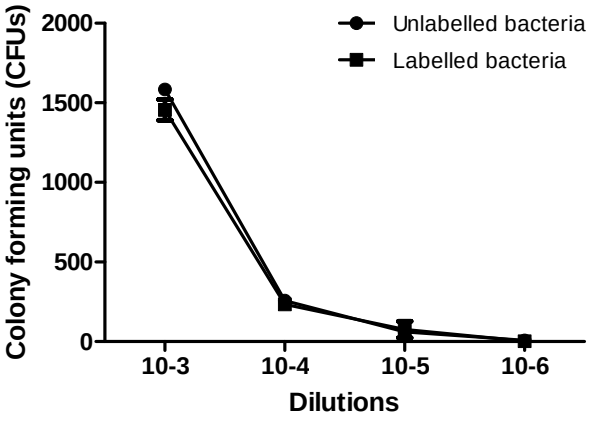


**Figure 2.4. Comparative viability of labelled and unlabelled MAP cultures.** The viability of Map incubated with 100 µg/ml FITC for 1 h was compared with that of unlabelled bacteria. Values are mean +/- SEM of three independent experiments. There was no significant difference in viability between the two treatments at any dilution (data analysed by 2-way ANOVA).

### 2.2.3 Killing bacteria

Mycobacteria are more tolerant to temperature and chemical stresses than many other pathogenic bacteria, exemplified by their ability to survive some pasteurisation techniques(Sung and Collins, 1998). It is thought this resistance is predominately due to their large and complex cell wall (Figure 1.4) and slow replication time (Figure 2.1). Heat treatment is a well established procedure for killing Map and other mycobacteria. Map in volumes less than 10 ml are killed after treatment at 72$^{o}$C for 25 seconds(Le Cabec et al., 2000; Yakes et al., 2008). For heat inactivation in the following experiments, a temperature and time well above the upper survival limit of Map (85$^{o}$C, 15 min) was used to ensure that all bacteria were killed. This protocol was also used to kill *E. coli* BL21, confirmed by no growth at 24 h when 50 µl of

bacterial suspension was plated onto blood agar. *E. coli* grow rapidly in RPMI media, therefore they were killed in these experiments to enable their use as a control at 48 h post infection.

Formaldehyde fixation, which reportedly kills Map in 5 minutes(Lilenbaum et al., 2007), was also used to treat Map, thereby overcoming the potentially confounding release of cytoplasmic contents from heat-killed bacteria. Additionally, formaldehyde treatment has the advantage of retaining an intact bacterial unit with similar antigenic presentation to a live bacterium for live/dead comparison experiments(Smit et al., 1974).

The viability of Map after 30 minutes incubation with 4% formaldehyde was tested by plating serially diluted bacteria on Middlebrook 7H9 agar and incubating the cultures for 6 weeks. This confirmed a loss of over 99.99% of viable bacteria when compared with Map incubated in PBS alone (data not shown). While mutants of MAP strain 43545 that were unable to persist in human cells would have been the ideal controls for these experiments, they do not exist for this strain. Therefore heat and formaldehyde killed MAP were used as in similar studies (Rumsey et al., 2006).

### 2.2.4 Generation of single bacterial cell suspensions

Mycobacteria are notorious for their ability to form clumps in culture. In nature, this behaviour may contribute to their resistance to heat and other stresses(Rowe et al., 2000). However, in culture, this ability to aggregate interferes with experimental doses and can inhibit growth(Lewin et al., 2008). There are several well-characterised methods to eliminate clumps and generate single mycobacteria in culture. Of these, the two that are predominantly used are sonication and passage through a 25 gauge needle(Parish and Stoker, 1998).

These two methods were compared to establish the most efficient way to generate single Map in solution. Bacterial suspensions were treated, then visualised by light microscopy using Ziehl Neelsen staining, an acid-fast stain that is specific for mycobacteria (Appendix 1). Light microscopy showed the optimum method for generating a suspension of single Map was sonication (Omniruptor 4000) of the bacterial suspension for 10 seconds, at 10% power with a 50% pulse (Figure 2.5).

This is in contrast to passage through a 25 gauge needle, which failed to remove many of the clumps (Figure 2.6).

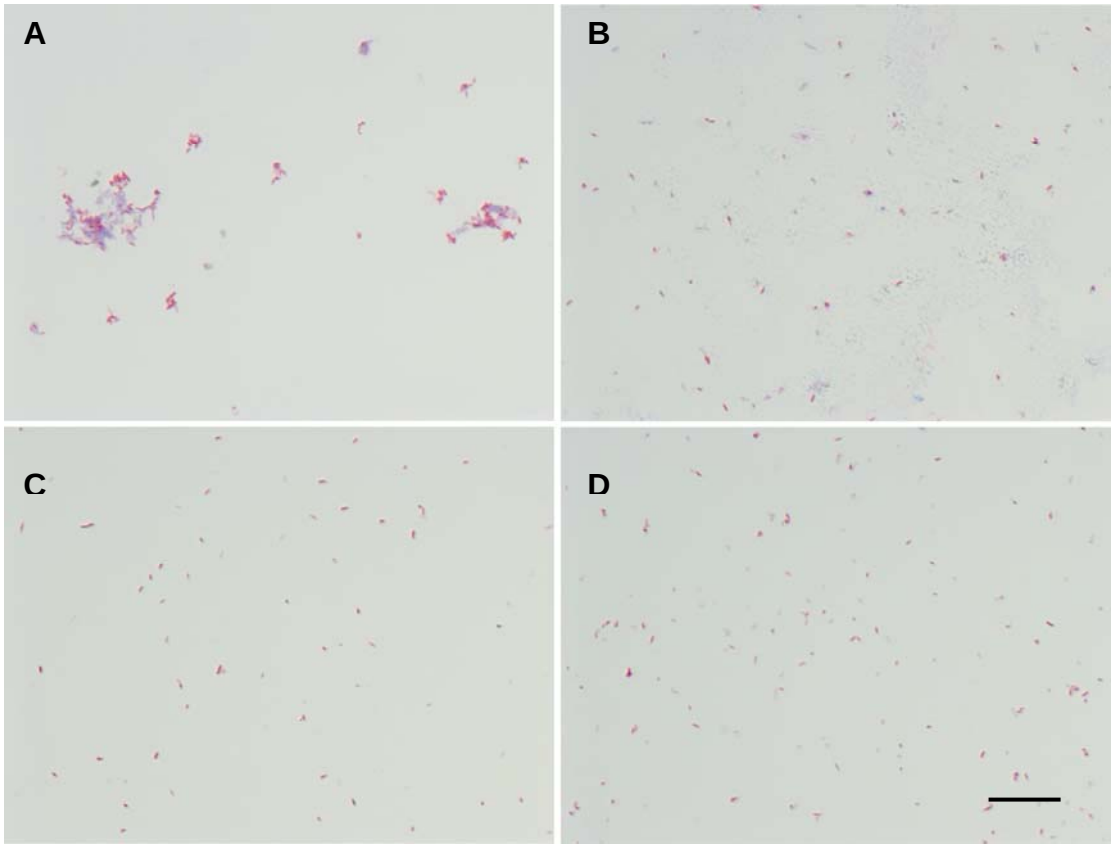


**Figure 2.5. Map bacteria after sonication.** Images show Map before (A) and after sonication for 10 (B), 20 (C), and 30 (D) seconds. The sonicator was set to 10% power with a 50% pulse (Omniruptor 4000 ultrasonic homogeniser). Scale bar indicates 10µm.

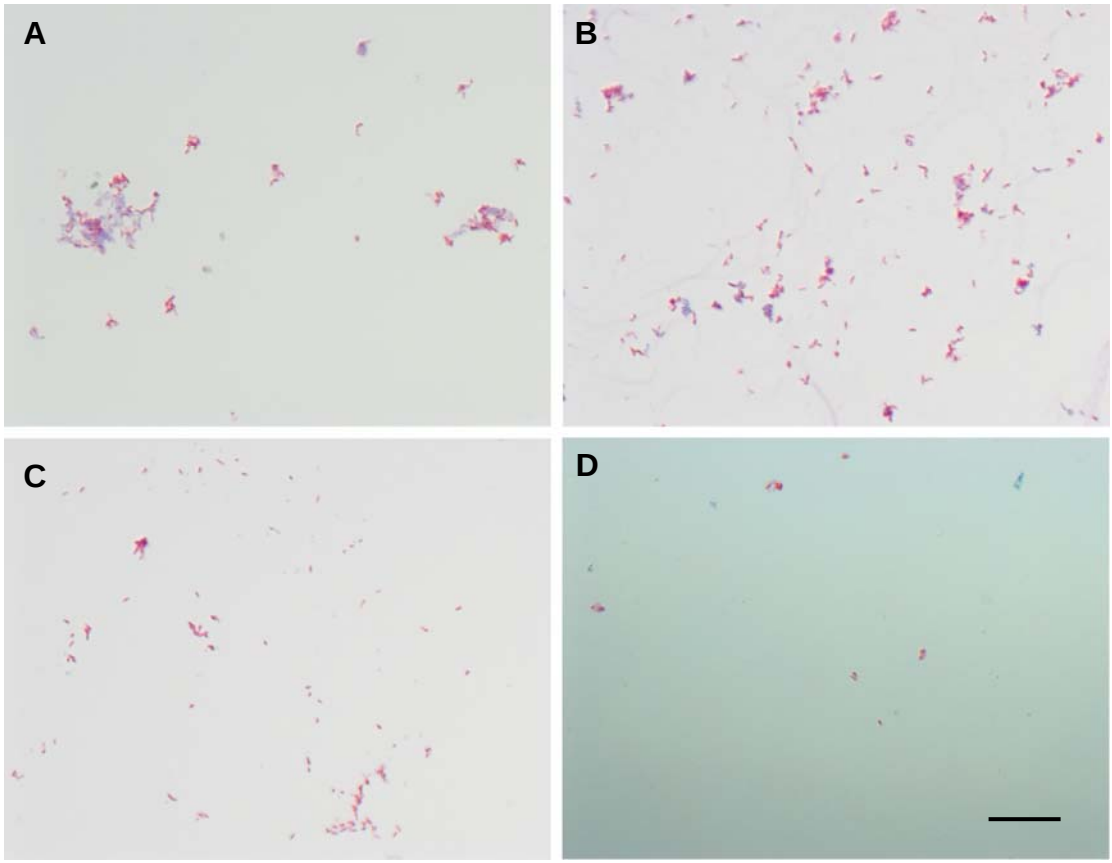


**Figure 2.6. Map bacteria after passage through a 25 gauge needle.** Images show a solution of Map before (A) and after passage through a 25 gauge needle 5 times (B), 10 times (C) or 20 times (D). The control in (A) is the same control as in figure 2.5. Scale bar indicates 10µm.

It was also important to ascertain whether the bacteria would stay homogenous during the course of an experiment, given the potential of reclumping to significantly affect experiments involving the cellular uptake of mycobacteria(Cougoule et al., 2002; Parish and Stoker, 1998). To analyse the extent and timeframe of re-clumping, Map bacteria (50 million/ml) were suspended in Middlebrook 7H9 medium. The solution was sonicated and a loopful was taken at time 0, 2 h, 4 h, 6 h and 24 h, spread onto a microscope slide, and Ziehl-Nelson stained. Relative bacterial clumping was analysed by light microscopy. There was no observable increase in the amount of clumped mycobacteria up to the 6 hour stage (Figure 2.7). A slight increase in bacterial clumping occurred at 24 hours post-sonication (Figure 2.8). However the majority of mycobacteria in suspension remained singular at this time point and this level of clumping was judged to be acceptable for experimentation. Reclumping was significantly decreased in the formaldehyde-treated bacterial cultures (Figure 2.8D).

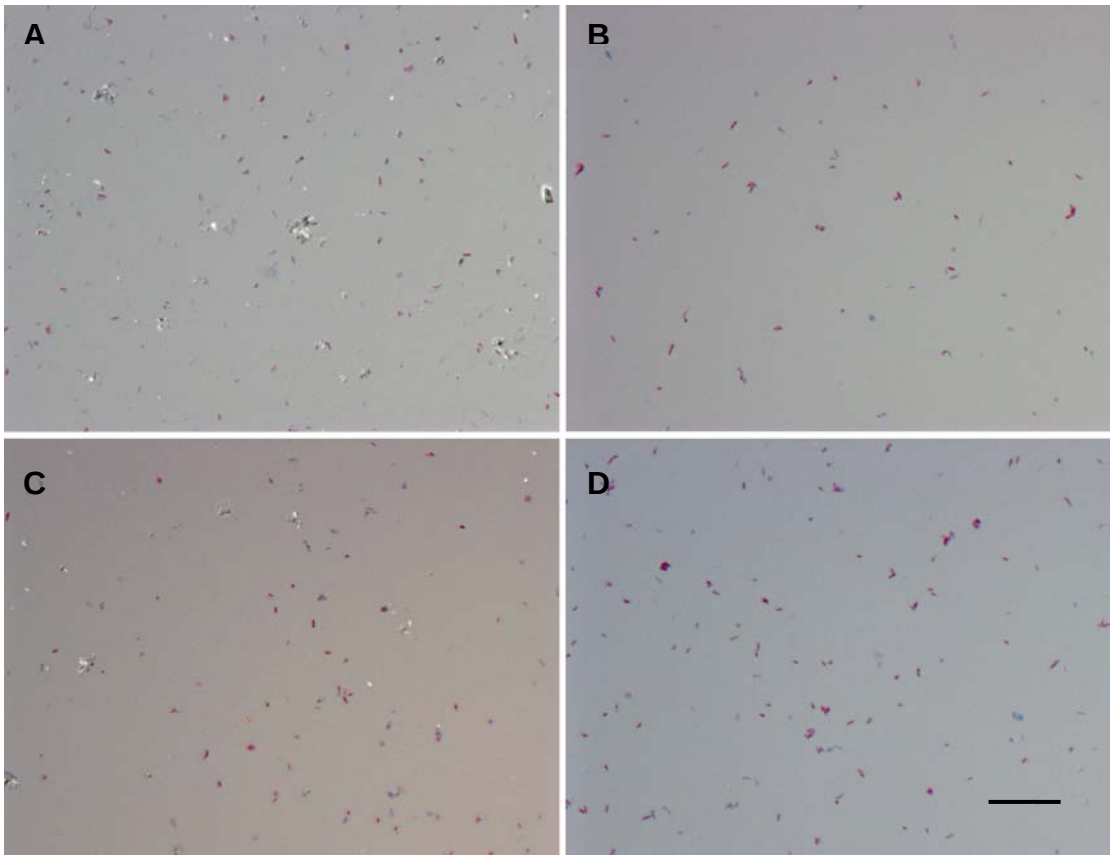


**Figure 2.7. Map bacteria 6 h after sonication.** Map bacteria before (A) and immediately after (B) sonication. The same bacteria 2 hours (C) and 6 hours (D) post-sonication. Scale bar indicates 10µm.

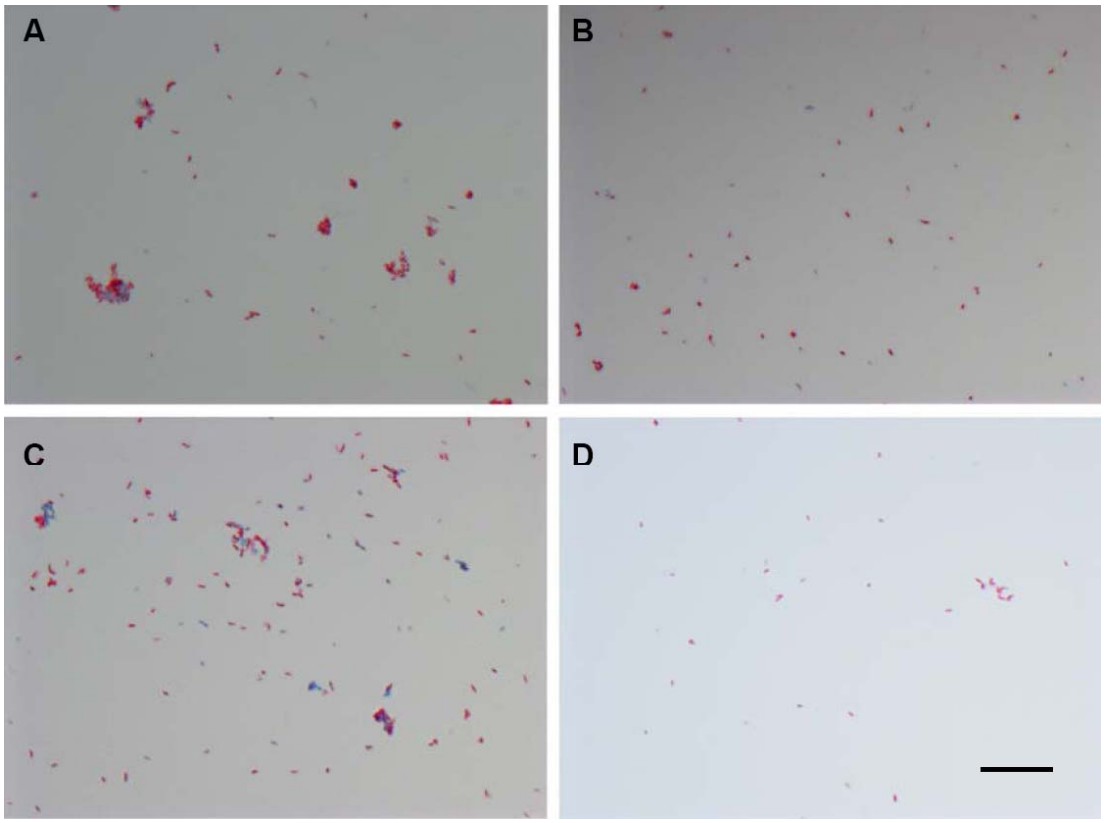


**Figure 2.8. Map bacteria 24 h after sonication.** A suspension of Map bacteria before (A) and immediately after (B) sonication. The same bacteria 24 hours post-sonication (C) and formaldehyde killed bacteria at 24 hours (D). Scale bar indicates 10 µm.

### 2.2.5 Simvastatin and growth of Map

Before examining the effect on cholesterol on Map uptake and persistence, it was first necessary to ensure that co-culture of these bacteria with simvastatin had no effect on Map growth. To test this, duplicate 2 ml aliquots (100 million bacteria/ml) with and without the addition of simvastatin (2.5 ug/ml) were grown in capped 5 ml tubes at 37$^{o}$C. Relative growth was assessed over a 7 day period (Figure 2.9). No significant difference was observed between treated and untreated Map (data analysed by one way ANOVA).

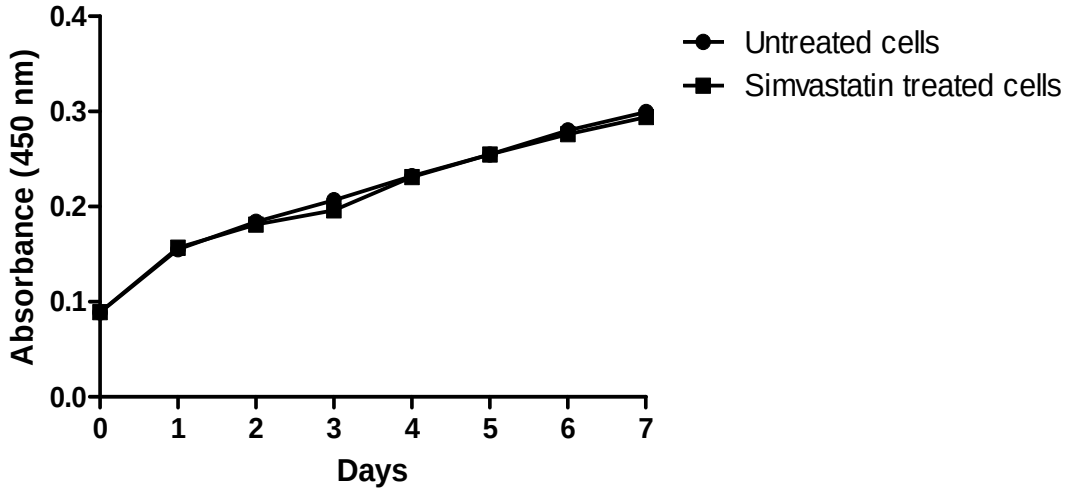


**Figure 2.9. Map growth with and without 2.5 µg/ml simvastatin.** Values are mean +/- SEM of three independent experiments. No significant difference was found between cultures with or without 2.5 µg/ml simvastatin (data analysed by one way ANOVA).

## 2.3 Cell culture of THP-1 human monocytes

THP-1 monocytes are a non-adhesive, phagocytic cell line originally derived from the peripheral blood of a 1 year old human male with acute monocytic leukemia(Tsuchiya et al., 1980). Cells were grown at 37$^{o}$C in RPMI-1640 with 10% FBS, 1 x Penstrep® antibiotic (Invitrogen, Auckland, New Zealand) and 1 x Glutamax® (Invitrogen), and maintained at approximately 5 x $10^{5}$/ml in culture. To count the cells, 20 µl of cell suspension was mixed with 20 µl trypan blue solution (250 µg/ml in PBS). Duplicate 10 µl volumes were pipetted into a haemocytometer and trypan blue negative cells in a given area were counted to give the number of viable cells per ml.

## 2.4 Co-incubation of THP-1 cells with Map bacteria

Phagocytosis was investigated by co-incubation of THP-1 cells with bacteria for 4 h(Feola et al., 1999; Neyrolles et al., 2006; Rumsey et al., 2006). This time allowed measurable uptake to occur, while minimising any unwanted confounding effects caused by longer term exposure to compounds such as simvastatin.

To determine the optimum number of Map per cell, THP-1 monocytes were exposed to different numbers of Map. Association of fluorescent bacteria with cells was measured by flow cytometry. It was found that a multiplicity of infection (MOI) of 100:1 (bacteria per cell) gave a reproducible value of approximately 25% bacterial association (Figure 2.10). This figure was higher than many published studies have used, but was most likely due to the suspended cells being less efficient in phagocytosing bacteria than adherent cells such as macrophages.

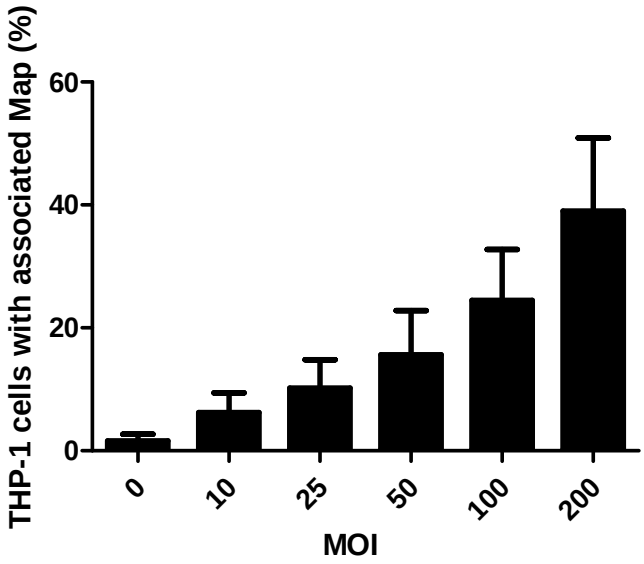


**Figure 2.10. THP-1 and Map MOI.** Increasing MOI of Map exposed to THP-1 cells over a 4 h incubation period. The percentage of THP-1 cells with associated Map was measured after 4 h incubation at 37°C (5% $CO_2$). Values are mean +/- SEM of three independent experiments.

An established method (Flaminio et al., 2002) was adapted to determine whether treating THP-1 cells affected association of mycobacteria. Two hundred thousand cells were incubated for 1 h with their respective treatments, washed once with 1x PBS containing 5% FBS, then incubated for 4 h with FITC-labelled Map (100:1 MOI). Cells were washed three times (to remove non-adherent extra-cellular bacteria) and resuspended in PBS/5% FBS containing 5 µg/ml propidium iodide (PI) incubated for 5 min at room temperature, then analysed by flow cytometry (Cytomics FC 500 MPL flow cytometer, Beckman Coulter). PI binds to DNA by intercalating between bases and is generally excluded from viable cells(Haugland, 2005). Any dead cells were

excluded by positive PI staining, and remaining non-adherent bacteria were removed from analysis by size stratification (Figure 2.11).

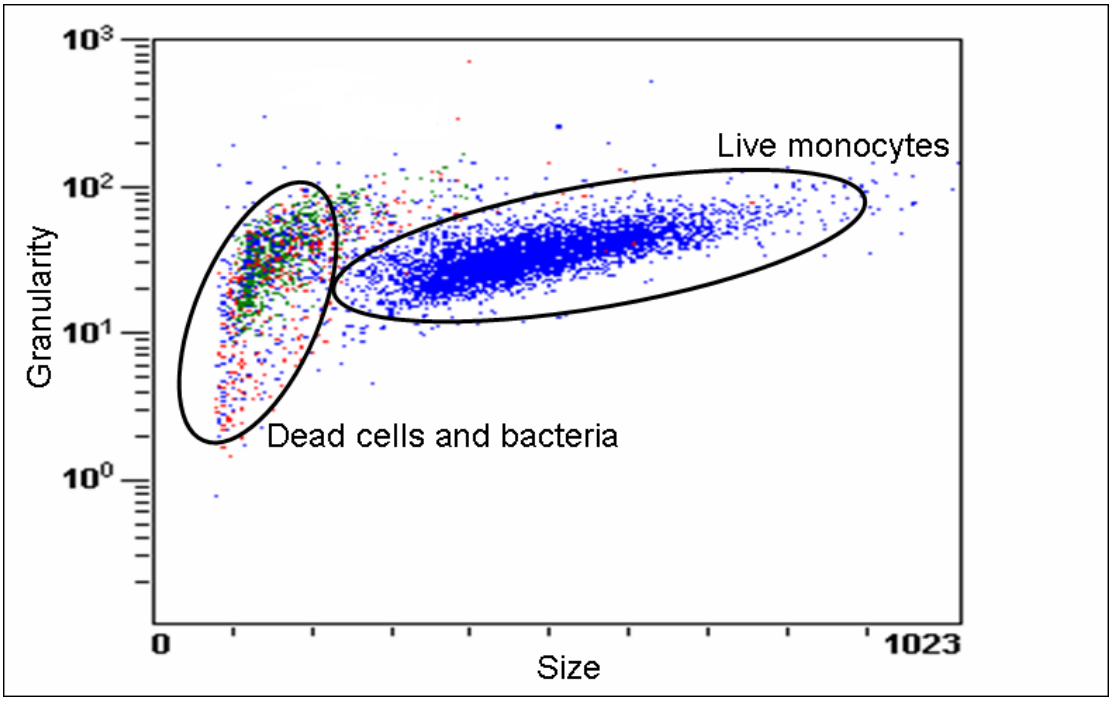


**Figure 2.11. Flow cytometry of THP-1 monocytes.** Live monocytes were isolated. Non-adherent bacteria were removed by size stratification. PI positive cells were also removed. Particles were plotted using granularity (Y axis) and size (X axis).

Those cells with bacteria associated were further stratified into total associated and intracellular. Trypan blue was added to the tubes after the initial flow cytometry run to quench any extra-cellular bacterial fluorescence. The suspension was run again, with the second result giving percentage intracellular bacteria(Wooldridge et al., 1996).

### 2.5 Depletion of THP-1 monocyte cholesterol levels

THP-1 monocytes were depleted of cholesterol using two different drugs. Statins have been used effectively in a variety of studies to inhibit cellular cholesterol production(Gatfield and Pieters, 2000; Lioke et al., 2004). Simvastatin (Sigma) was used to reduce endogenous cholesterol synthesis in the cell(Almog et al., 2004; Lioke et al., 2004; Rise et al., 1997), while methyl-ß-cyclodextrin (MßCD) (Sigma) was used to actively sequester cholesterol away from the plasma membrane(Christian et al., 1997). These drugs were used in tandem to create a decreasing cholesterol

concentration gradient, with which the dependence of bacterial uptake on host cell cholesterol status could be measured(Gatfield and Pieters, 2000; Lamberti et al., 2008; Lioke et al., 2004). MßCD complexed with cholesterol was used as a control to demonstrate there were no MßCD-related, cholesterol-independent effects. To create a negative gradient of cholesterol, cultured cells were incubated with 2.5 µg/ml simvastatin for 48 h and then resuspended at a concentration of 200,000 cells/ml with increasing concentrations of MßCD for 1 h.

### 2.6 THP-1 cell proliferation following cholesterol depletion

In these experiments, THP-1 cells were incubated with 2.5 µg/ml simvastatin a concentration well below the 4.19 µg/ml (10µM) value shown to inhibit proliferation by 35% over 48 h in the closely related U937 monocyte cell line (Fujino et al., 2005).

MßCD-treated THP-1 cell proliferation was assessed because of evidence that this drug may inhibit cellular proliferation(Choi et al., 2004; Pottosin et al., 2007). Cells were treated with MßCD for 24 h, then permeablised (70% EtOH) to let the normally membrane-impermeable propidium iodide (PI) into the cells. Flow cytometry was used to quantitate the relative amount of DNA in each cell, allowing cell stages (G1, S, G2) to be categorised (Toba et al., 1992). The relative proliferation of each cell preparation was quantified by comparing the number of cells in S phase between treatments (Figure 2.12).

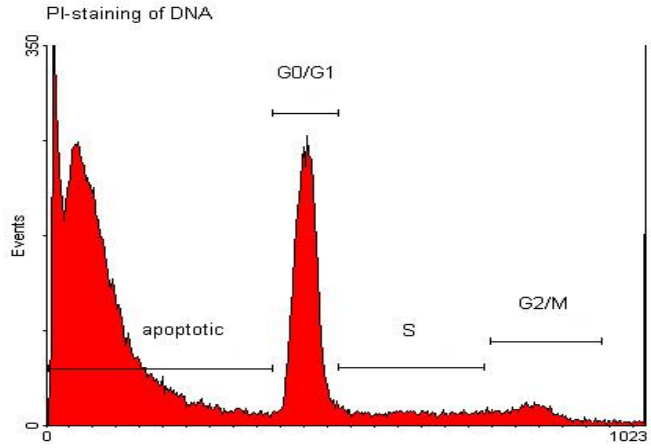


**Figure 2.12. Cell cycle pattern using propidium iodide.** Quantitative PI stain and corresponding cell cycle phase. Y axis is number of events and X axis is PI concentration. Note the large S phase plateau between the G0/1 and G2 phases; this is used as a measure of percentage proliferating cells in a suspension. Image modified from Macleod and Aldaz (2008).

The cytometry profile for THP-1 cells was too compact to give reliable values for the S phase (Figure 2.13). Accordingly, the combined results of three independent experiments showed no significant difference in cell proliferation following MßCD-treatment (Figure 2.14). This finding was contrary to other studies(Choi et al., 2004), suggesting that the technique lacked the sensitivity required to reveal any differences induced by MßCD.

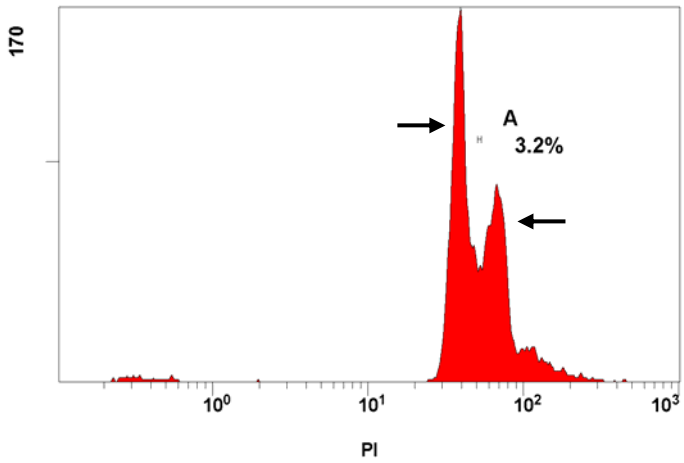


**Figure 2.13. Cell cycle pattern using propidium iodide in THP-1 cells.** Representative flow cytometry readout for THP-1 monocyte cells DNA content analysis. Note the lack of a suitable S phase "gap" (only 3.2% of cells) between the G0/G1 and G2/M phase peaks (arrows). The apoptotic peak is likely hidden.

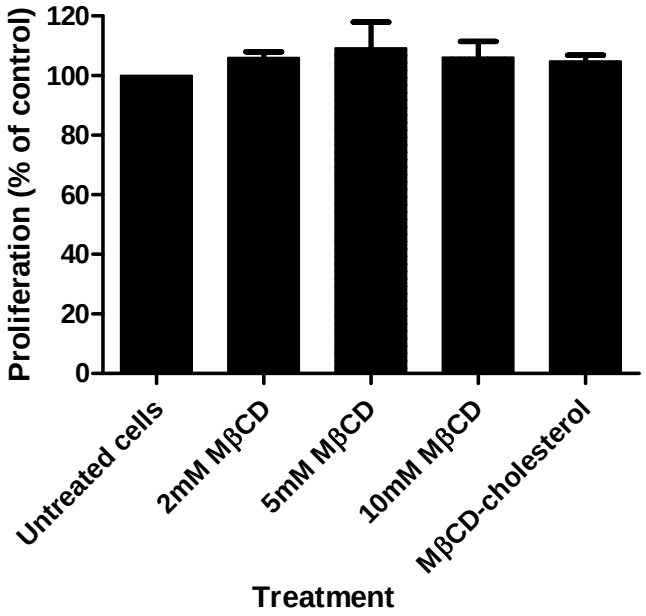


**Figure 2.14. PI cell cycle assay to measure proliferation of THP-1 cells exposed to MßCD.** Relative proliferation of cells treated with MßCD was measured using the PI cell cycle method. Values are mean +/- SEM of three independent experiments. No significant difference was found between any of the treatments (data was analysed by a one-way ANOVA).

Another measure of cell proliferation was used to test the hypothesis that overlapping G phases of the DNA cell cycle analysis profile obscured significant differences between the S phases of different treatments. Bromodeoxyuridine (BrdU) is integrated into dividing cells where it replaces thymidine during DNA synthesis. Detected using an antibody, BrdU quantification can be used as a measure of relative cell proliferation. The assay was carried out using a BrdU colorimetric ELISA kit (Roche, Mannheim, Germany) as per the manufacturer's instructions. The results showed that MßCD significantly reduced proliferation of the THP-1 cells in a dose dependent manner (Figure 2.15). Addition of exogenous MßCD complexed to cholesterol partially restored cell proliferation.

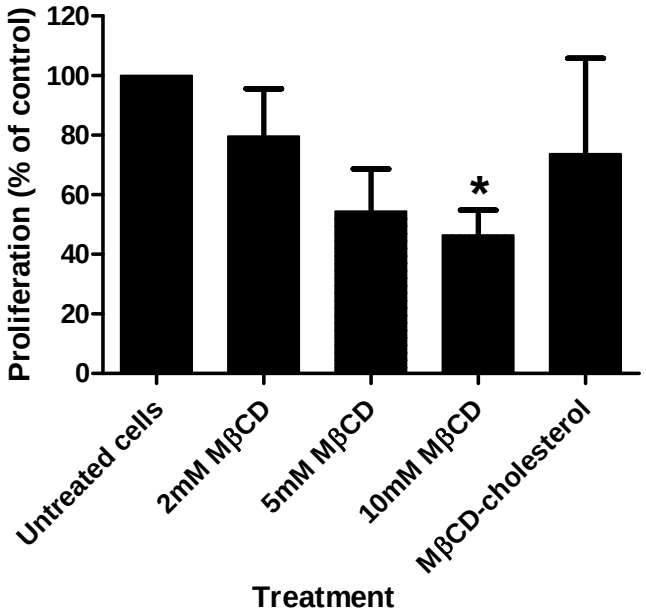


**Figure 2.15. BrdU assay to measure proliferation of THP-1 cells exposed to MßCD.** Effects of MCßD on proliferation of THP-1 monocytes was measured by BrdU assay. MβCD complexed with cholesterol was used to partially restore cholesterol. Results are expressed as percentage proliferation of control cells. Values are mean +/- SEM of three independent experiments. 10mM MßCD was significantly different from the untreated control (data analysed by one way ANOVA. * indicates $P < 0.05$).

## 2.7 THP-1 cell viability

To ensure that simvastatin and MßCD did not have a deleterious effect on cell viability, relative cell death was measured by staining cells with PI (5µg/ml for 5min). Flow cytometry was used to determine that at least 90% of THP-1 cells were PI negative (and therefore viable) at the end of each experiment. The results of these experiments showed PI values for cells treated for 1 h with 10 mM MßCD were approximately twice that of all other treatments. In contrast, the concentrations of simvastatin used throughout the following experiments did not significantly alter cell viability (Figure 2.16).

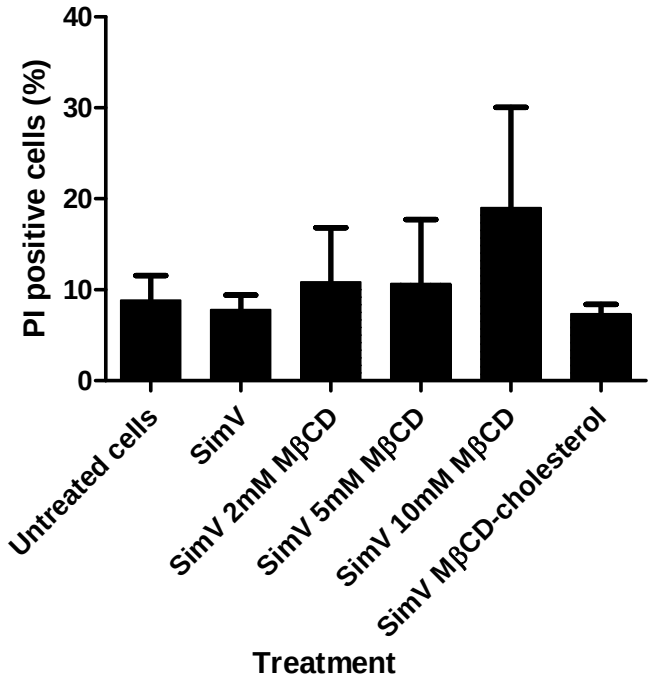


**Figure 2.16. THP-1 cell death after treatment with simvastatin (SimV) and MßCD.** The Y axis indicates the percentage of PI positive (dead) cells. No significant difference in cell death was found between any of the treatments and the cells only control. However, 10mM MßCD did show an observable, but not significant, increase in cell death. Values are mean +/- SEM from three independent experiments (data was analysed using a one way ANOVA).

The observation that 10 mM MßCD had an significant effect on THP-1 cell proliferation (Figure 2.15), and decreased THP-1 cell viability (Figure 2.16) resulted in an amended regimen for the cholesterol depletion experiments. This included simvastatin (2.5 µg/ml) and MßCD concentrations of 2 and 5 mM. These combinations had no significant effect on THP-1 cell proliferation (Figure 2.15) or viability (Figure 2.16).

## 2.8 Measurement of THP-1 cellular cholesterol

Simvastatin and MßCD were used to create a negative cholesterol gradient to analyse a role for cholesterol in Map uptake by THP-1 cells. Cellular cholesterol levels were measured following treatment using a commercially available kit (Roche). Control serum was reconstituted in water to give a stock solution (2.78 g/L) that was further diluted to produce a standard curve (Appendix 2).

To assay THP-1 cell cholesterol content, 200,000 cells were incubated with the treatment solution, then washed twice with PBS and resuspended in 50 µl lysis buffer (Appendix 3). Cells were vortexed briefly, then incubated at 37$^{o}$C (shaking for 15 min. One hundred and fifty microlitres of milliQ $H_2O$ was then added to give a final lysate volume of 200 µl. For analysis, duplicate 100 µl aliquots of lysate were added to wells of a 96 well plate, and cholesterol CHOD-PAP reagent (100 µl) added to each. The plate was incubated at 37$^{o}$C (shaking) for 15 minutes to allow colour development, then read on a spectrophotometer (Spectromax 190) at 490 nm. Cholesterol content was expressed as micrograms of cholesterol per milligram of cellular protein, measured used an established method(Sandermann and Strominger, 1972), detailed in Appendix 4. A negative gradient of cholesterol was created, although the values were not significantly different (Figure 2.17).

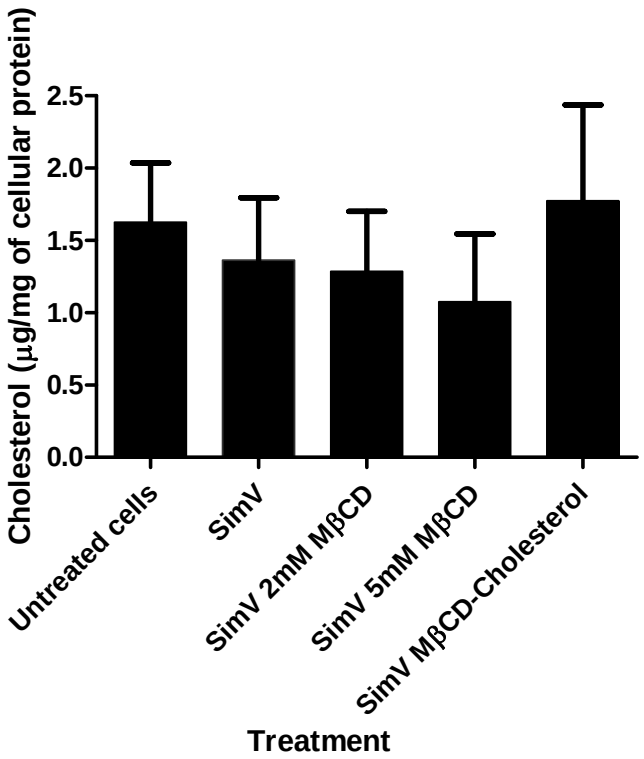


**Figure 2.17. Cholesterol depletion of THP-1 monocytes.** THP-1 cells were treated with simvastatin (SimV) and methyl-β-cyclodextrin (MßCD) to create a negative cholesterol gradient. Cellular cholesterol levels were measured using an ELISA kit (Roche). Results are expressed as µg of cholesterol/mg of cellular protein. Values are means +/- SEM from three independent experiments. While a negative cholesterol gradient was created, no significant differences were found between any of the treatments (data was analysed using a one-way ANOVA).

## 2.9 Visualisation of cellular cholesterol by filipin fluorescence

Fluorescence microscopy was also used to visualise differences in the cholesterol content of treated and control cells (Figure 2.18). Filipin is a polyene antibiotic that binds cholesterol in mammalian cells(Drabikowski et al., 1973; Gatfield and Pieters, 2000). Treated cells were incubated with 0.05% filipin (30 min) at 37°C, then visualised using fluorescence microscopy with excitation (360 nm) and emission (405 nm) through a standard UV filter block. Filipin fluorescence decreased with simvastatin and MßCD-mediated cholesterol depletion (Figure 2.18).

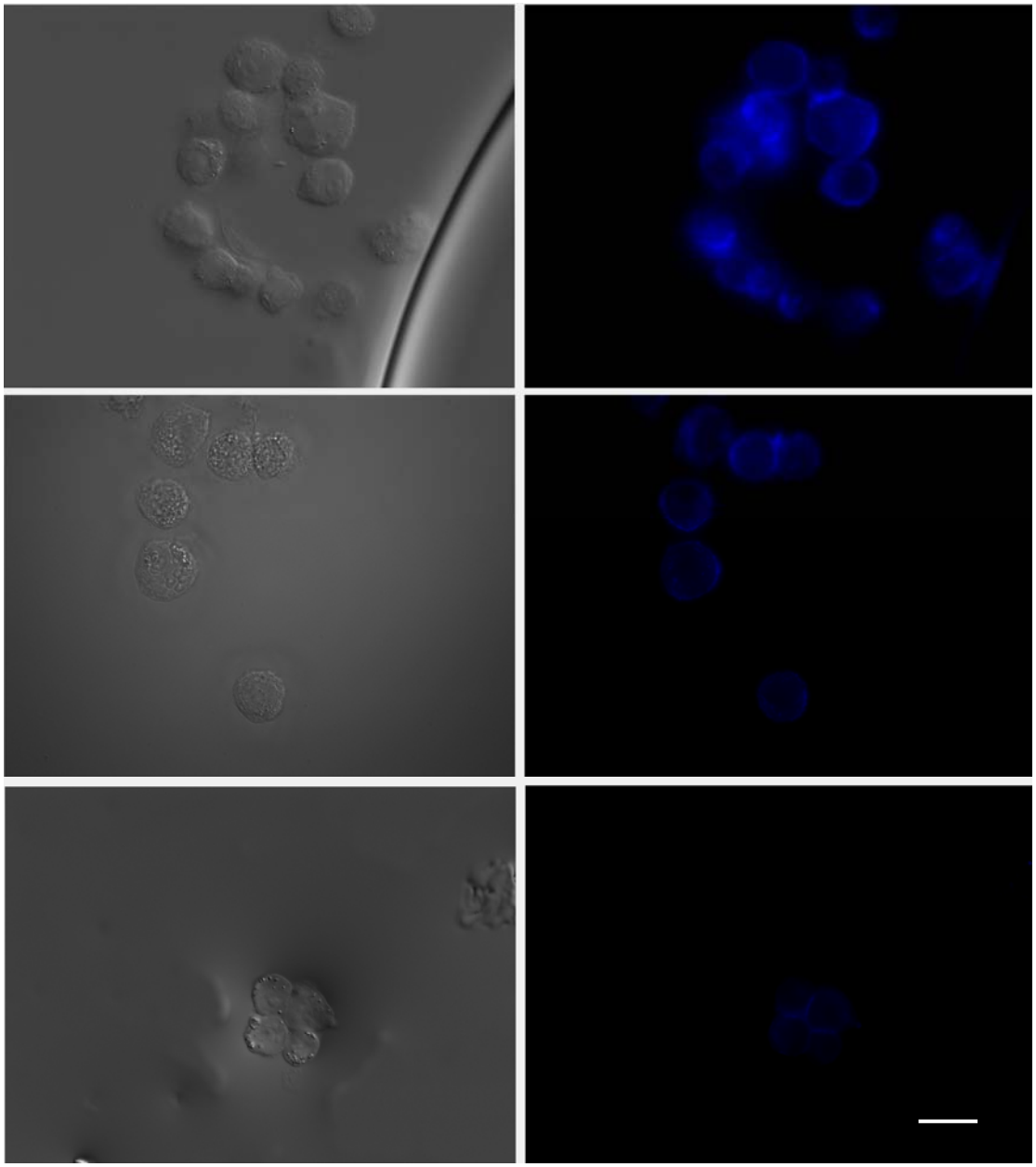

**Figure 2.18. Cholesterol content of THP-1 cells.** Filipin staining (blue) of cellular cholesterol in untreated THP-1 cells (top) and following treatment with 2.5 µg/ml simvastatin (middle) and 2.5 µg/ml simvastatin with 5 mM MßCD (bottom). Corresponding images (left) are of the same cells using differential interference contrast (DIC). Scale bar indicates 20 µm.

## 2.10 Flow Cytometry

For flow cytometry, cells were prepared as above (Section 2.4) and analysed on a Cytomics FC 500 MPL flow cytometer (Beckman Coulter). FITC and PI were detected in FL1 and FL2 channels respectively (green and red fluorescence). Preliminary

samples were used to adjust compensation settings (to ensure no cross-wavelength contamination) and optimise the protocol.

### 2.11 Microscopy

Fluorescent imaging was carried out on an Axio-imager Z1 upright microscope with a 40x EC plan neofluar lens (1.3 numerical aperture) (Zeiss, Oberkochen, Germany). An axiocam MRm camera was used to capture images with axiovision software. Immersion oil was Immersol 518 F (Zeiss).

A generic method for immunofluorescence microscopy was derived from several studies(Kelley and Schorey, 2003; Rumsey et al., 2006). Cells infected with bacteria were cytospun onto coverslips (500 rpm, 5 min), then fixed with 4% formaldehyde for 30 min. The cells were permeablised with PBS containing 0.1% Triton X-100 (10 min) and formaldehyde-induced auto-fluorescence quenched with PBS containing 1.5 mg/ml glycine. The cells were washed once more with PBS/2.5% FBS, then blocked for 1 hour at 37$^{o}$C (PBS/5% FBS) before being exposed to primary antibody (raised in rabbit, specific antibody details given in relevant sections) diluted 1:250 in PBS/2.5% FBS overnight at 4$^{o}$C. After washing twice more with PBS/0.1% Triton X-100 and once with PBS-2.5% FBS, cells were incubated with chicken anti-rabbit secondary antibody (conjugated to the red fluorophore Texas-red) diluted 1:1000 in PBS-2.5% FBS for 4 h at room temperature. A final two washes (PBS/0.1% Triton X-100) were carried out, then cell nuclei were were stained with PBS/2.5% FBS containing Hoechst (0.25 µg/ml) for 5 minutes at 37$^{o}$C. Coverslips were blotted dry and mounted onto slides with 10 µl Phenylenediamine to reduce fading and imaged. In addition to fluorescent images, differential interference contrast images

By taking slices through the cell, bacteria could be localised within cells in 3 dimensions. The fluorescent images generated from these experiments are presented in three parts. The central image (A) is in two dimensions, through the X and Y planes. The outer rectangular images (B, C) show sections through the Z axis, thus allowing discrimination between extra- and intra-cellular bacteria (Figure 2.19).

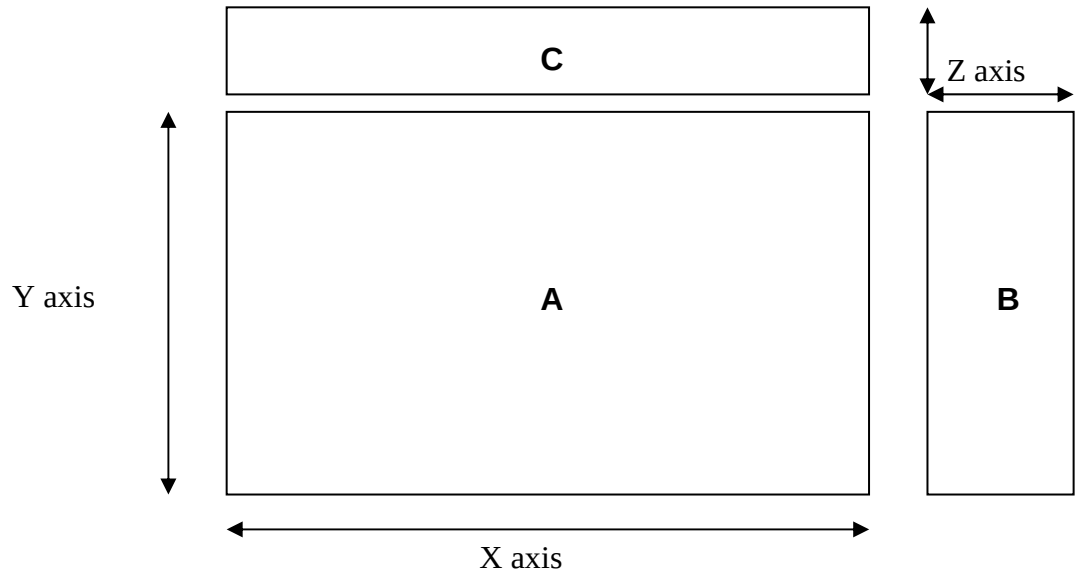


**Figure 2.19. Layout of pictures.** Schematic of image presentation. The central image (A) shows cells in 2D (X and Y axes), while the outer boxes (B, C) show slices through the cell (Z axis),

## 2.12 Chemical generation of spheroplasts forms of Map

Spheroplasts of Map strain Dominic were generated using the method of Hines and Styer (2003). Briefly, 1 million bacillary Map were suspended in 1 ml of Middlebrook 7H9 media containing 1% glycine for 96 h at 37$^{o}$C (shaking) before being resuspended in a 1 ml solution containing 7H9 broth, 0.5 M sucrose, 20 mM $MgCl_2$, 1% glycine and 30 µg/ml lysozyme. Bacteria were then incubated for a further 10 days in this solution. Untreated control bacteria were maintained for 14 days in 7H9 media.

# Chapter 3. Trafficking of Map through THP-1 monocytes

## 3.1 Introduction

Mycobacteria are masters of intracellular persistence. They have adapted many tools to survive the hostile environment inside phagocytes, even when faced with a competent immune response(Britton et al., 1994). These adaptations make mycobacteria extremely successful pathogens of animals and humans.

### 3.1.1 The phagocytic pathway

The phagocytic pathway is split into three phases, based on the phagosome's sequential interaction with endocytic organelles. Typically, a bacterium is taken up by the cell and immediately deposited into a phagosome, which fuses with early endosomes, then late endosomes, and finally lysosomes. Bacteria are destroyed by the acidic pH and hydrolytic enzymes present in the mature phagolysosome(Beron et al., 2002; Desjardins et al., 1994a; Desjardins et al., 1994b).

Early and late phagosomal compartments are differentiated by their Rab protein composition. These small GTP-binding proteins of the Rab subfamily are a series of molecular switches that control membrane traffic in eukaryotic cells. They oscillate between an inactive, soluble, GDP-bound form and an active, membrane-bound form(Bruckert et al., 2000). Rab 5a and Rab 7 are associated with the endocytic pathway of almost every cell type(Bruckert et al., 2000).

The active form of Rab 5a is acquired immediately after phagocytosis and formation of the phagosome. It works with a phosphatidylinositol 3-kinase (PI 3-kinase) to recruit early endosomal antigen 1 (EEA1) to early phagosomes. This results in the docking and fusion of further early endosomal machinery, and facilitates maturation from an early to a late phagosome(Kurosu and Katada, 2001; Vieira et al., 2002).

Rab 7 is a marker of late phagosomes. It is recruited to the phagosomal membrane where it interacts with RILP (Rab 7-interacting lysosomal protein) which then bridges phagosomes with dynein-dynactin, a motor protein associated with microtubules(Harrison et al., 2003). This complex mediates transport of the phagosome along microtubules towards the microtubule organising centre, and facilitates the construction of tubular extensions which facilitate fusion of the phagosome with late endosomes and lysosomes. Although the processes governing the functioning of late endosomal/phagosomal molecules are incompletely understood, markers such as Rab 7 are thought to facilitate the hybridisation of late phagosomal components with lysosomes. This generates the mature acidic/hydrolytic phagolysosomal compartment(Harrison et al., 2003; Vieira et al., 2002).

### 3.1.2 Mycobacterial manipulation of the phagocytic pathway

After being phagocytosed, pathogenic mycobacteria interrupt phagosome trafficking and persist in compartments that are much less acidic than normal(Anes et al., 2006; Hart et al., 1987; Malik et al., 2000). Several mechanisms are thought to contribute to a reduction in acidity in the mycobacterial phagosomal compartments. Some mycobacterial pathogens arrest phagosome maturation, and persist inside an early endosomal compartment. Disruption of proteins facilitating the transition from early to late endosomal compartments has been implicated in *M. tuberculosis* and *M. bovis* infection models(Clemens et al., 2000a; Clemens et al., 2000b; Sun et al., 2007). Despite acquisition of the lysosomal marker Lamp-1, phagosomes containing *M. avium* actively inhibit fusion of vacuoles containing cellular ATPase with its phagosomal membrane. This impairs acidification of the mature *M. avium* containing compartment(Sturgill-Koszycki et al., 1994). While growth of most mycobacteria including *M. tuberculosis* is halted by exposure to a mature phagolysosome, *M. avium* is still able to replicate even in this harsh environment. This suggests different susceptibility to the toxic phagosomal environment between species, despite similar strategies to prevent phagosome-lysosome fusion(Gomes et al., 1999).

TACO (tryptophan aspartate-containing coat protein), also known as coronin 1a (hereafter referred to as TACO), transiently associates with late endosomes under normal conditions. However there is evidence that TACO is retained on the

phagosomes of some pathogenic bacteria and mycobacteria for extended periods(Ferrari et al., 1999; Schuller et al., 2001; Zheng and Jones, 2003). This extended association is thought to contribute to the attenuated fusion of phagosomes with lysosomes by interfering with the recruitment of lysosome delivery machinery to the phagosome. Interestingly, the resident macrophages of the liver (termed Kupffer cells) lack the TACO protein and are able to rapidly process mycobacteria-containing phagosomes and facilitate fusion with lysosomal organelles(Ferrari et al., 1999).

### 3.1.3 Trafficking of Map through cells

Map inhibit phagosome maturation in murine and bovine cells. They persist and replicate in sub-epithelial macrophages in the face of a robust immune response from the host(Chacon et al., 2004; Hostetter et al., 2005; Woo et al., 2007). Despite comprehensive debate about the role of Map in human disease, there is a paucity of data concerning the fate of Map in human phagocytes(Rumsey et al., 2006).

This chapter examines the uptake and trafficking of Map by human THP-1 cells, asks whether live bacteria can arrest the phagocytic pathway and, if so, seeks to identify the compartments to which these bacteria traffic. This was investigated by determining whether intracellular compartments containing live Map exhibited reduced acidity compared with those containing dead bacteria. Map-containing compartments were also examined using antibodies to early (Rab 5a) and late (Rab 7) endosomal markers, and to the TACO protein.

## 3.2 Results

### 3.2.1 Acidity of Map-containing phagosomes

Phagosomes containing pathogenic mycobacteria are recalcitrant to fusion with lysosomes, and are less acidic than compartments that contain inactivated bacteria(Clemens and Horwitz, 1995; Woo et al., 2007). The following experiments were designed to investigate whether Map bacteria traffic to acidic phagolysosomes (the product of lysosomal fusion with a phagosome) over 48 h. To establish whether a cell wall constituent was responsible for impaired co-localisation, or whether the

inhibition of fusion is an active process, comparisons were made between live mycobacteria and cells killed with either heat or with formaldehyde which conserves the majority of the antigenicity of whole bacterial cells(Cryz et al., 1982). The acidity of bacteria-containing compartments was analysed first using neutral red, and confirmed using lysotracker red.

Percentage intracellular bacterial co-localisation with acidic areas of the cell, marked by neutral red fluorescence (Figure 3.1), was compared between live Map and formaldehyde- (4% for 1 h) and heat-killed (85$^{o}$C for 15 min) controls. 50:1 FITC-labelled bacteria were incubated with 2500K/ml cells in antibiotic free media. After 4 h incubation, the cells were washed three times with media to remove extracellular bacteria, then incubated for the remaining 44 h. Neutral red (final concentration 5µg/ml) was added for the final 2 h of incubation (Ghigo et al., 2002). Bacteria were revealed by direct immunofluorescence of FITC, and neutral red was observed using excitation and emission filters for Texas Red. The Z stack function (p32 section 2.11) was used to obtain a 3 dimensional view of the cells, allowing exclusion of extracellular bacteria from enumeration. The number of bacteria co-localising with neutral red positive compartments was enumerated by counting 50 bacteria/preparation. Significantly fewer live Map were found in acidic compartments at 48 h when compared with heat- and formaldehyde-treated Map (Figure 3.2).

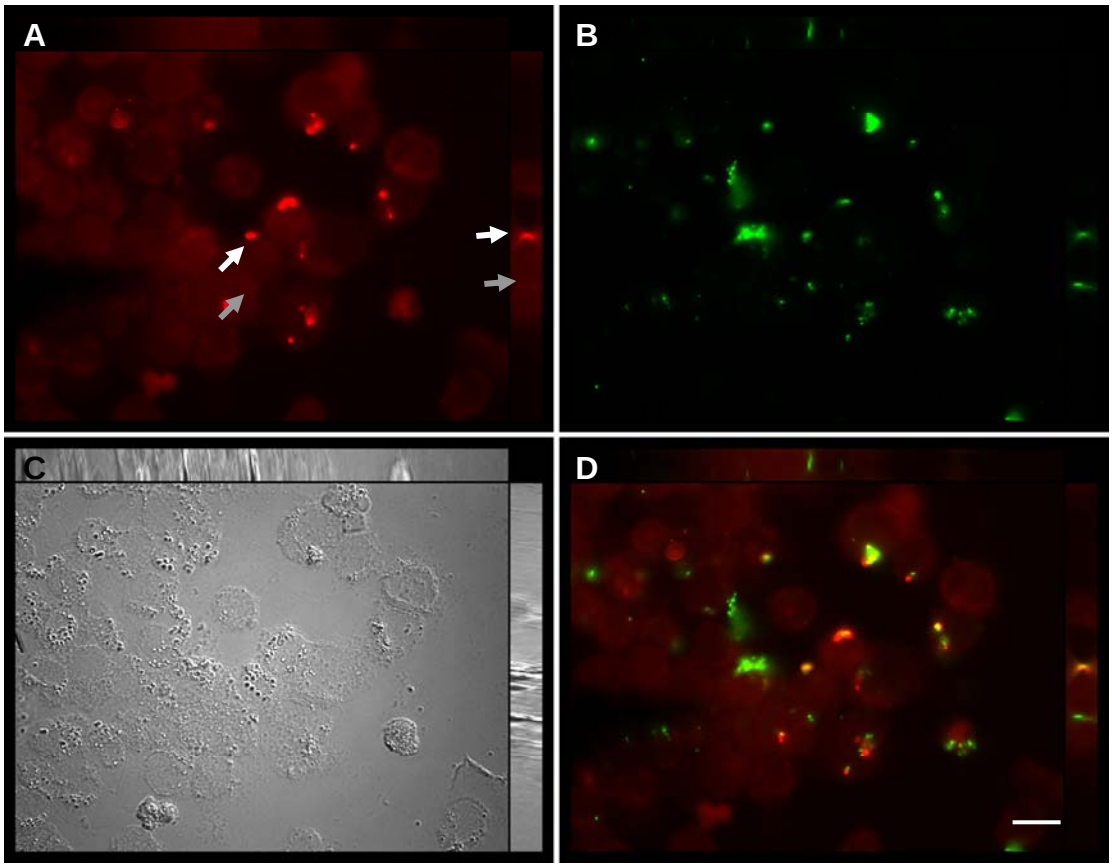


**Figure 3.1. Map and acidic compartments.** Map co-localised with neutral red stained acidic compartments inside THP-1 monocytes. The Z-stack function (top and right bars) confirmed that bacteria were intra-cellular. Images show acidic (white arrow) and non acidic (grey arrow) compartments inside the cell (A), containing FITC-labelled Map (B). A DIC image (C) fluorescent merged image (D) are also shown. Images represent three independent experiments. Scale bar indicates 20 µm.

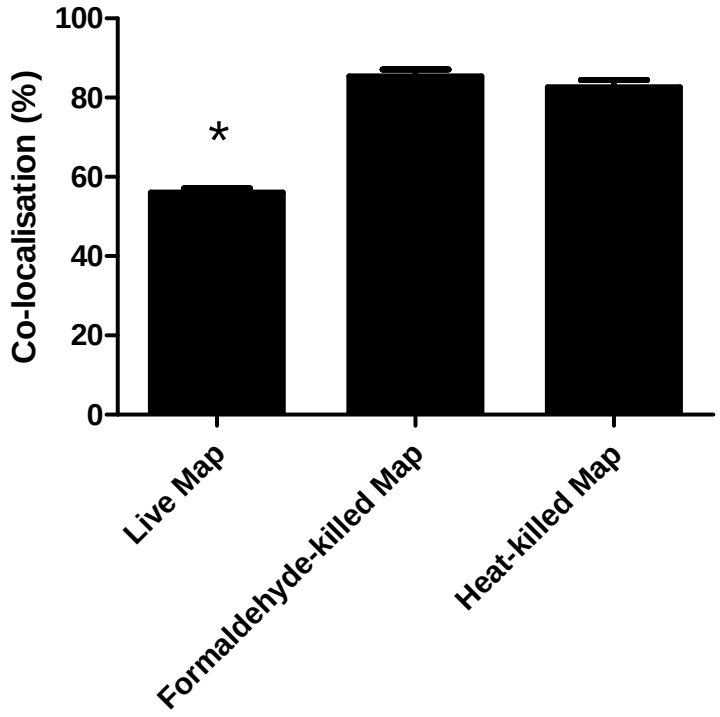


**Figure 3.2. Co-localisation of Map bacteria with neutral red staining.** Values are mean +/- SEM from three independent experiments. Live Map co-localised with significantly fewer neutral red positive vacuoles than formaldehyde or heat-killed Map (* = P<0.001, data was analysed using a one way ANOVA).

A more robust technique was used to confirm and expand on these findings. Lysotracker red is a fluorescent dye that migrates to acidic organelles. It is widely used in the literature to label lysosomes(Via et al., 1997; Zheng and Jones, 2003). Bacteria were incubated with cells as in the neutral red experiments (p 37, section 3.2.1). Lysotracker red (final concentration 500nM) was added to the media for the final 2 h of incubation. Cells were fixed with 4 % formaldehyde and visualised using fluorescence microscopy. Phagosomes were classed as strongly staining, weakly staining or not stained, all counts were verified by an independent observer.

Lysotracker red confirmed that live Map and *M. bovis* reside in compartments with reduced acidity compared with formaldehyde (Figure 3.3) and heat-treated Map (not shown). Live Map, as well as *M. bovis*, co-localised significantly less with strongly staining/acidic areas of the cell compared with formaldehyde- and heat-killed Map (Figure 3.4).

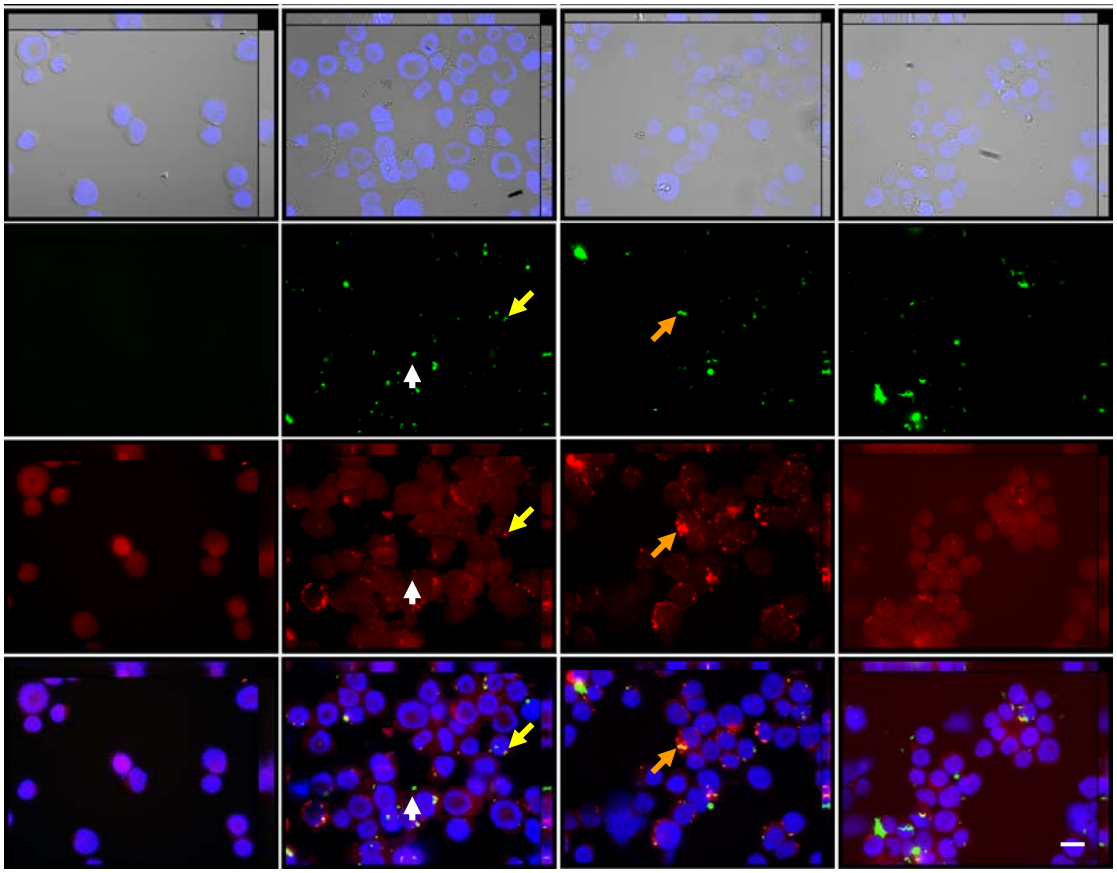

**Figure 3.3 Bacteria and lysotracker.** Bacteria and lysotracker-labelled acidic compartments at 2 h post infection. Lysotracker channel images were taken at the same exposure. Rows are (from top) nuclei (blue) and DIC images merged, bacteria (green), Lysotracker (red), and a nuclei, bacteria and lysotracker merged image. Columns are (from left) cells without bacteria, live Map, formaldehyde-killed Map, live *M. bovis*. Arrows indicate no acidity (white), weakly acidic (yellow) and strongly acidic compartments (orange). Images represent three independent experiments. Scale bar indicates 20 µm.

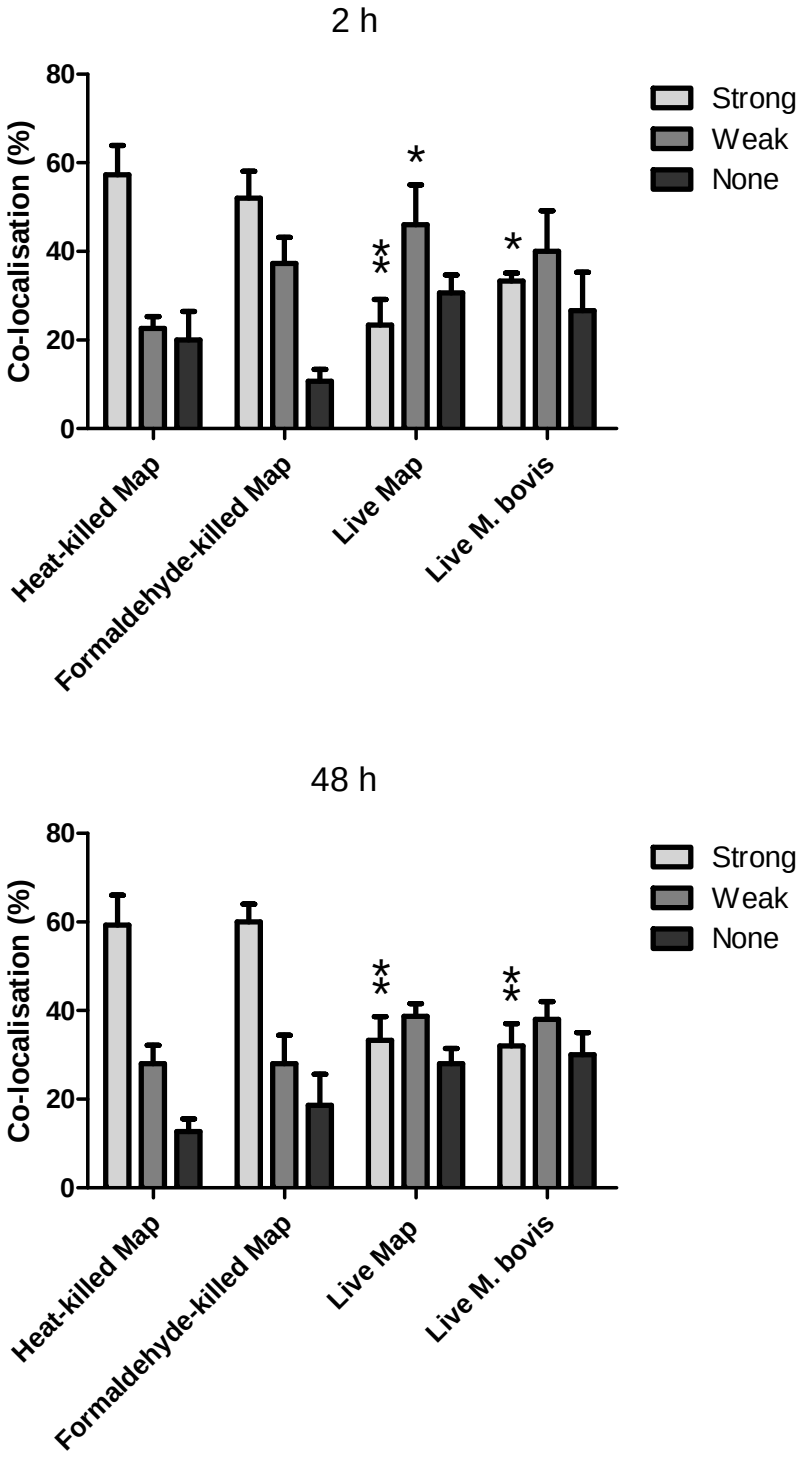


**Figure 3.4 Bacterial co-localisation with lysotracker.** Proportion of bacteria co-localising with lysotracker-labelled acidic compartments at 2 (top) and 48 h (bottom) post infection. Bacterial phagosomes were visualised by microscopy, and classed as strongly stained, weakly stained or not stained. Values are mean +/- SEM from three independent experiments. At 2 and 48 h, live Map and *M. bovis* co-localised significantly less with strongly staining acidic compartments compared with heat-killed Map. (**, $P < 0.01$; *, $P < 0.05$; data was analysed by one way ANOVA).

To further examine the acidity of Map-containing compartments, images were quantified with ImageJ software (MBF (McMaster Biophotonics Facility), National institute of Health, Bethesda, MD, USA). After subtraction of background, the fluorescence intensity for each bacterial type (live Map, *M. bovis*, formaldehyde-killed Map and heat-killed Map) was calculated for 10 fields containing at least 20 bacteria each. Fluorescence intensity data was averaged and compared (Figure 3.5).

These experiments showed that at 2 h post infection, live Map and *M. bovis* resided in compartments with reduced acidity compared with formaldehyde-treated Map. Unexpectedly, heat killed Map compartments also showed reduced acidity compared with formaldehyde-killed Map. This difference was significant. This could be due to membrane compromised bacteria 'leaking' cytoplasmic contents into the lumen of the phagosome, resulting in a temporary decrease in acidity. At 48 h, no difference was seen between heat- and formaldehyde-killed Map, or interestingly, *M. bovis* containing phagosomes. However Map containing compartments showed reduced acidity. This difference was not significant. Why *M. bovis* compartments did not show reduced acidity compared with killed bacteria at 48 h is still unclear. This data supports the neutral red and lysotracker results for live Map, and further suggests that a component secreted from bacteria may affect phagosomal acidity.

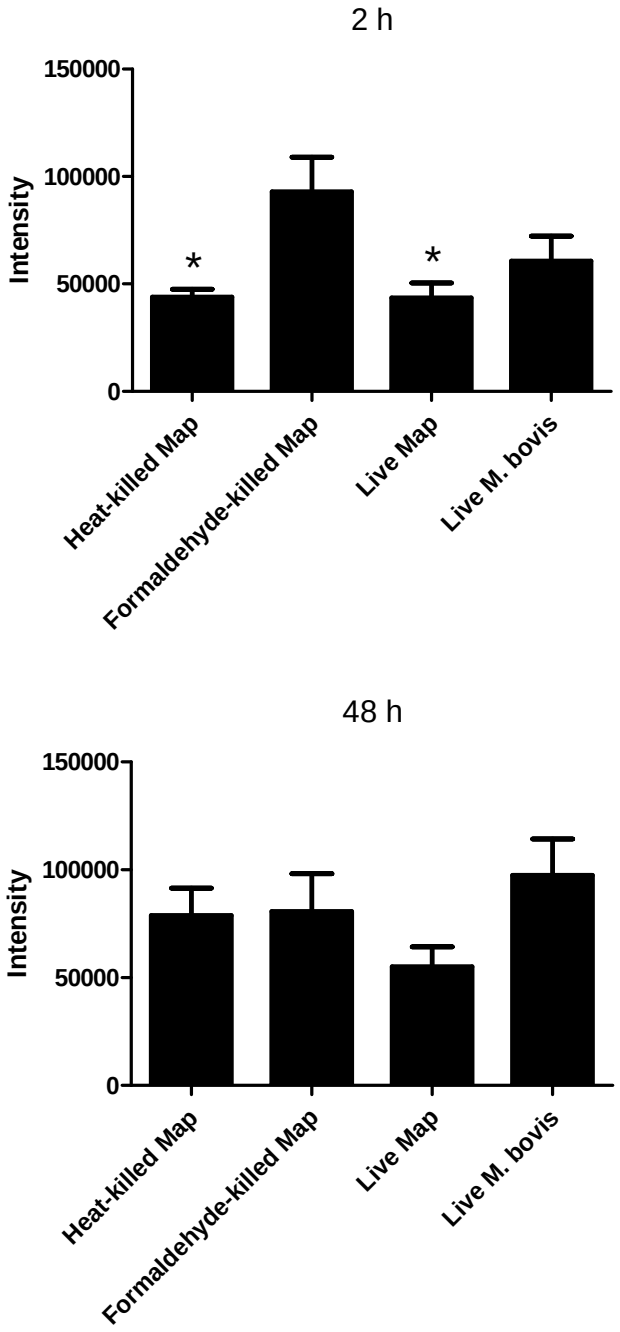


**Figure 3.5. Lysotracker fluorescence intensity of bacterial phagosomes.** Lysotracker fluorescence of bacterial phagosomes at 2 (top) and 48 h (bottom) post infection. Ten separate fields (each containing at least 20 bacterial phagosomes) were analysed per bacterium. Average lysotracker fluorescence was calculated using ImageJ software. At 2 h, heat-killed and live Map containing compartments showed significantly reduced acidity compared with formaldehyde-killed Map containing compartments. *M. bovis* intensity was also reduced, although this difference was not significant. At 48 h, the intensity of Live Map phagosomes was observably lower compared with heat and formaldehyde-killed bacteria, and also *M. bovis*. However this difference was not significant. Values are mean +/- SEM (* = $P < 0.05$, data was analysed by one way ANOVA).

### 3.2.2 Using endosomal markers to characterise Map-containing phagosomes

Antibodies against Rab 5a (found on early endosomal compartments) and Rab 7 (found on late endosomal compartments) were used to label Map-containing phagosomes, to determine bacterial progression through the phagocytic pathway. Bacteria (MOI 50:1) were pulsed for 1 h and chased for 2 h, or pulsed for 4 h and chased for 48 h as described previously (p. 33, section 2.11). Briefly, the cells were then mounted on coverslips, fixed, and stained with anti-Rab 5a antibody (Santa-Cruz Biotechnology, Heidelberg, Germany), diluted 1:250. After washing, bound antibody was detected with a secondary antibody conjugated to Texas-red, diluted 1:1000. Live and formaldehyde-killed Map were compared with live *M. bovis*, as well as heat-killed *E. coli* BL21.

There was no evidence of mycobacterial co-localisation with Rab 5a at either time point (Figure 3.6). Diffuse staining of what appeared to be small vacuoles was seen, but no punctate Rab 5a, as reported elsewhere in *M. avium* infected macrophages(Kelley and Schorey, 2003). Few intact heat-killed *E. coli* were visualised inside the cells at 48 h, indicating that trafficking and destruction were most likely complete by this time (Root et al., 1972).

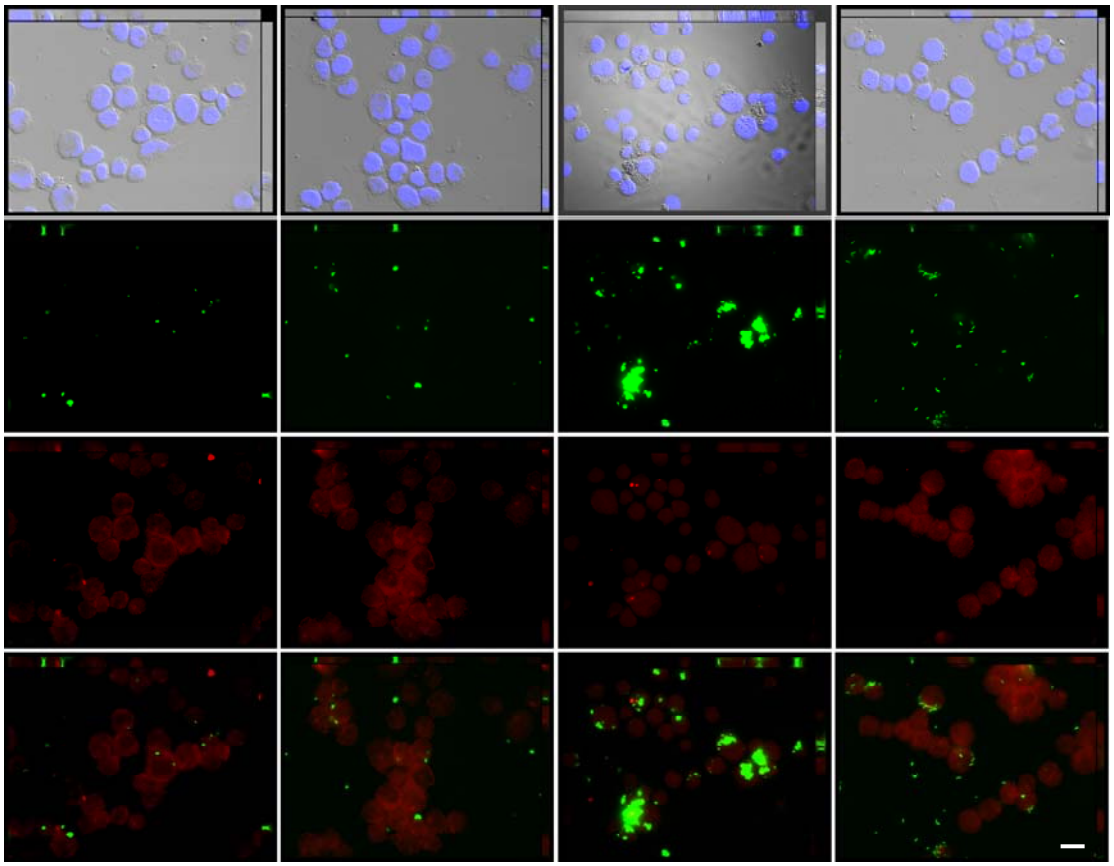

**Figure 3.6. Bacteria and Rab 5a.** Representative images of bacteria and the early endosomal marker Rab 5a inside THP-1 monocytes at 2 h post infection. Rab 5a did not co-localise with any of the bacteria investigated, at any time point. Columns are (from left) live Map, formaldehyde-killed Map, *M. bovis*, heat killed *E. coli* BL21. Rows are (from top) nuclei (blue) and DIC images merged, bacteria (green), Rab 5a (red), and nuclei, bacteria and Rab 5a merged image. Images represent three independent experiments. Scale bar indicates 20 µm.

To investigate whether the failure to visualise bacteria in Rab 5a-containing compartments was related to Rab 5a disappearance from the THP-1 cell phagosomes by the 2 h time point or simply an inability to visualise Rab 5a, heat-killed *E. coli* containing phagosomes were analysed immediately after phagocytosis, when Rab 5a recruitment and activity is reportedly maximal (Kitano et al., 2008). THP-1 cells were exposed to heat-killed *E. coli* (MOI 50:1) for 15 mins only before being washed, fixed, stained and imaged as described above (p43, section 3.2.2). However, no Rab 5a co-localisation with heat-killed *E. coli* was observed. Different concentrations of primary anti-Rab 5a antibody (1:200, 1:100) were used in an attempt to increase sensitivity, with no success.

Bacterial co-localisation with Rab 7 was visualised using an anti-Rab 7 antibody (Santa-Cruz Biotechnology) and the same labelling conditions as for Rab 5a. Rates of Rab 7 co-localisation were compared to pathogenic *M. bovis*, as well as heat-killed *E. coli* BL21.

These experiments indicated that the majority of live Map-containing phagosomes had acquired Rab 7 by 2 h post infection. This was not significantly different from *M. bovis*, formaldehyde- or heat-killed Map or *E. coli* strain BL21. At 48 h, the majority of *M. bovis*, live Map and formaldehyde killed-Map resided in Rab 7 positive compartments (Figure 3.8, 3.7). In contrast, few heat-killed *E. coli* were visualised at 48 h post infection.

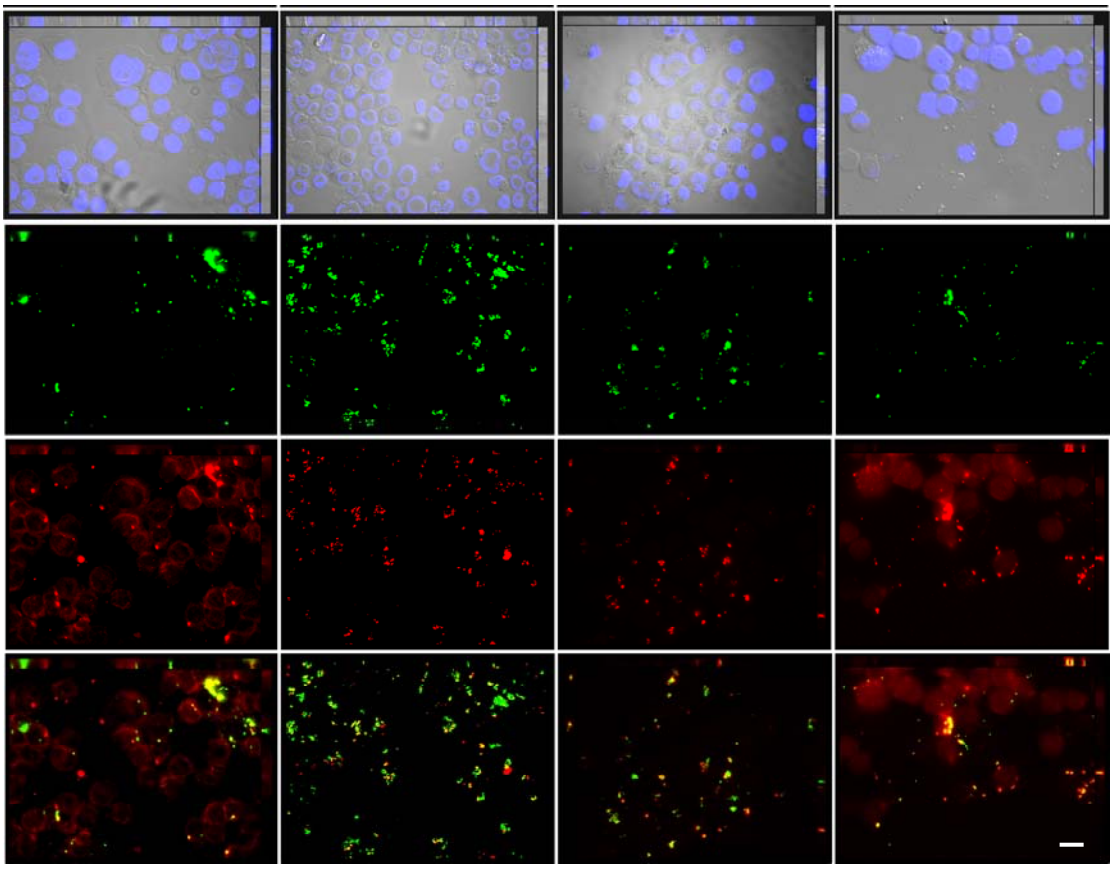

**Figure 3.7. Bacteria and Rab 7.** Representative image of Map bacteria co-localising with the late endosomal marker Rab 7 inside THP-1 monocytes at 2 h post infection. Columns are (from left) live Map, formaldehyde-killed Map, *M. bovis*, heat killed *E. coli* BL21. Rows are (from top) nuclei (blue) and DIC images merged, bacteria (green), Rab 7 (red), and nuclei, bacteria and Rab 7 merged image. Images represent three independent experiments. Scale bar indicates 20 μm.

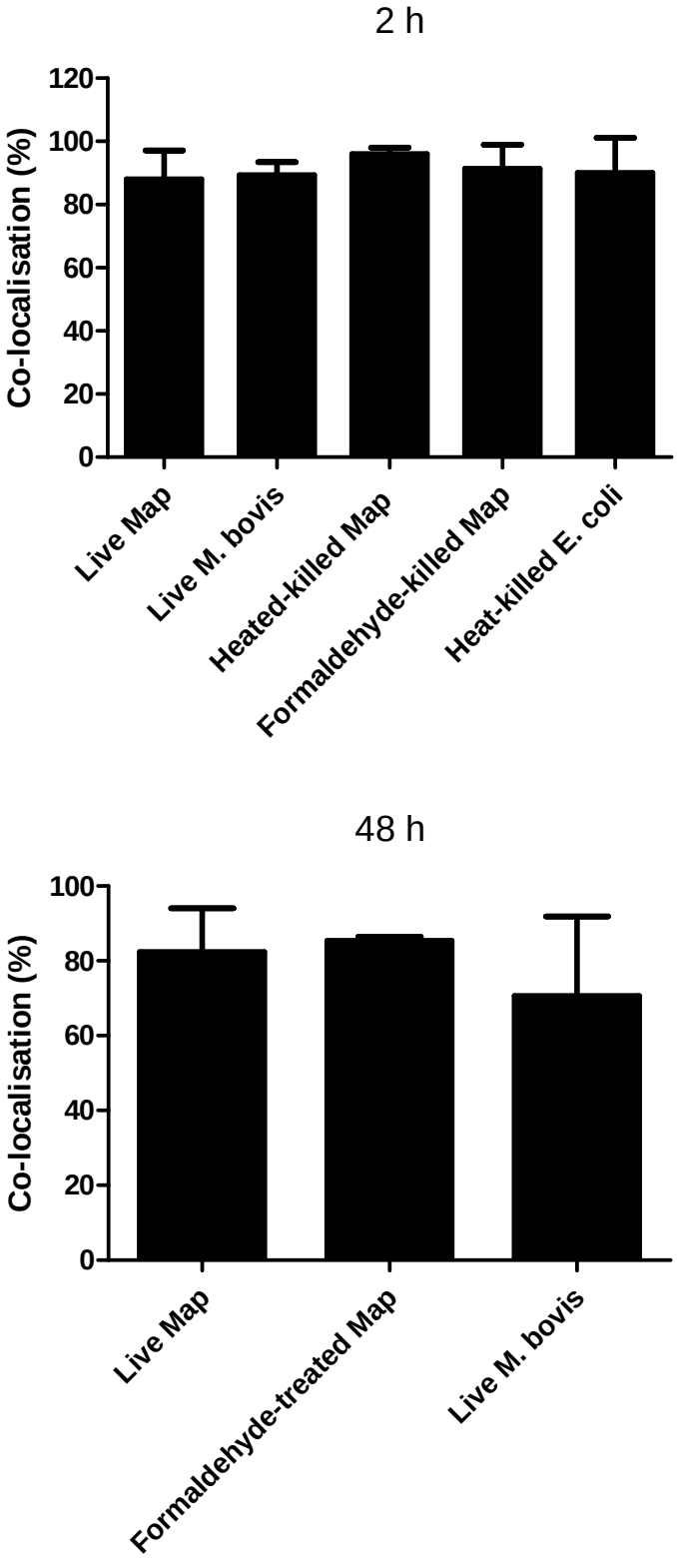


**Figure 3.8. Co-localisation of bacteria with Rab 7.** These graphs indicate bacterial containing phagosomes exhibit co-localisation with Rab 7 at 2 h (top) and 48 h (bottom) post infection. Values are mean +/- SEM from three independent experiments. No significant difference was found between bacteria at either time. (Data was analysed using a one-way ANOVA).

### 3.2.3 TACO (Coronin-1a)

To examine whether Map bacteria co-localised with the TACO protein at 2 and 48 h, cells were prepared and exposed to bacteria as for Rab 5a, then stained with anti-TACO antibody raised in rabbit (Bethyl Laboratories, Murarrie, Queensland, Australia) diluted 1:250. Cells were washed, then bound antibody was probed using a secondary antibody conjugated with a red fluorophore as described above (p43, section 3.2.2). These experiments showed little TACO localisation with bacterial phagosomes at 2 h post infection. However, at 48 h post infection, approximately 40% of both *M. bovis* and Map containing compartments showed evidence of TACO. No association was seen with phagosomes containing heat killed *E. coli* BL21 at 2 h (Figure 3.9, 3.10).

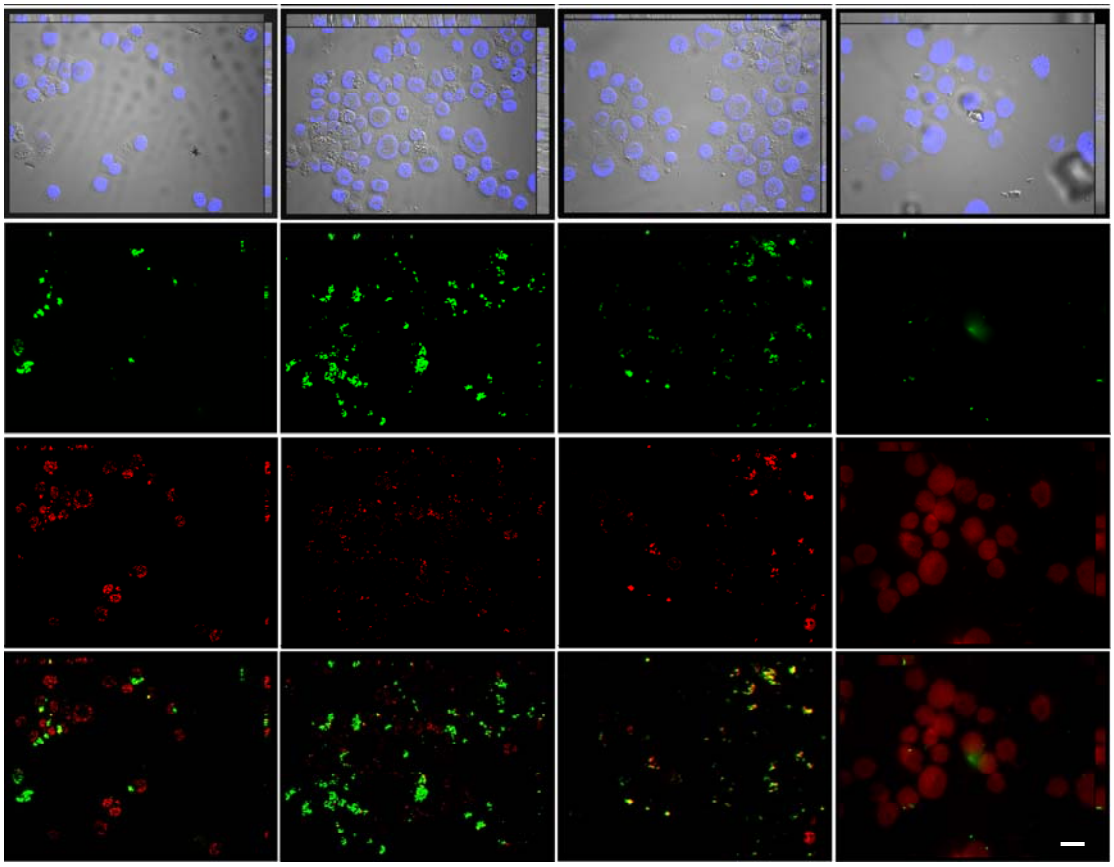

**Figure 3.9. Bacteria and the TACO protein.** Representative picture of bacteria and TACO inside THP-1 monocytes at 48 h post infection. Columns are (from left) live Map, formaldehyde-killed Map, *M. bovis*, heat killed *E. coli* BL21. Rows are (from top) nuclei (blue) and DIC images merged, bacteria (green), TACO (red), and a nuclei, bacteria and TACO merged image. Images represent three independent experiments. Scale bar indicates 20 µm.

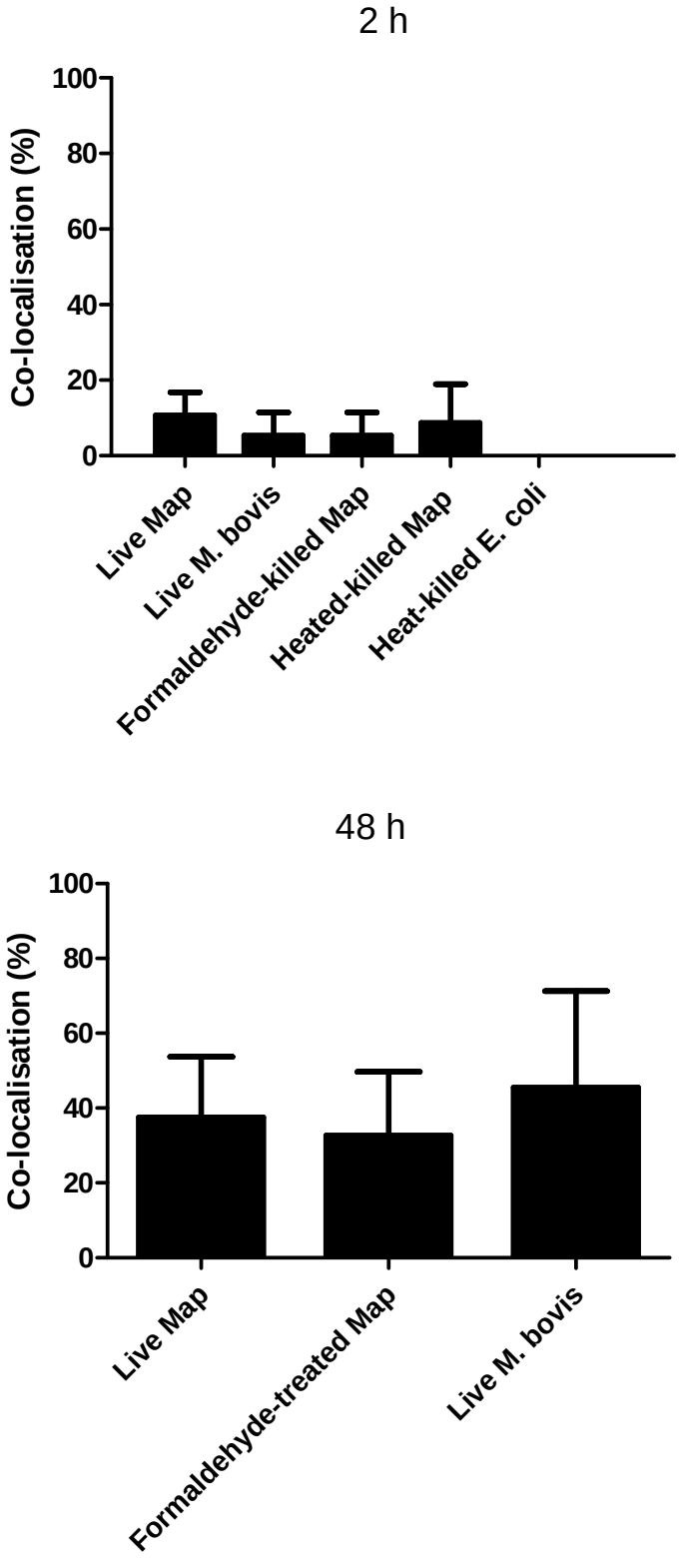


**Figure 3.10. Co-localisation of bacteria with TACO.** These graphs indicate bacterial containing phagosomes exhibiting co-localisation with TACO at 2 h (top) and 48 h (bottom) post infection. Values are mean +/- SEM from three independent experiments. No TACO staining was seen at 2 h. No significant difference was found between other bacteria at either time. (Data was analysed using a one way ANOVA)

## 3.3 Discussion

Despite the isolation of Map in tissue and blood from CD patients (Abubakar et al., 2008), there have to date been few studies of Map trafficking and persistence in human derived cells. Results presented in this chapter show that live Map phagocytosed by THP-1 human monocytes reside in compartments that exhibit reduced acidity when compared with compartments containing formaldehyde- or heat-killed bacteria. This observation suggests the presence of cell wall antigens alone is insufficient to interrupt phagosome trafficking and that Map disruption of acidification of the phagosome is most likely an active process. The observation that heat-killed (and membrane compromised) Map show reduced lysotracker intensity at 2 h post infection indicates this may be due to a secreted component.

Manipulation of the phagocytic pathway and persistence in compartments recalcitrant to fusion with lysosomes is well characterised in *M. tuberculosis*, *M. leprae* and *M. bovis* infection of human cells(Anes et al., 2006; Hart et al., 1987; Sun et al., 2007). There is also evidence of altered trafficking of live Map in peripheral polymorphonuclear cells (PMNCs) isolated from patients with CD, ulcerative colitis (an inflammatory bowel condition similar to CD) and healthy individuals(Rumsey et al., 2006). The observation that Map survival in PMNCs from CD and healthy patients is comparable to that of *M. tuberculosis*(Rumsey et al., 2006). Collectively, these findings support the results presented here, which suggest that live Map has the ability to manipulate the phagocytic pathway in human phagocytic cells in the same way as it does in murine and bovine infection(Woo et al., 2007).

In this study, the use of 3Dimensional microscopy proved to be invaluable in distinguishing extra-cellular bacteria from those inside cells. Normally, antibiotic protection assays are used, where extra-cellular bacteria are killed before enumeration of intra-cellular bacteria (by plate counts) following cell lysis. However, this technique was not ideal as, like all mycobacteria, Map are extremely slow growing. By staining the plasma membrane and using 3D microscopy, intra-cellular bacteria could be clearly identified and counted. Furthermore, compared to conventional microscopy, 3D microscopy reduces the chance of false positives as a

result of bacteria being cytospun (technique to spin non-adherent cells onto a coverslip surface for staining and viewing under a microscope) onto the cell surface.

The failure to detect Rab 5a co-localisation with bacterial phagosomes at any time point was unexpected, given the punctate staining around bacterial phagosomes described by Kelley and Schorey (2003). The diffuse staining that was observed suggested a number of possibilities. Expression levels of Rab 5a in THP-1 monocytes may be too low for accurate visualisation using this technique. Other possibilities are that the antibody was impaired and unable to bind to Rab 5a, or that the majority of Rab 5a was already removed from the phagosomal membrane at the time of staining. However, *E. coli* treated THP-1 cells stained immediately after phagocytosis (15 min) showed no evidence of bacterial co-localisation as reported elsewhere (Perskvist et al., 2002). *M. avium* reportedly resides in a Rab 5a-containing compartment (Kelley and Schorey, 2003), and was analysed as an additional control. However, no Rab 5a staining was seen. Collectively, these results suggest that the immuno-labeling technique used here lacked the sensitivity to detect of Rab 5a in THP-1 cells. There is not enough evidence to class the lack of Rab 5a on phagosomal membranes as a true negative.

In marked contrast to Rab 5a, Rab 7 co-localisation was seen with live, formaldehyde- and heat-killed Map in THP-1 monocytes. Likewise, live *M. bovis* were also observed in compartments which stained strongly for Rab 7 at 48 h post infection. Rab 7 is a crucial molecule for the survival of mycobacteria in host cells; both *M. tuberculosis* and *M. bovis*-containing phagosomes display strong Rab 7 staining(Clemens et al., 2000b; Sun et al., 2007). In macrophages, live *M. bovis* secretes a protein that inactivates Rab 7, rendering it unable to interact with the Rab 7-interacting lysosomal protein (RILP). As a result, the inactive, GDP-bound form of Rab 7 predominates in cells infected with live *M. bovis* whereas, conversely, the majority of Rab 7 in cells containing killed *M. bovis* is in the active GTP-bound form. Intriguingly, live *Salmonella typhimurium* also secretes a factor that interferes with Rab 7 signalling via impaired association with RILP, leading to significantly reduced lysosomal fusion(Catron et al., 2004). The failure of *M. bovis* containing phagosomes to acquire RILP arrests phagosome trafficking and impairs fusion with lysosomes(Sun et al., 2007). This suggests that Rab 7 is a key player in the manipulation of cells by *M. bovis* and *S. typhimurium*. The antibody mediated visualisation used in these

assays does not allow the characterisation of Rab 7 into the active/inactive form. However, given the attenuated acidification of live Map phagosomes in THP-1 monocytes, live Map bacteria may use a similar system to reduce acidification of their phagosomes. A role for Rab 7 inactivation in Map infection is currently under investigation by the helicobacter research lab.

The role of the TACO protein in the persistence of some pathogenic mycobacteria has been shown in several studies(Gatfield and Pieters, 2000; Kaul, 2008; Kaul et al., 2004). However, to date, the association of Map bacteria with the TACO protein has not been investigated. In this study, Map (live and formaldehyde-killed)-containing phagosomes showed evidence of TACO staining at 48 h post infection. *M. bovis*-treated cells displayed similar staining. It is unclear whether this association is specific to these mycobacteria in THP-1 monocytes as the majority of heat-killed *E. coli* had been processed at this time point. However the involvement of the TACO protein with related mycobacteria makes this likely.

Chemically-mediated down-regulation of the TACO gene transcription in THP-1 monocyte-derived macrophages significantly reduces both the uptake and survival of *M. tuberculosis* (Anand and Kaul, 2005) whereas live *M. bovis* actively retains the TACO protein on its phagosomal membrane by secreting a coronin-interacting protein (CIP). This protein is also expressed by *M. tuberculosis*, but not the non-pathogenic *M. smegmatis*(Deghmane et al., 2007). When the interaction between CIP and TACO is reduced (after treatment with interferon gamma), increased phagolysosome fusion of BCG-containing compartments is observed(Deghmane et al., 2007). In the present study, phagosomes containing formaldehyde-killed Map phagosomes also exhibited TACO protein staining, suggesting that cell wall constituents may play a role in the retention of TACO in THP-1 cells.

The role of TACO is currently a subject of debate in the literature(Schuller et al., 2001), with some contending that TACO is a crucial mediator of intracellular mycobacterial survival(Jayachandran et al., 2008; Jayachandran et al., 2007; Kaul, 2008). TACO typically associates only transiently with the maturing phagosome.

However, in mycobacterial infection, it can remain associated with the phagosome in a cholesterol-dependent manner, leading to reduced fusion of the compartment with lysosomes(Deghmane et al., 2007). In light of this and other recent studies that reveal a role for cholesterol in the inactivation of Rab 7 in other cell systems(Deghmane et al., 2007; Huynh et al., 2008), further experiments were designed to explore the role of cholesterol in Map infection (Chapter 4).

# Chapter 4. Cholesterol involvement in Map uptake and fate

## 4.1 Introduction

Cholesterol is ubiquitous in the mammalian cell; it is found in the plasma membrane and intracellular membranes, which are enriched to varying degrees (Soccio and Breslow, 2004). Cholesterol is an essential constituent of these membranes, affecting a wide variety of processes such as receptor-mediated signalling, ion flow and enzymatic activity (Gimpl et al., 1997).

Cholesterol has been implicated in the uptake of several pathogenic bacteria and mycobacteria into host cells. Moreover, uptake via cholesterol-dependent pathways, and recruitment of excess cholesterol to the phagosomal membrane, is hypothesised to enhance survival and persistence of some bacterial (*B. pertussis* and *S. enterica*) and mycobacterial pathogens (*M. avium, M. tuberculosis, M. bovis*) inside the cell (Gatfield and Pieters, 2000; Goluszko and Nowicki, 2005; Peyron et al., 2000; Rosenberger et al., 2000). In contrast, depletion of cellular cholesterol results in decreased viability for bacteria such as *Salmonella typhimurium* and *M. tuberculosis* (Catron et al., 2004; Lamberti et al., 2008; Pandey and Sassetti, 2008).

Bacteria taken up in this way persist in compartments recalcitrant to fusion with lysosomes. One hypothesis is that by entering at cholesterol-rich areas of the cell, microbes are transferred directly into the endocytic rather than phagocytic pathway of cells (Naroeni and Porte, 2002; Rodriguez et al., 2001). The TACO protein interacts only briefly with late endosomes under normal conditions but it is retained on the phagosomes of some pathogenic bacteria and mycobacteria for extended periods (Ferrari et al., 1999; Zheng and Jones, 2003). This extended association is thought to contribute to the attenuated fusion of phagosomes with lysosomes by interfering with the recruitment of lysosome delivery machinery to the phagosome. In *M. bovis*-infected cells, retention of the TACO protein on phagosomes depends on cholesterol (Gatfield and Pieters, 2000). In addition, a recent study demonstrated

that cholesterol-rich compartments inside the cell are intrinsically less likely to fuse with lysosomes (Huynh et al., 2008).

Despite involvement in several bacteria and mycobacterial infections, the role of cholesterol in Map infection has yet to be elucidated. The aim of this chapter was to determine whether the uptake and persistence of Map bacteria in THP-1 monocytic cells is mediated by cholesterol. The role of cholesterol in uptake of Map was investigated using depletion and co-localisation techniques while the association of Map with membrane-bound cellular cholesterol was explored using microscopy. In addition, the effect of cholesterol depletion on Map persistence was analysed by enumeration of viable bacteria following long term co-culture.

## 4.2 Results

### 4.2.1 Map uptake by THP-1 monocytes and cholesterol

Flow cytometry was used to quantify the association and uptake of FITC-labelled bacteria into THP-1 cells. First, a decreasing gradient of cholesterol in the cells was created by pre-treatment with simvastatin (2.5 µg/ml) and MβCD (2 and 5 mM) for 48 and 1 h, respectively (p23, section 2.5). Bacteria were added and the combined culture of bacteria, cells, simvastatin and MβCD were incubated for 4 h at 37$^{o}$C (5% $CO_2$) The cells were then centrifuged (1400 rpm for 5 min) to remove media and non-adherent bacteria, before being resuspended in 1 ml of PBS containing 5% FBS and 5 µg/ml PI, then analysed by flow cytometry (p 21, section 2.4). Each sample was run twice, with trypan blue (final concentration 0.25%) added between runs to quench extra-cellular bacterial fluorescence (Wooldridge et al., 1996). This gave values for total associated, as well as internalised bacteria. Non-adherent bacteria and dead cells (PI positive) were removed from analysis using size segregation and isolation (gating) of the live monocyte smear, respectively (Figure 2.9).

Two species of bacteria were used as controls to prove this approach could accurately visualise differences between cholesterol-dependent and independent uptake. *M. bovis*, a mycobacterial relative of Map, enters macrophage cells via a cholesterol-dependent pathway (Gatfield and Pieters, 2000) and was used as a positive control whereas *E. coli* strain BL21, which is internalised into macrophages

via a cholesterol-independent mechanism (Gatfield and Pieters, 2000), provided a negative control.

The control experiments showed that both the association and internalisation of FITC-labelled *M. bovis* decreased with decreasing cellular cholesterol over a 4 h period. This decrease was significant at the lowest concentration of cholesterol (Figure 4.1). In contrast, *E. coli* uptake was not significantly affected by lowered cholesterol. However, total association of *E. coli* was significantly decreased in the MβCD treatments (2 and 5 mM). This was most likely due to general anti-adherence effects, resulting from the removal of cholesterol from the plasma membrane (Figure 4.2).

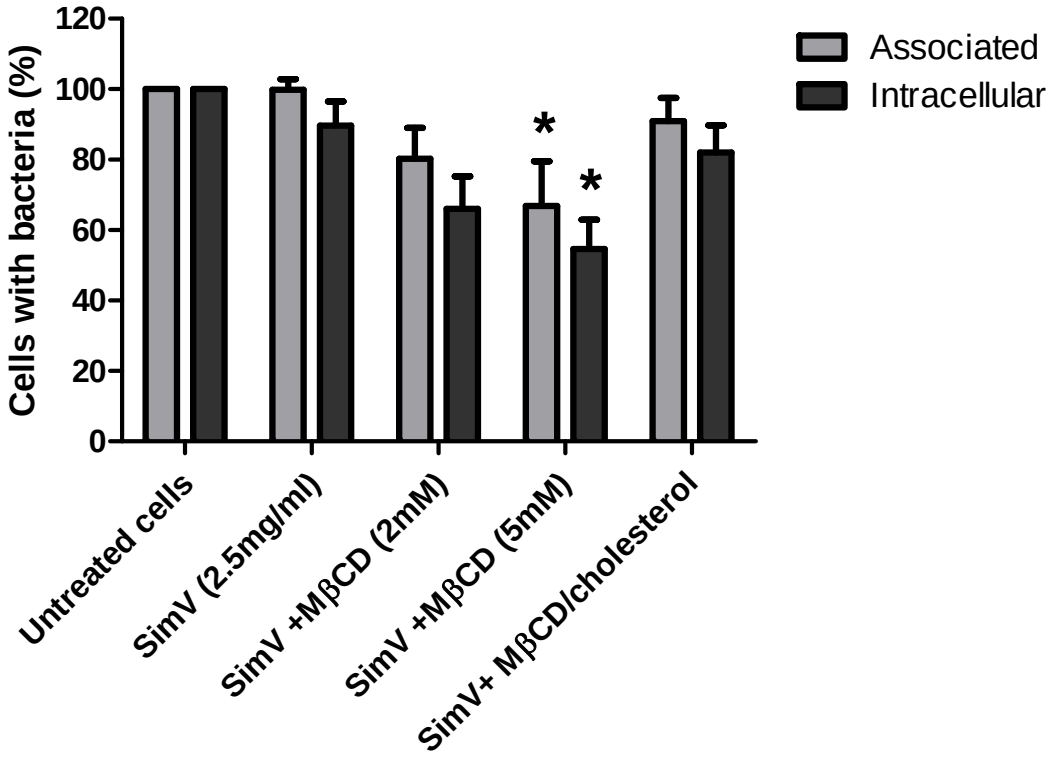


**Figure 4.1. Association and internalisation of *M. bovis* into THP-1 monocytes over 4 h along a negative cholesterol gradient.** Results show bacteria associated/internalised for each treatment as a percentage of control treatment. Values are mean +/- SEM of three independent experiments. (Data was analysed by one way ANOVA. * indicates $P < 0.05$).

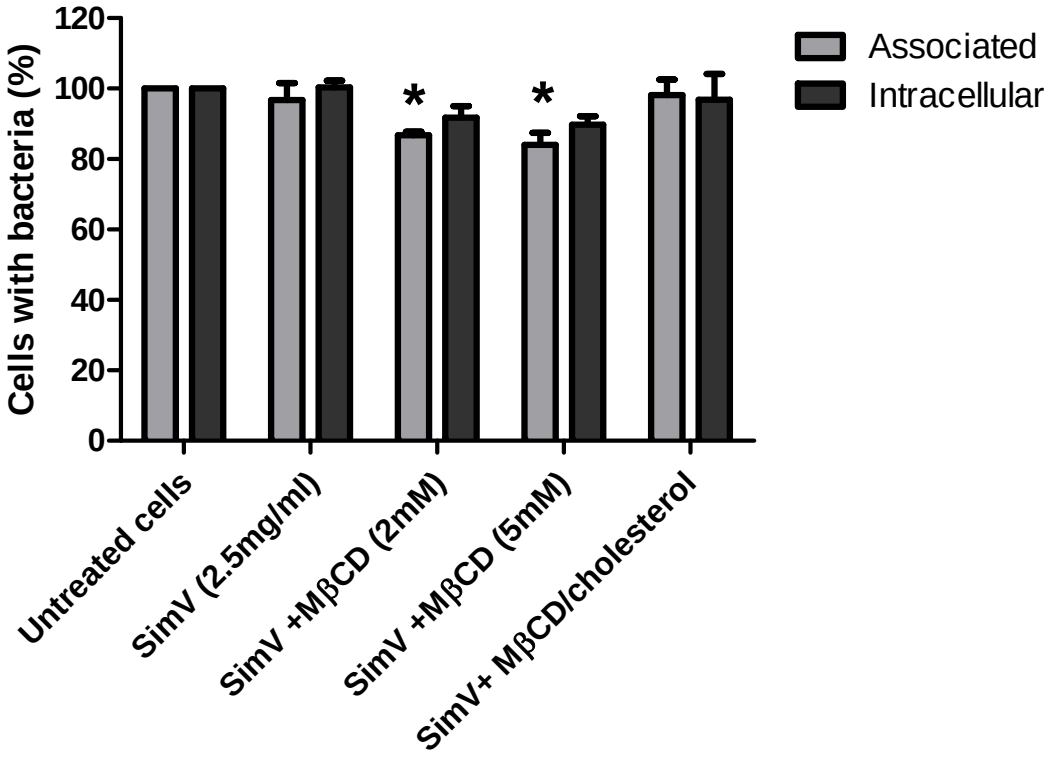


**Figure 4.2. Association and internalisation of *E. coli* into THP-1 monocytes over 4 h along a negative cholesterol gradient.** Results show bacteria associated/internalised for each treatment as a percentage of control treatment. Values are mean +/- SEM of three independent experiments. (Data was analysed by one way ANOVA. * indicates $P < 0.05$).

While decreasing cellular cholesterol caused little or no changes in the association and internalisation of *E. coli*, the uptake of living Map into THP-1 monocytes was significantly reduced by cholesterol depletion with simvastatin and MβCD (Figure 4.3). Moreover, re-addition of cholesterol restored Map uptake and association. Similar results were obtained with formaldehyde-killed Map, with cholesterol depletion again causing decreased association and uptake (Figure 4.4). Thus, Map are taken up into THP-1 monocytes via a cholesterol-dependent mechanism.

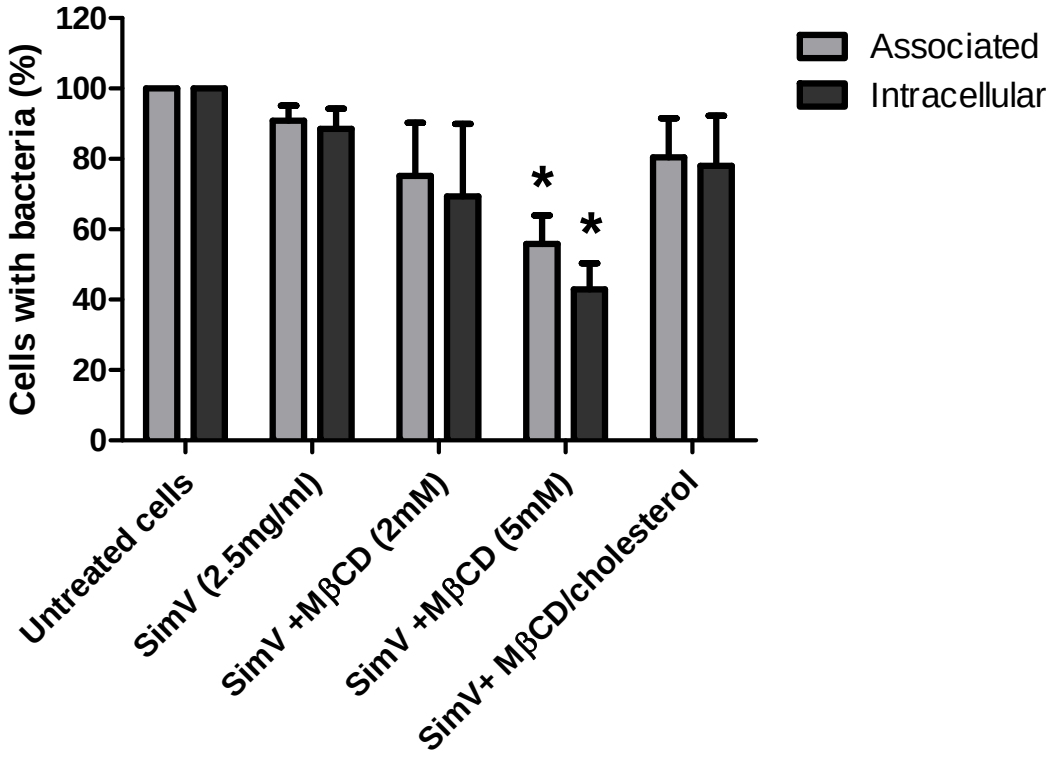


**Figure 4.3. Association and internalisation of live FITC-labelled Map into THP-1 monocytes over 4 h along a negative cholesterol gradient.** Results show bacteria associated/internalised for each treatment as a percentage of control treatment. Values are mean +/- SEM of three independent experiments. (Data was analysed by one way ANOVA. * indicates $P < 0.05$).

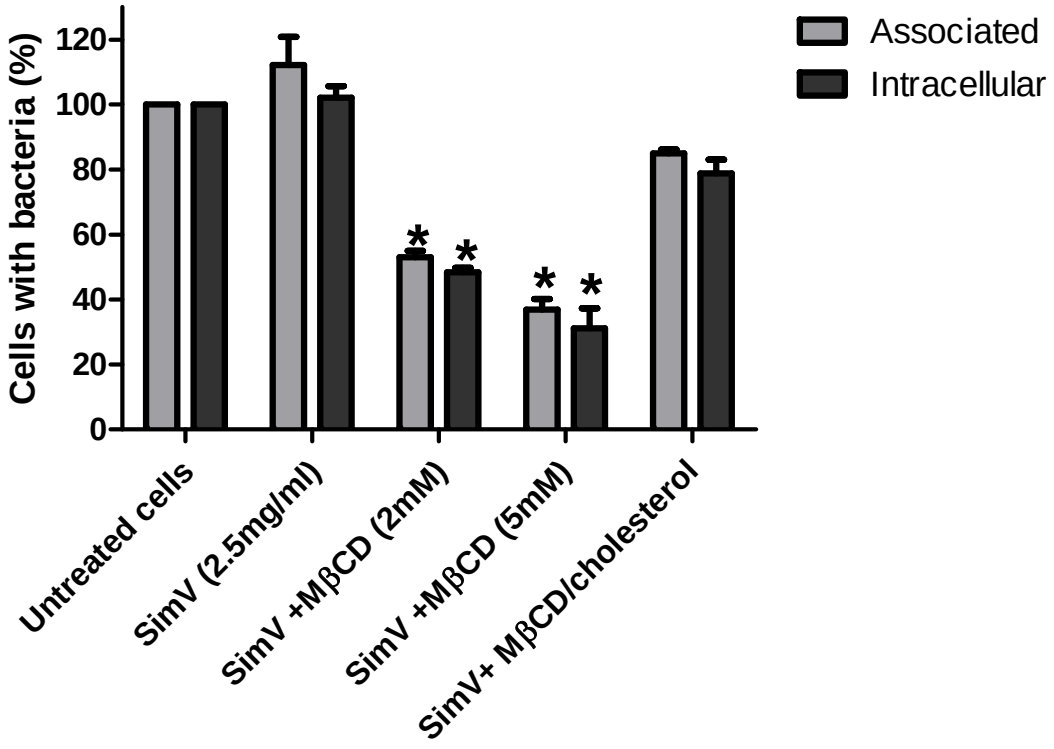


**Figure 4.4. Association and internalisation of formaldehyde-killed, FITC-labelled Map into THP-1 monocytes over 4 h along a negative cholesterol gradient.** Results show bacteria associated/internalised for each treatment as a percentage of control treatment. Values are mean +/- SEM of three independent experiments. (Data was analysed by one way ANOVA. * indicates $P < 0.05$).

Fluorescence microscopy was used to extend these observations. FITC-labelled bacteria were incubated for 4 h with THP-1 cells, which were then fixed. Cell membrane cholesterol was labelled with the fluorophore filipin, as described previously (p 30, section 2.9). Additionally, the actin cytoskeleton of the cells was labelled with Texas-red phalloidin (Molecular Probes, Invitrogen). This fluorescently-tagged actin-binding peptide allowed visualisation of actin polymerisation associated with the entry of bacteria into cells. In these experiments, it was used as a marker of bacterial internalisation (Ibrahim-Granet et al., 2003).

These experiments showed cholesterol aggregation at the site of the majority of *M. bovis* entering THP-1 (Figure 4.5). In contrast, although actin polymerisation was observed, there was little evidence for cholesterol aggregation at the site of *E. coli* entry (Figure 4.6).

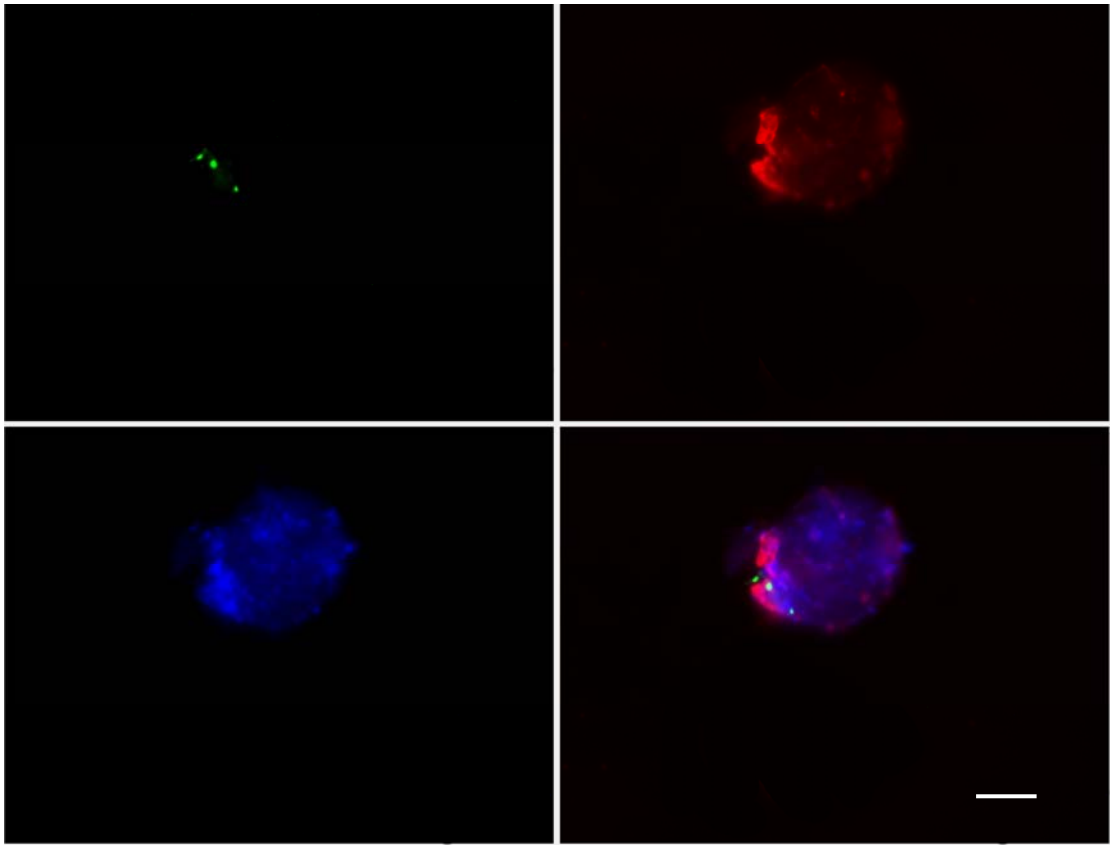

**Figure 4.5. Cholesterol aggregation at the site of internalisation of live FITC-labelled *M. bovis* into a THP-1 monocyte.** FITC-labelled mycobacteria (green, top left), phalloidin-stained actin (red, top right), filipin-labelled cholesterol (blue, bottom left) and the merged image (bottom right). The image is representative of the majority of phagocytic events in three representative 4 h experiments. Scale bar indicates 10 μm.

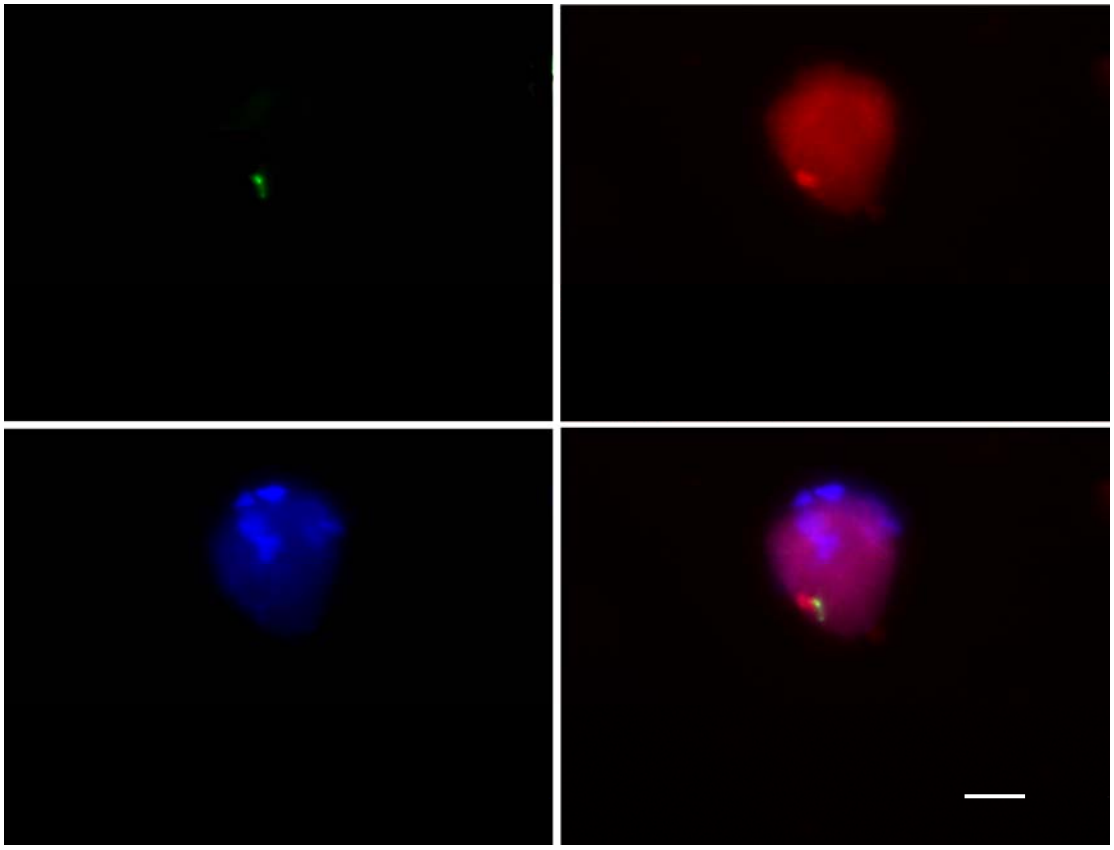

**Figure 4.6. Cholesterol independent internalisation of live FITC-labelled *E. coli* into a THP-1 monocyte.** FITC-labelled bacteria (green, top left), phalloidin-stained actin (red, top right), filipin-labelled cholesterol (blue, bottom left) and merged image (bottom right). This image is representative of the majority of phagocytic events in three representative 4 h experiments. Scale bar indicates 10 µm.

FITC-labelled Map (live and formaldehyde-killed) uptake by THP-1 cells was analysed using the same parameters. The results showed cholesterol aggregated at the site of entry of the majority of both live and formaldehyde-killed Map bacteria observed (Figures 4.7 and 4.8) and are concordant with the flow cytometry data (Figures 4.3 and 4.4).

Collectively, these results suggest that the majority of Map are internalised via a cholesterol-dependent process, at areas of the plasma membrane enriched for cholesterol. Furthermore, the observation that formaldehyde-treatment of Map had no significant effect on uptake suggests involvement of a Map cell wall component in this process, unaffected by cell fixation, rather than an active process. These findings do not rule out cholesterol independent uptake of Map into THP-1 cells, as uptake was not completely abrogated with cholesterol removal.

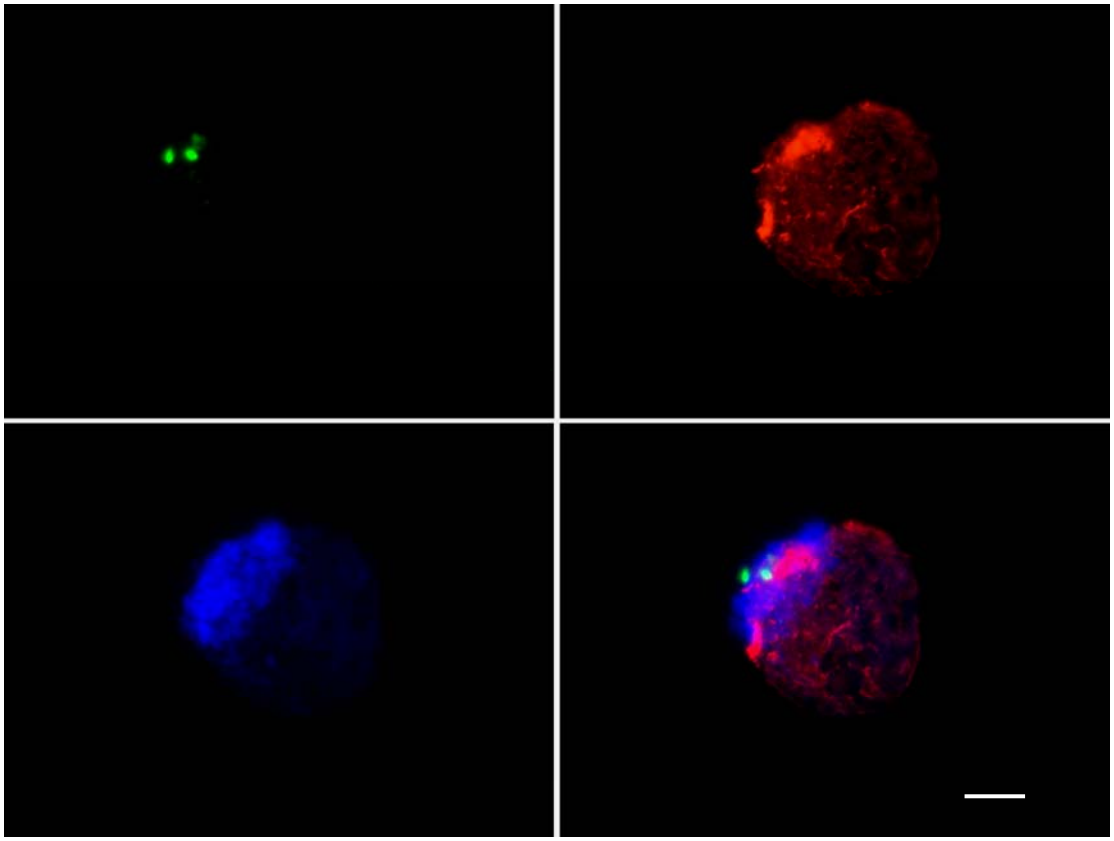

**Figure 4.7. Cholesterol aggregation at the site of internalisation of live FITC-labelled Map into a THP-1 monocyte.** FITC-labelled bacteria (green, top left), phalloidin-stained actin (red, top right), filipin-labelled cholesterol (blue, bottom left) and the merged image (bottom right). The image is representative of the majority of phagocytic events in three representative 4 h experiments. Scale bar indicates 10 μm.

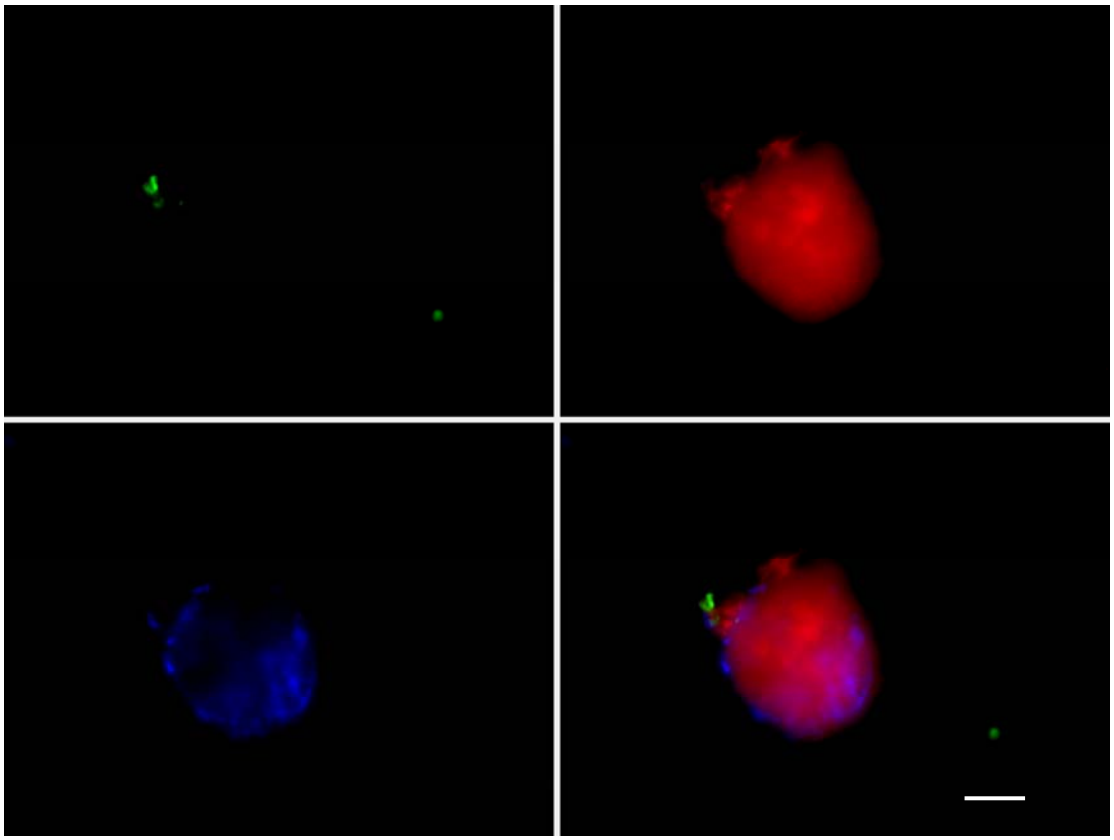

**Figure 4.8. Cholesterol aggregation at the site of internalisation of formaldehyde-killed, FITC-labelled Map into a THP-1 monocyte.** FITC-labelled bacteria (green, top left), phalloidin-stained actin (red, top right), filipin-labelled cholesterol (blue, bottom left) and merged image (bottom right). This image is representative of the majority of phagocytic events in three representative 4 h experiments. Scale bar indicates 10 μm.

### 4.2.2 Map associates with cholesterol rich areas inside THP-1 cells

To determine whether Map continued to associate with cholesterol-rich compartments at 48 h post infection, cells were cultured and incubated in cholesterol-depleting agents (simvastatin and MβCD) before being stained with filipin, washed and resuspended in 10 μl of AF1 antifade solution, (Citifluor, London, England). Ten microlitres of the cell suspension was aliquoted onto a microscope slide, covered with a cover glass, and sealed with nail polish (L'Oreal).

This experiment showed live Map bacteria in compartments with cholesterol-rich membranes 48 h post infection. Moreover, bacterial density within the compartment appeared to affect cholesterol aggregation. In cells with 3 or more Map bacteria,

comparatively large amounts of cholesterol aggregated around bacteria containing compartments (Figure 4.9). A similar effect was also observed in cells co-incubated with formaldehyde- and heat-killed Map (not shown).

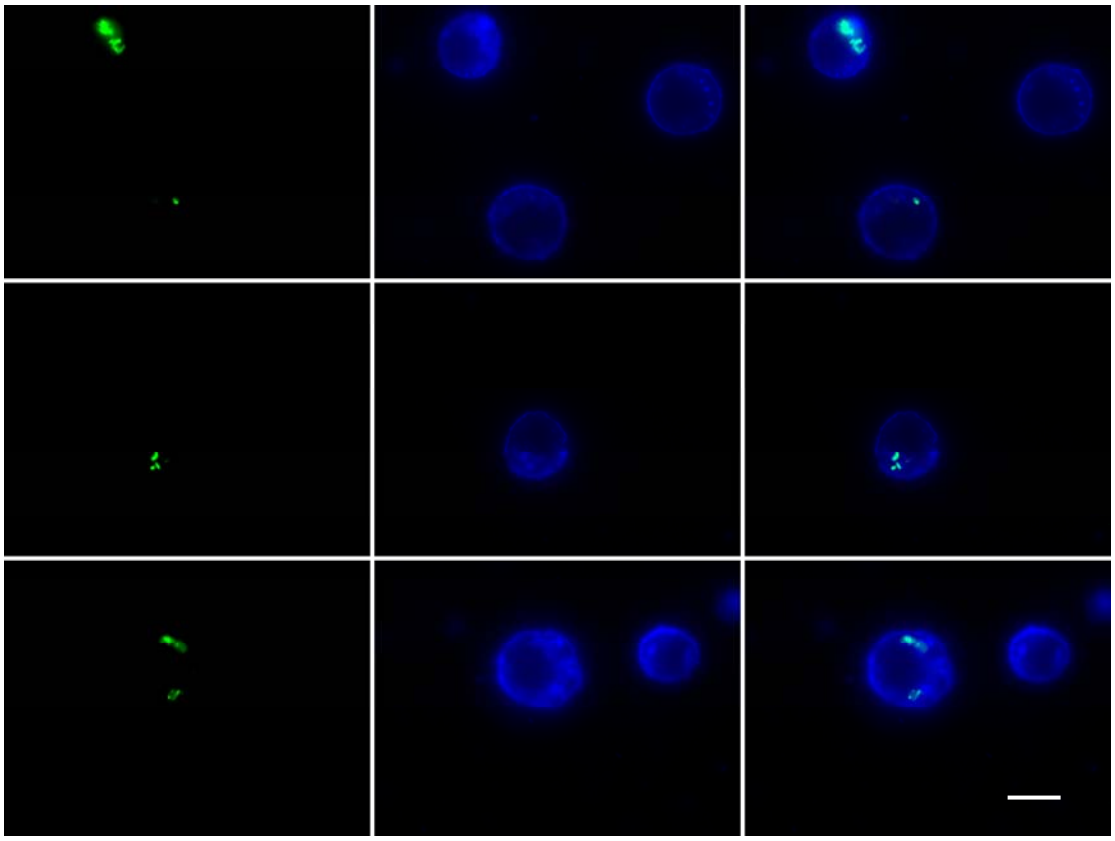

**Figure 4.9. Live Map bacteria and cholesterol co-localisation.** FITC-labelled live Map (green) and filipin-labelled cholesterol (blue) co-localisation within THP-1 cells. Images show (Top row) a single bacterium, (Middle row) Several bacteria and (Bottom row) large aggregations of bacteria associated with cholesterol-rich areas of the cell. Scale bar indicates 10 µm.

To visualise the association between Map and cholesterol inside the cell in more detail, confocal microscopy was used to collect optical sections through THP-1 cells co-incubated with Map, and 3D models of the cells constructed. Cells were exposed to FITC-labelled Map for 48 h, then washed and stained with filipin. After washing to remove excess stain, cells were resuspended in AF1 antifade solution and imaged by confocal microscopy (Leica model SP5, Wetzlar, Germany) with a 40x oil-immersion NA 1.3 lens using optical step size of 500 nm. Filipin was excited at 405 nm light

(violet) and emission collected at 460 nm, while FITC was excited with 488 nm (blue) light and fluorescence collected from 500-550 nm. Live Map bacteria residing in cholesterol-rich areas of the cell were visualised using this approach. Optical sections were converted into 3-dimensional models of the infected cells (Figure 4.10).

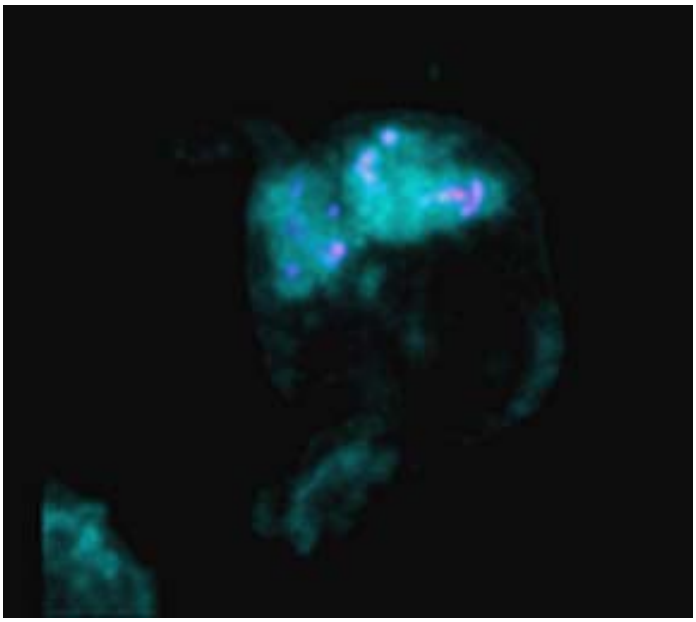

**Figure 4.10. Three dimensional model of Map and cholesterol.** A section through a Map containing cell with labelled cholesterol (white) and live Map (blue). The 3D model can be viewed on the University of Canterbury confocal website - link.

### 4.2.3 Effect of cholesterol depletion on lysotracker co-localisation

To investigate whether cellular cholesterol depletion had an effect on phagosomal acidification to 48 h post infection, THP-1 cells were exposed to Map (MOI 50:1) for 4 h with and without simvastatin (2.5 µg/ml), then washed three times with media and incubated for a further 48 h in media with and without simvastatin. At 48 h, the number of Map co-localising with acidic areas of the cell was compared between simvastatin treated and untreated cells using lysotracker as described previously (p 36, section 3.2.1). No significant difference in phagosome acidification was found between simvastatin treated- and untreated cells (Figure 4.11).

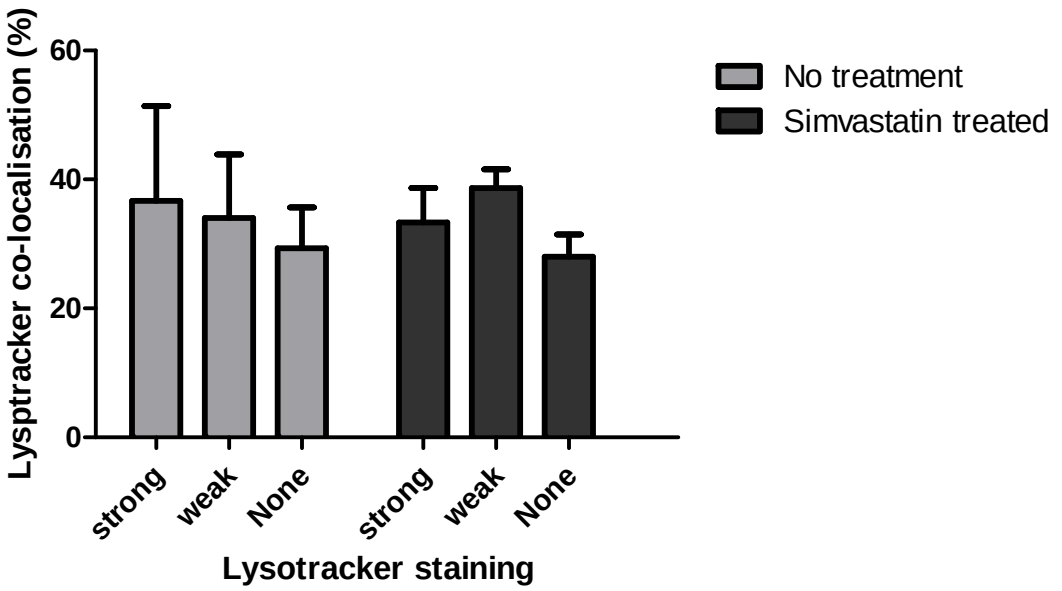


**Figure 4.11. Effect of simvastatin on lysosome co-localisation of live labelled Map.** The intensity of lysotracker staining was compared between Map in untreated and simvastatin treated cells. Values are mean +/- SEM from three independent experiments. No significant difference was seen at 48 h post infection (Data was analysed using a one way ANOVA).

### 4.2.4 Cholesterol and the long term survival of Map

To determine the effect of cholesterol on the intracellular processing and, therefore, the survival of Map in human monocytes over longer times, bacteria were co-incubated with THP-1 cells with and without pre-treatment with 2.5 µg/ml simvastatin. Duplicate THP-1 cell cultures were seeded at 100,000 cells/ml, and incubated with Map (MOI 50:1). The medium (with or without simvastatin) was changed every 2 days, and the cells were split to prevent cell overgrowth at 7 and 12 days. At 2, 7 and 14 days post infection, duplicate 100 µl aliquots were taken from each sample, cytospun onto microscope slides and stained with the mycobacteria-specific ZN stain (Appendix 1). The number of cells with visible intracellular Map was counted in triplicate (3 x 100 cells per treatment per time point) using light microscopy. All counts were carried out blinded.

This experiment showed no significant difference in the number of Map in simvastatin-treated and untreated cells at 2 days. However, at 7 and 14 days, there

were fewer intracellular bacilli in simvastatin-treated cells compared to the untreated controls, although these differences were not significant (Figure 4.12).

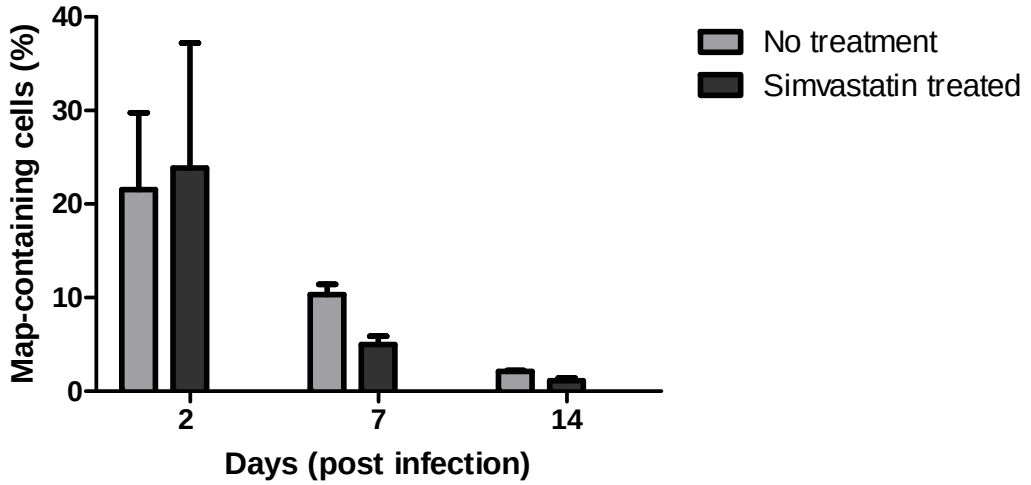


**Figure 4.12. THP- cells containing Map bacteria after extended incubation.** The percentage of THP-1 monocytes containing Map bacteria was determined in the absence and presence of simvastatin (2.5 µg/ml). Values are mean +/- SEM from three independent experiments. Although there were observably fewer Map bacteria in simvastatin treated cells at 1 and 2 weeks post infection, no significant difference was found between treated and untreated cells (data was analysed using a two way ANOVA).

To elucidate whether simvastatin treatment was associated with a reduction in live Map and not simply reduced bacterial staining under these conditions, intracellular Map were enumerated by plate counts. Aliquots (1 ml) of the cell suspension were collected at days 2, 7 and 14. The cells were washed twice in PBS containing 2.5 % FBS (PBS/FBS), then resuspended at 250,000 cells/ml in PBS/FBS before being split into two equal aliquots. The cell in one tube were resuspended in PBS with 0.1 % Triton X-100, vigorously vortexed and incubated for 10 min at 37°C to ensure cell lysis before the addition of amakacin (an aminoglycocide antibiotic, final concentration 200 µg/ml). In contrast, amakacin was added to the second tube (final concentration 200µg/ml) prior to cell lysis, to kill extra-cellular bacteria (Patel et al., 2006). After 2 h incubation at 37°C, the cells were washed three times with PBS/FBS before being lysed. Both lysates were serially diluted and plated on 7H9 agar. After a minimum of 5 weeks incubation at 37°C, colonies on the plates were counted.

Viable intracellular bacteria were determined and normalised to colony forming units (CFUs) per 100,000 cells for each dilution. For each experiment, normalised results for each dilution were averaged, and then combined to give one replicate value. Any colonies found growing on the control plates were, counted, combined, and then subtracted from replicates to give the final number of intracellular bacteria (Figure 4.13).

Concordant with light microscopy findings, fewer viable Map were recovered from simvastatin-treated cell preparations than untreated controls at 1 and 2 weeks post infection. However, these differences were not significant.

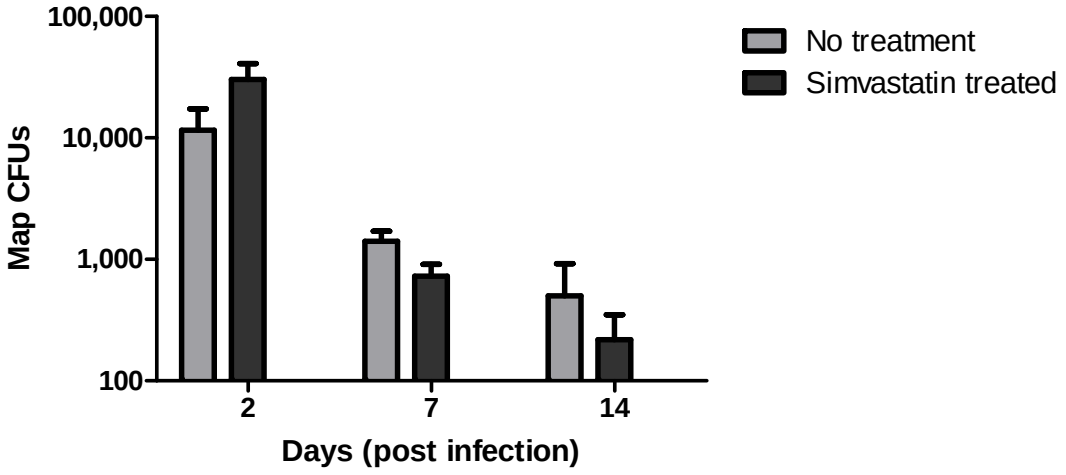


**Figure 4.13. Map CFU's after incubation with control and simvastatin (2.5µg/ml) treated cells to two weeks post infection.** Map bacteria were plated at three dilutions. These were adjusted to CFUs per 100K cells, and combined to give one replicate value. Values are mean +/- SEM from three independent experiments. Although there were fewer viable Map bacteria in simvastatin treated cells at 1 and 2 weeks post infection, no significant difference between was found between treated and untreated cells (data was analysed using a two way ANOVA).

## 4.3 Discussion

The work presented here shows for the first time that Map uptake and survival is associated with cell membrane cholesterol. Map associate with and are internalised into THP-1 monocytes in a cholesterol-dependent manner. They are found to persist in cholesterol-rich compartments two days post infection, and their ability to persist inside THP-1 cells is cholesterol-dependent.

Cholesterol has been implicated in many aspects of bacterial and mycobacterial pathogenesis. Uptake via a cholesterol-dependent pathway increases the survival of many intracellular pathogens including *M. tuberculosis* (Martens et al., 2008; Miner et al., 2009; Naroeni and Porte, 2002) but the mechanism(s) involved are largely unknown. Evidence of a cholesterol specific receptor ($C_k$) on the surface of *M. tuberculosis* implies bacterial binding directly with membrane cholesterol (Kaul et al., 2004). Cholesterol-mediated uptake reportedly circumvents the oxidative burst (Lamberti et al., 2008; Rodriguez et al., 2001), a potent antibacterial mechanism that might otherwise kill the intracellular bacteria. It is also hypothesised that by entering via cholesterol-rich areas, pathogens traffic only as far as endosomal compartments and are spared from undergoing lysosomal degradation (Naroeni and Porte, 2002; Rodriguez et al., 2001). In addition to direct advantages such as a supplemental carbon source and phagosome remodelling, cholesterol-rich intracellular membranes are intrinsically resistant to fusion with lysosomes. This is attributed, in part, to Rab 7, which remains in an inactive form in cells treated to increase intracellular cholesterol concentrations (Huynh et al., 2008).

Mycobacterial persistence inside the host cells is also facilitated in part by association with cholesterol-rich areas in the cell. Depleting the cellular cholesterol of *M. avium*-containing macrophages results in a stimulation of phagosomal maturation, leading to increased fusion of compartments with lysosomes (de Chastellier and Thilo, 2006). *M. tuberculosis* induce accumulation of cholesterol in macrophages (Kurup and Mahadevan, 1982), and reside in cholesterol-rich areas in these cells. Hyper-cholesterolemic mice fed a cholesterol rich diet are extremely susceptible to *M. tuberculosis* infection. These animals exhibit severe pathology, a greatly increased bacterial load and significantly decreased survival compared with their wild type counterparts (Martens et al., 2008).

Intracellular cholesterol is shown to assist the persistence of pathogenic mycobacteria by several different mechanisms. There is evidence that *M. tuberculosis* accumulate cellular cholesterol in the free-lipid zone of their cell wall, even when there are other carbon sources available (Pandey and Sassetti, 2008). Furthermore, when deprived of a carbon source, *M. tuberculosis* is able to metabolise this cholesterol (Brzostek et al., 2009; Miner et al., 2009), a trait that is likely to be highly advantageous in the nutrient-deficient environment of the phagosome.

In this study, a proportion of the Map-containing compartments were observed to stain positive for the cell membrane protein TACO, a late endosomal protein that is also reportedly retained on the phagosomes of pathogenic mycobacteria. TACO is implicated in attenuating the fusion of the mycobacterium-containing compartments with lysosomes (Kaul et al., 2004), and related studies show *M. tuberculosis* and *M. bovis* secrete a coronin-interacting protein that is dependent on cholesterol in its interaction with cellular TACO (Deghmane et al., 2007). Interestingly, the cholesterol receptor found on *M. tuberculosis* also up-regulates transcription of the TACO protein in infected cells (Kaul et al., 2004). It is unclear at this stage whether the association of TACO with Map-containing phagosomes shown here is a result of cholesterol accumulation in the compartment, or whether it is actively retained on Map containing phagosomes.

Long term persistence of pathogenic mycobacteria in host cells is associated with an altered bacterial phenotype, demonstrated by the emergence of spheroplast (or cell wall deficient) forms after extended intracellular incubation. These forms lack many cell wall components (Hines and Styer, 2003), which may enhance bacterial survival by reducing antigenicity (Chandler and Hamilton, 1975). In the following chapter, the morphology of Map to inside monocytes is followed over time.

# Chapter 5. Map bacterial morphology during long term survival

## 5.1 Introduction

Mycobacteria are some of the most persistent pathogens known, with a third of the human race thought to be latently infected with *M. tuberculosis* (Gatfield and Pieters, 2000). In the short term, these bacteria have evolved to manipulate the host phagosome in order to persist inside host cells. However, longer term persistence, especially in chronic infections, is less well characterised.

Pathogenic mycobacteria are renowned for their ability to circumvent the host cell's immune response, and to persist within professional phagocytes via many different mechanisms (Nguyen and Pieters, 2005). Many bacteria adopt a viable but non-culturable form that is specialised for an intracellular existence (Beran et al., 2006). The development of an intracellular bacterial phenotype has been implicated in the persistence of some mycobacterial species (Bermudez et al., 2004).

Many species of bacteria and some mycobacteria (including *M. tuberculosis*) can develop these cell wall deficient (CWD) forms. More commonly known as spheroplasts, these bacteria are often characterised by a change in cellular shape, most commonly from rod-shaped to round (Beran et al., 2006). By discarding their cell wall, it is thought that they lose much of their antigenicity, allowing them to "fly under the radar" of the intracellular immune response (Rinno et al., 1980). Consequently, spheroplasts have been implicated in the aetiology of numerous diseases, including Crohn's disease (Beran et al., 2006; Chiodini et al., 1986; Willet and Thacore, 1967). However, it is unclear if they have a role in disease, or if they are a form that facilitates persistence in nature (Mattman, 2001).

This question is particularly relevant to many mycobacterial diseases, where spheroplasts are often found (Beran et al., 2006). Spheroplasts are a form of Map not documented in ruminant Johne's disease. They have, however, been identified by long term culture in the white blood cells, breast milk, and intestinal biopsies of

patients with CD (Beran et al., 2006; Cho et al., 1986; Hines and Styer, 2003; Moss et al., 1992; Naser et al., 2004). However, whether CWD forms of Map are actively involved in infection and disease remains unknown, and is still a subject of much debate.

Spheroplast forms are fastidious and extremely slow growing, with cultivation taking months or years (Chiodini et al., 1986). Furthermore, they require specific protoplast media for extended growth and rapidly revert to their bacillary (cell wall competent) forms when grown on conventional media (Markesich et al., 1988). In 2003, the first chemical method to generate Map (strain 19698) spheroplasts in culture was published. This study also analysed the chemical and structural constituents of the generated spheroplasts. Significant attenuation of cell wall features integral for diagnosis, virulence, pathogenicity, immunological response and spectrum of disease were reported (Hines and Styer, 2003). This technique provides a means to shed light on some of the mystery surrounding a role for spheroplasts in Map pathogenesis.

The following experiments investigated whether spheroplasts could be chemically generated from Map strain Dominic. In addition, THP-1 monocytes infected with Map were cultured for up to 5 weeks to explore whether Map developed a spheroplast-like form as a result of long term infection. A combination of light and transmission electron microscopy (TEM) was used to visualise differences in bacterial morphology and ultrastructure following chemical treatment and/or long term intracellular culture.

## 5.2 Results

### 5.2.1 Chemical generation and visualisation of spheroplasts

To visualise the bacteria with light microscopy, a 10 µl aliquot of bacterial suspension was spread and heat fixed to a microscope slide before ZN staining (Appendix 1). Concurrent with previous studies (Hines and Styer, 2003), light microscopy showed that Map bacteria change their morphology after chemical treatment (p11, section. 2.12). In addition to long rod-shaped bacilli, shorter rod shapes and acid-fast coccoid

forms were seen after 14 days. Furthermore, the propensity of Map bacteria to form large clumps during culture appeared to be affected by the chemical treatments, demonstrated by an observable decrease in the number of large clumps of Map at this time (Figure 5.1).

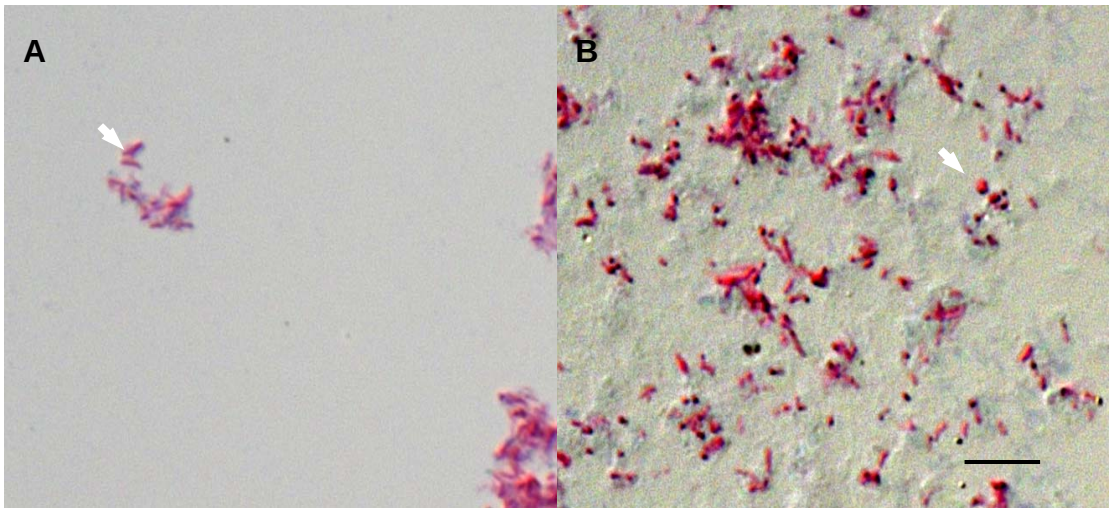


**Figure 5.1. Chemically generated spheroplasts by light microscopy.** Map bacteria treated with the spheroplast generating protocol were stained with ZN stain at 0 (A), and 14 days culture (B). Note the rounded but acid fast forms at 14 days compared with day 0 (arrows). Scale bar indicates 10 µm.

Negative-staining transmission electron microscopy was used to examine in more detail the morphological changes associated with chemical treatment of Map. First, a 5 µl aliquot of bacterial suspension was aliquoted onto formvar film, copper mesh grids (ProSciTech, Thuringowa Central, Queensland, Australia) and allowed to adhere. Adherent bacteria were stained with 2 % phosphotungstic acid (PTA) for 1 h. Grids were washed twice with Pipes buffer (60 mM pH 6.8) to remove excess stain, then imaged on a CM 12 scanning-transmission electron microscope (Phillips).

Examination of treated and untreated Map revealed densely-stained bacillary forms of various sizes (Figures 5.2A, B), as well as several translucent coccoid forms (figure 5.2D). In addition, intermediate forms were also observed. These were roughly coccoid, with what appeared to be cell wall material being sloughed off (Figure 5.2C). This observation could also suggest the presence of pseudo-spheroplast

forms, with partial loss of their cell wall. The translucent, coccoid-shaped forms (figure 5.2D) lacked the opaque consistency of bacillary forms, which may be indicative of a lost cell wall. Protrusions were seen on both opaque rods and translucent coccoid forms. These may be microspherules, which are reportedly an indicator of metabolic activity (Chiodini et al., 1986). If so, it would suggest that these chemically-generated spheroplast forms of Map may remain viable even after cell wall removal (Figures 5.2B,D, arrows).

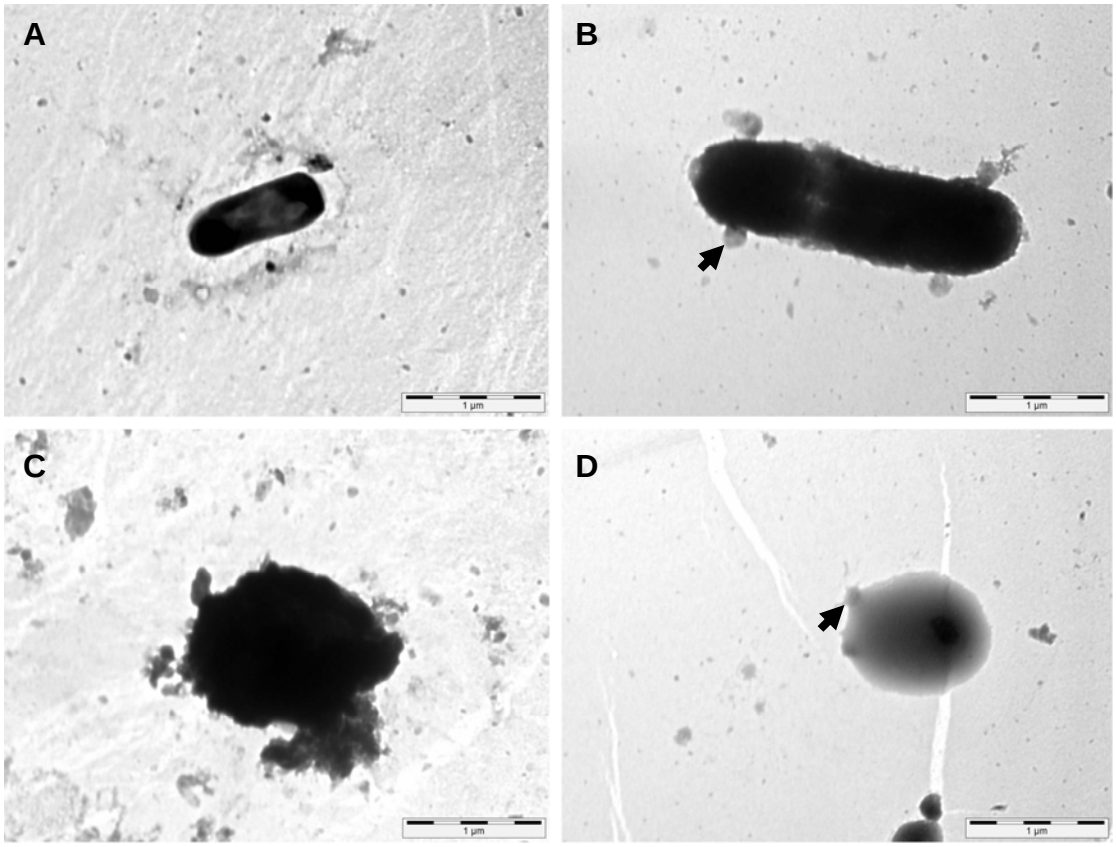


**Figure 5.2. Chemically generated spheroplasts by transmission electron microscopy.** Images are untreated bacillary Map (A, B), and chemically treated Map (C,D). The untreated mycobacterial suspension shows the typical bacillary form, with the opaque staining suggesting the presence of the characteristic thick cell wall. In the treated mycobacterial suspensions, intermediate forms were also observed in addition to bacilli. These forms appeared to have lost their rod morphology but retained the dense cell wall material (C). Translucent coccoid forms were also present (D). Scale bars indicate 1 µm.

Ultrastructural differences in the bacteria were examined using modifications to established methods (Day 1995, Appendix 5). Briefly, bacteria were fixed in 2.5% gluteraldehyde for 1 h at room temperature, then washed twice and resuspended in 50 µl of 3% liquid agarose (warm). The bacteria/agarose solution was mixed gently by pipetting up and down, then aliquoted onto a microscope slide and left to set. Bacteria-rich areas of the agarose (plugs) were cut out of this agarose smear and transferred to an eppendorf tube. Plugs were stained, dehydrated and blocked in resin as described previously (Day, 1995, Appendix 6). Blocks were cut into 70 nm slices using an EM-UC6 microtome (Lecia), mounted on formvar film, copper mesh grids and imaged.

Examination of treated bacteria revealed short rods typical of Map bacilli. These were approximately 1 µm in length, with a width of between 300 and 500 nm. Longer forms up to 1.5 µm in length were also observed. Map bacilli contained an electron dense cytoplasm, with numerous internal structures, as reported by (Hines and Styer, 2003). The characteristic double cell wall was visualised, however only in a small proportion of bacteria (Figure 5.3A, arrow). In others, this wall could only be visualised as a halo around the bacterium, as reported in studies of *M. avium* (Frehel et al., 1991) (Figure 5.3B, arrow). Considerably fewer bacillary Map were observed among the chemically-treated bacteria (Figure 5.3C,D). Instead, the majority of forms were found to be amorphous or coccoid, with notably less electron dense internal structure than untreated bacilli. Bacilli that were still present were elongated or showed atypical rod morphology suggestive of transition to the coccoid form (Figure 5.3C, arrow). Despite poor camera resolution, there was evidence that the majority of chemically-treated bacteria more closely resembled spheroplast than bacillary forms, similar to findings reported elsewhere (Markova et al., 2008b; Udou et al., 1982).

The loss of cell wall in the treated bacteria was not confirmed. However, the differences in morphology seen by ZN staining, the presence of translucent forms seen by grid-TEM, and the similarity of these forms to spheroplasts generated from other mycobacterial species (Yabu and Takahashi, 1977), suggest cell wall deficient forms of Map strain Dominic are generated after 14 days of chemical treatment.

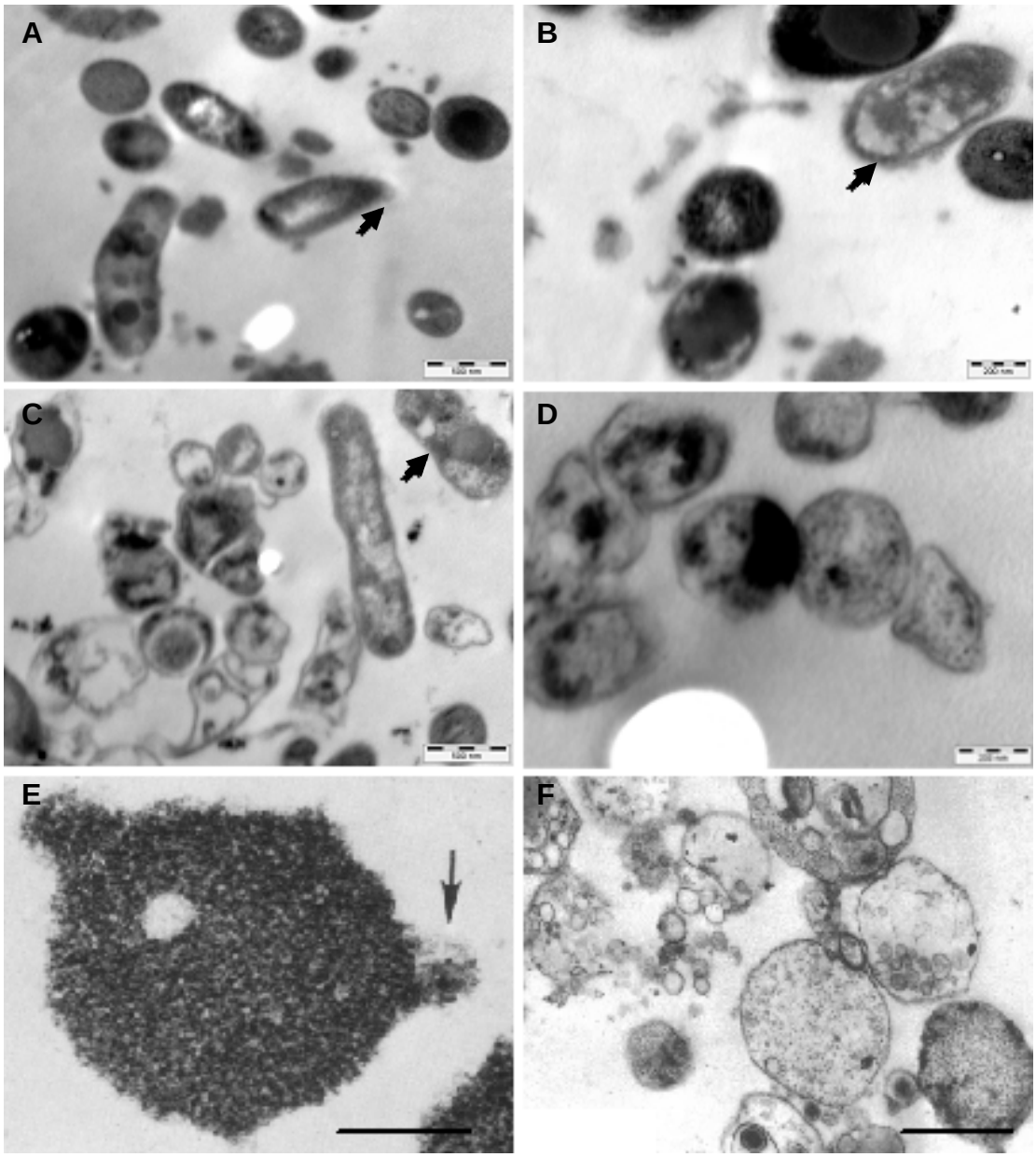


**Figure 5.3. Chemically generated spheroplasts by transmission electron microscopy.** Images are untreated Map showing characteristic rod morphology and double cell wall (A,B), Map bacilli treated for 14 days to generate spheroplasts, bacteria have lost their electron dense cytoplasm and rod shaped morphology (C,D). Transmission electron micrographs of Map spheroplast forms isolated from a CD patient (note the membrane protrusion similar to that seen in figure 5.2E) (E- image adapted from (Chiodini et al., 1986)), and chemically generated spheroplasts of *M. smegmatis* (F- image adapted from (Yabu and Takahashi, 1977). Scale bars indicate 200 nm (B, D), 500 nm (A, C, E) and 1 μm (F).

### 5.2.2 Bacterial morphology after long term infection

For long term co-incubation experiments live Map bacteria were added to 200,000 THP-1 cells at an MOI of 100:1. Media was changed every 2 days, and the cells were split (with 25% retained) every 7 days to prevent overgrowth. After 1 and 5 weeks of co-incubation, a 100 µl aliquot of cells was cytospun, then heat fixed to a microscope slide and ZN stained (Appendix 1). One ml of cell suspension was resuspended in 2.5% gluteraldehyde and processed for electron microscopy (Appendix 5). The morphology of ZN positive forms inside the cells was analysed by light microscopy, while the ultrastructure of cells and bacteria was analysed using electron microscopy.

Intracellular Map, as detected by ZN staining, were predominantly bacillary after one week. However, at 5 weeks post infection, ZN positive forms inside the cells were exclusively spherical, and varied in size from approximately 0.5 to 1.5 µm (Figure 5.4).

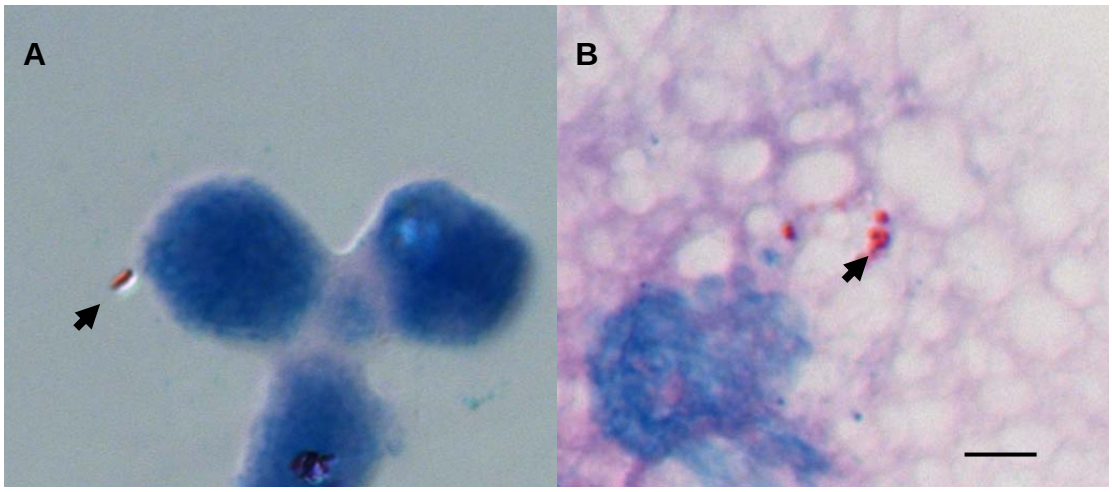


**Figure 5.4. ZN positive organisms in THP-1 cells at 1 and 5 weeks.** Representative ZN-positive forms after incubation of Map bacteria with THP-1 monocytes at 1 (A) and 5 (B) weeks post infection. Scale bar is 10 µm.

Intriguingly, the spherical forms observed in the 5 week cultures closely resemble ZN-positive structures observed following the culture of peripheral blood taken from patients with Crohn's disease (John Aitken, unpublished results), with the larger size (approximately 3-4 µm) of some forms found in CD patient blood the only observable difference (Figure 5.5).

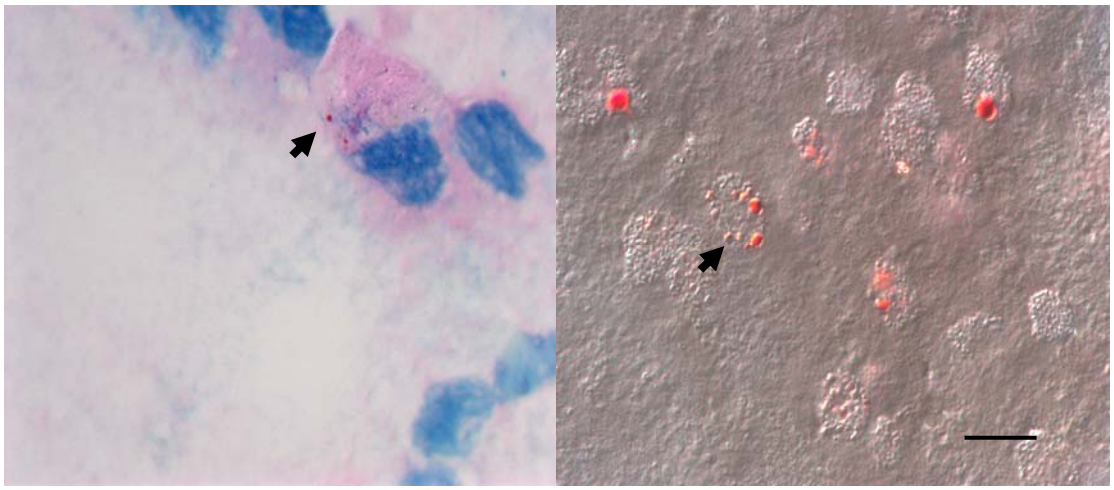

**Figure 5.5. Comparison of ZN positive forms in THP-1 and CD patient cells.** Spherical, ZN positive forms inside THP-1 monocytes after 5 weeks incubation with Map (left), and similar forms in cytospun peripheral blood of a CD patient. Scale bar indicates 10 µm.

Using transmission electron microscopy, bacteria resembling bacillary Map were seen inside THP-1 cells at 1 week post infection (Figure 5.6D, arrows). These bacteria displayed similar morphology and ultrastructure to Map bacilli analysed previously (Hines and styer et al 2003). In addition, amorphic/coccoid forms were also observed in the Map-exposed cells (Figure 5.6C, arrow). Many of these forms were bounded by electron light space (Figure 5.6C, arrow), suggesting they were in membrane bound compartments. Some, however, were not (Figure 5.6E, white arrow). The intracellular structure was homogeneous in most forms, with several organelles/vesicles visible in some (Figure 5.6E, black arrow).

Whether these forms are organelles generated by the presence of bacteria in the cell, or whether they are Map bacteria in an intracellular form is unknown. However, the morphology and interior structures shown here are similar to the cell wall

deficient form of *M. bovis* BCG, which was recently shown to develop into a spheroplast form after an extended incubation period in the peritoneal cavity of guinea pigs (Figure 5.6F). While viability cannot be inferred from TEM, the close apposition of the phagosomal membrane to bacteria (Figure 5.6D, arrow), is often seen in phagosomes containing live mycobacteria (de Chastellier, 2009).

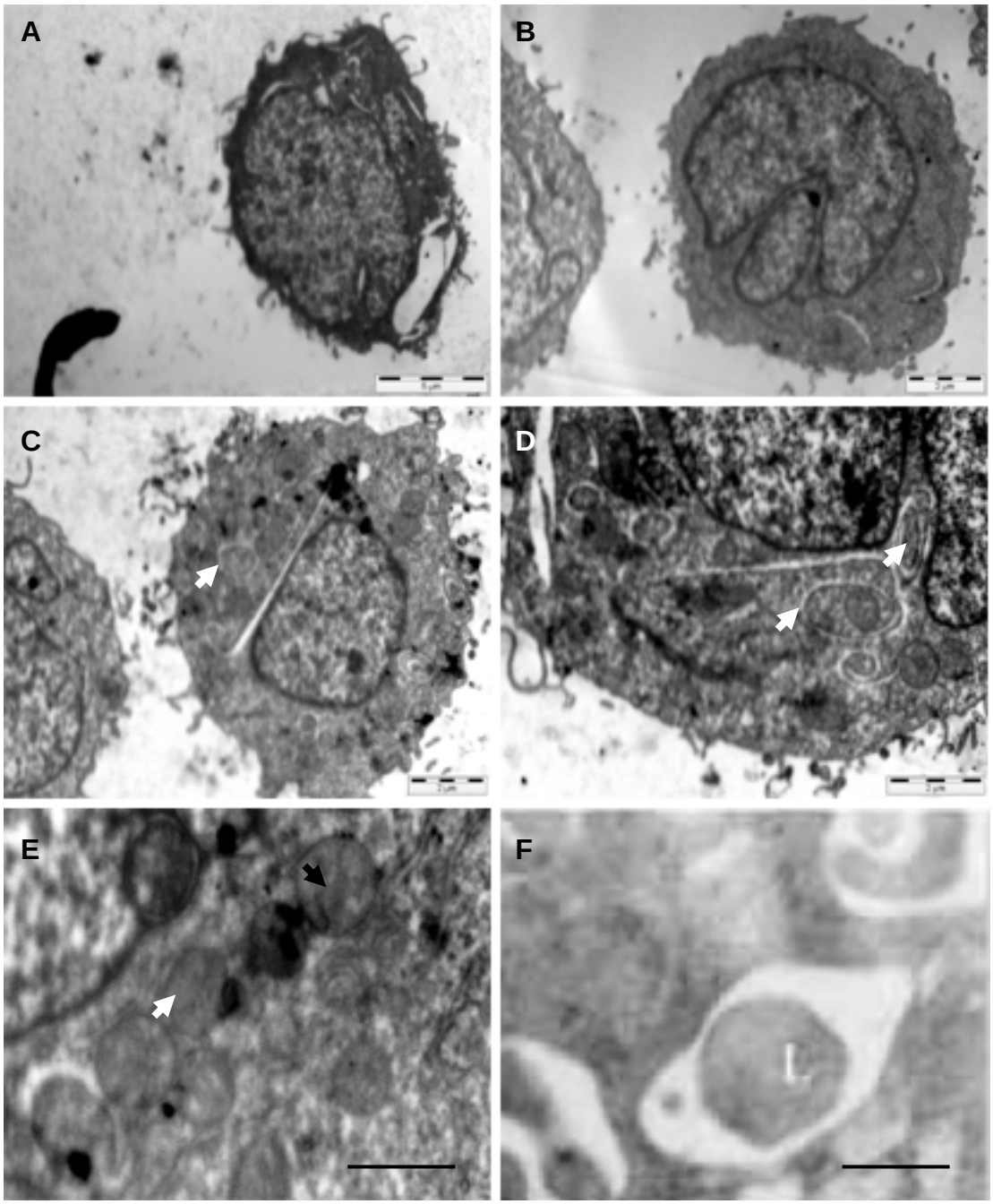


**Figure 5.6. Map inside THP-1 monocytes at 1 week post infection (TEM).** (A) bacteria-free control cells, (B-F) Map-exposed THP-1 monocytes, containing intracellular bacteria, and bacteria-like forms of various morphology (B-E), (F) an *M. bovis* BCG derived spheroplast, after incubation inside a Guinea pig peritoneal macrophage (image adapted from (Markova et al., 2008a)). Scale bars indicate 5 µm (A), 2 µm (B, C, D) and 500 nm (E, F).

No bacillary forms were seen in THP-1 cells at 5 weeks post infection, but similar amorphic/coccoid forms were present in many cells (Figure 5.7). These spheroplast-like forms were larger than those seen at the one week time point but exhibited the same homogeneous internal architecture. Interestingly, they were a similar size to the ZN positive forms observed in the peripheral blood of a CD patient (Figure 5.5), and also exhibited ultrastructural characteristics (such as a homogeneous interior) similar to that of spheroplasts generated chemically from other mycobacteria such as *M. bovis* and *M. smegmatis* (Figures 5.6F, 5.7F). These coccoid forms were mostly present in what appeared to be membrane bound compartments, but several were in the process of phagocytosis, confirmed by the presence of a phagocytic cup (Figure 5.7C, arrow). There was also some evidence of a double membrane, bounding these forms (Figure 5.7E, arrow), similar to that reported for *M. smegmatis* bacteria after treatment to remove their cell wall (Udou et al., 1982) (Figure 5.7F, arrow). This is intriguing, as no such structure was seen at 1 week post infection. The presence of a double membrane could indicate reversion of a spheroplast form to a ZN positive form.

In sharp contrast to the Map exposed THP-1 cells, many of the bacteria-free cells were apoptotic, showing nuclear condensation, shrinking and cytoplasmic vacuolization typical of monocyte apoptosis (Lang et al., 2002) (Figure 5.7A). Inhibition of apoptosis has been reported for pathogenic mycobacteria inside host cells. It is thought that by inhibiting the apoptotic pathways in host cells, these bacteria extend the life of their host cell, prolong their intracellular stay, and therefore maximise replication time (Berger and Griffin, 2006; Hasan et al., 2006).

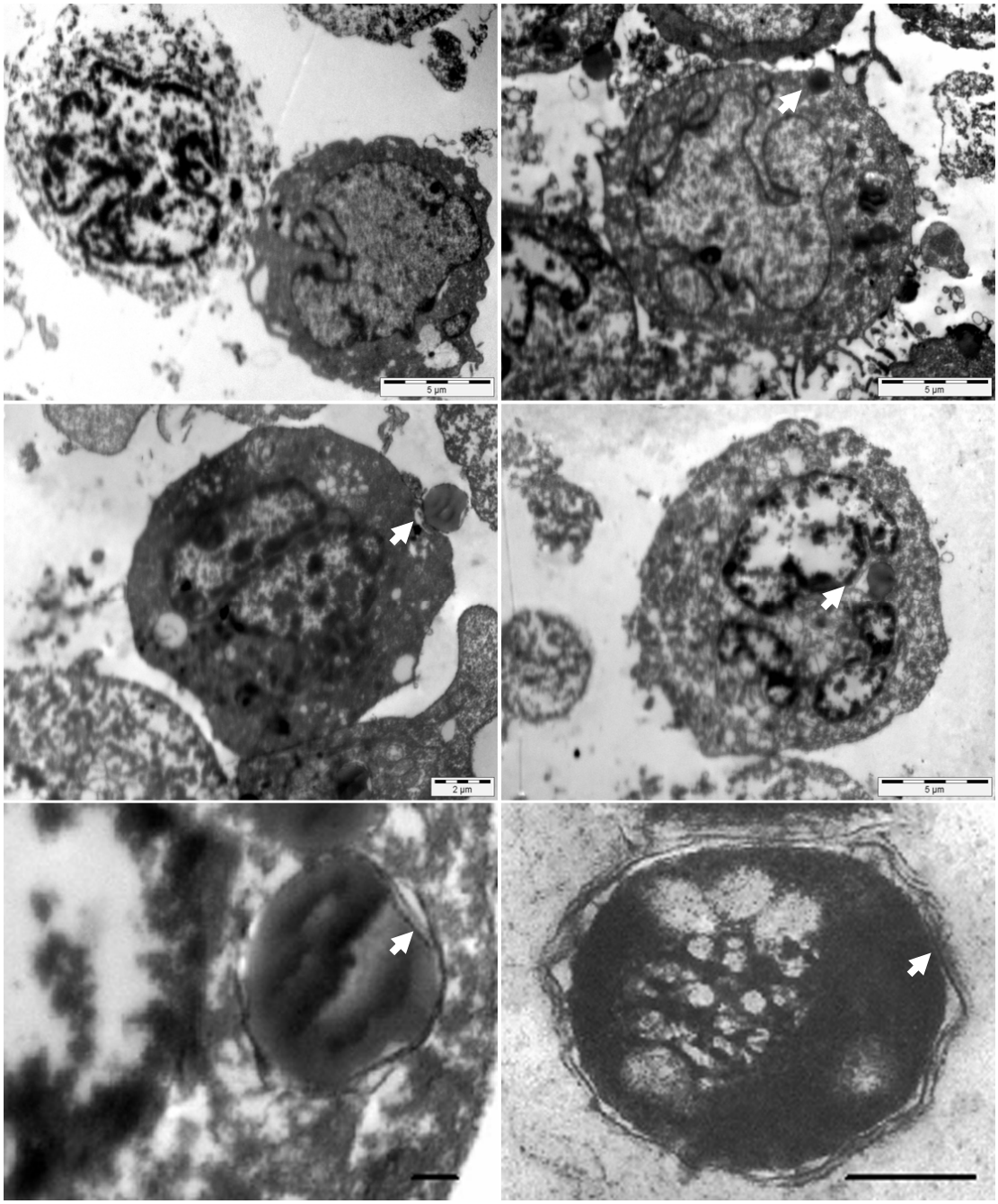

**Figure 5.7. Spheroplast like forms in Map exposed cells at 5 weeks post infection by transmission electron microscopy.** (A), bacteria free cells, (B-E) cells with atypical forms inside and (F) a chemically generated *M. smegmatis* spheroplast, showing cell wall exfoliation from the membrane (Image adapted from (Udou et al., 1982)). Scale bars indicate 5 µm (A, B, D), 2 µm (C) and 200 nm (E, F).

## 5.3 Discussion

This study demonstrated that, as with other mycobacteria, spheroplasts could be generated chemically from Map strain Dominic. This confirms that the technique developed by Hines and Styer (2003) is potentially applicable to many strains of Map. Furthermore, experiments showed that coccoid forms, not present in control cells, existed in Map exposed THP-1 monocytes at 1 and 5 weeks post infection. Coccoid forms observed at 5 weeks post infection showed similarities to chemically generated spheroplasts. In addition, they were of a similar size to ZN positive forms found in THP-1 monocytes at 5 weeks post infection by light microscopy, as well as in CD patient peripheral blood cells. Interestingly, in contrast to the coccoid forms in THP-1 monocytes observed at 1 week, forms at 5 weeks incubation showed evidence of a double membrane, indicative of a mycobacterial cell wall. This is an intriguing connection to the ZN positive forms seen in CD patient blood cells.

These observations support the possibility that a proportion of Map may loose all or part of their cell wall and develop a spheroplastic, intracellular phenotype after prolonged intracellular incubation. Map spheroplasts, such as the translucent bacteria visualised by negative staining TEM, may not have a cell wall. If so, these forms may not be acid fast. This has implications for detection using conventional mycobacterial screening techniques such as ZN staining (Sechi et al., 2004).

Spheroplast forms of mycobacteria are regularly documented in mycobacterial infection and are implicated in a variety of diseases (Beran et al., 2006). An L-form of *M. tuberculosis* develops in rat macrophages after 5 weeks incubation and is more drug tolerant, and faster growing than the bacillary form (Markova et al., 2008a; Markova et al., 2008b). Spheroplast forms of *M. tuberculosis* (Beran et al., 2006; Markova et al., 2008a; Thacore and Willett, 1966), *M. bovis* (Markova et al., 2008b) and *M. smegmatis* (Udou et al., 1982) have also been characterised. Spheroplast forms of Map, confirmed by genetic analysis and reversion to the bacillary form, have also been isolated from CD patient blood and tissue in several different studies (Chiodini et al., 1986; Hines and Styer, 2003). Given the difficulties inherent in isolation, how these forms occur and whether they have a role in CD remains unclear. The results presented in this chapter support the possibility that Map spheroplasts may develop after prolonged intracellular persistence. While this idea is

thought-provoking, further research is required to determine the true nature of these forms. Specifically, are they organelles produced after prolonged culture in Map exposed cells, or an intracellular form of Map?

Given the frequent splitting of cells and media changes, the length of culture, and the low number of samples analysed, the potential for the presence of other factors is significant. To confirm if the forms found inside THP-1 monocytes after an extended incubation are Map, or whether they are simply cellular structures brought about by the extended culture period and bacterial exposure, more research is needed. A mycobacteria- or Map-specific proceedure such as FISH could be used for this purpose. Another approach could be to label Map exposed cells with a gold-labelled, (non-cell wall) mycobacteria specific antibody, then process and image as above using TEM. These experiments are beyond the scope of this study. Therefore the above concerns must be kept in mind, and any interpretation of the results presented in this chapter must be made with caution.

# Chapter 6. General Discussion

## 6.1 Manipulation of the phagocytic pathway

Evidence is emerging that Map bacteria are able to persist in human cells as they do in murine and bovine macrophages (Rumsey et al., 2006). However, there are few studies investigating the interaction(s) of Map bacteria with human cells (Britton et al., 1994; Rumsey et al., 2006). This study has shown that Map behaviour in THP-1 monocytes mimics that of *M. bovis*. Moreover, the mechanisms of Map uptake and persistence in these cells show intriguing similarities to pathogenic bacteria and mycobacteria.

The role of cell wall components in the fate of Map in host cells remains unclear at this stage. The observation that formaldehyde-killed Map were also taken up into THP-1 cells via a cholesterol-mediated process (Chapter 4) suggests this uptake may be a passive process, mediated by cell wall constituents. Cell wall molecules of other mycobacteria have previously been shown to affect fate after phagocytosis. Mannose receptor-dependent uptake facilitates the development of a safe intracellular niche for *M. tuberculosis*. It is not, however, known whether this, or similar pathways or molecules exist for other mycobacteria (Kang et al., 2005).

Cell wall components also affect pathways inside host cells. Mannosylated lipoarabinomannan (ManLAM) is a cell wall component from slow growing mycobacterial species such as *M. tuberculosis* and *M. bovis*. It is integral in mediating bacteria/host interactions (Rojas et al., 2000), with evidence that ManLAM from these species is able to inhibit macrophage activation as well as apoptosis (Chan et al., 2001; Sibley et al., 1990). Interestingly, long-term Map colonisation of THP-1 monocytes also appeared to inhibit cellular apoptosis (p76, section 5.2.2). However, more research is needed to qualify this observation.

Lipid rafts are cholesterol-rich areas within cell membranes (Goluszko and Nowicki, 2005). Cholesterol is integral to raft formation because removal (with compounds such as methyl-β-cyclodextrin) results in a disassociation of the raft as a whole, as well as the disassociation of proteins from raft domains (Christian et al., 1997;

Lawrence et al., 2003). Many pathogenic microbes (bacteria, viruses) use lipid raft-dependent processes to augment their pathogenesis (Shin and Abraham, 2001; Zass et al., 2005). The cholesterol dependent uptake and fate of Map in THP-1 cells suggests a role for lipid rafts or lipid raft signalling.

Lipid rafts domains are also found on endosomal membranes inside cells, meaning their effects extend beyond internalisation (Rosenberger et al., 2000; Zass et al., 2005). The association between Map and lipid rafts is strengthened by the observation that Map and *M. bovis* reside in cholesterol-rich areas inside the cell 48 h post-infection. Other pathogenic bacteria, including *Salmonella typhimurium* and *M. bovis* also traffic to areas of the cell that are rich in cholesterol (Catron et al., 2004; Harrison et al., 2004; Sun et al., 2007). It is thought that this cholesterol facilitates the formation of these membrane micro-domains or rafts, which aid in manipulation of cell signalling and processing (Catron et al., 2004). In addition, there is also evidence that these cholesterol-rich domains are intrinsically resistant to fusion with lyosomes. This effect is thought to be mediated by inactivation of Rab 7 (Huynh et al., 2008).

In THP-1 cells, both Map and *M. bovis* phagosomes exhibit strong Rab 7 staining 48 h post infection. Rab 7 is a marker of late phagosomes; the active, GTP-bound form is instrumental for the fusion of pathogen-containing compartments with lysosomes (Vieira et al., 2002), while there is evidence that conversion of Rab 7 to the inactive GDP-bound form inhibits phagosomal maturation (Sun et al., 2007).

Some pathogenic bacteria secrete factors that inactivate Rab 7 on nearby phagosomes. This results in the extended association of Rab 7 with phagosomes, and decreased fusion of the compartments with lysosomes (Sun et al 2007). Lipoamide dehydrogenase, the enzyme responsible, is secreted by *M. tuberculosis* and *M. bovis*, but not by the non-pathogenic *M. smegmatis* (Deghmane et al., 2007). Given the similarities between Map and *M. bovis* trafficking shown here, the potential exists for Map to also resist fusion of the phagosome with lyosomes via inactivation and retention of Rab 7. However, this hypothesis remains to be tested.

Recent studies in other cell systems suggest that cholesterol and Rab 7 may be interlinked. Lysosomal degradation of low density lipoprotein (LDL), a major source

of exogenous cholesterol, is under the control of Rab 7 in aortic cells (Bruckart et al 2000). In thyroid cells, treatment with lovastatin (an analogue of simvastatin) up-regulates Rab 7 expression (Bruckert et al., 2000). These studies suggest that the inactivation of Rab 7 by pathogens such as *M. bovis*, *Salmonella typhimurium* and *M. tuberculosis* may occur through dual mechanisms; cholesterol aggregation, as well as direct Rab 7 inactivation by lipoamide dehydrogenase (Deghmane et al., 2007; Harrison et al., 2004; Sun et al., 2007). Despite these links, the connection between bacteria-containing phagosomes, cholesterol and Rab 7 has yet to be fully elucidated.

A further dimension to this story was added with the discovery of the TACO protein. TACO is a leucocyte-specific, intracellular protein, shown to facilitate the persistence of pathogenic mycobacterial species in host cells (Anand and Kaul, 2005; Jayachandran et al., 2008; Jayachandran et al., 2007; Kaul, 2008). It was recently shown that the retention of the TACO protein on mycobacteria-containing phagosomal membranes is dependent on cholesterol (Deghmane et al., 2007). Map's association with TACO has not been documented previously. However, TACO's association with Map-containing phagosomes suggests another mechanism by which Map bacteria may persist in human cells.

Simvastatin-mediated depletion of cellular cholesterol had no effect on Map viability or clearance 48 h post-infection. However at 1 and 2 weeks post infection, less Map were observed (by light microscopy and plate counts) in cells treated with simvastatin. Similar research suggests cholesterol acquisition is less important for early *M. tuberculosis* infection in mice. *M. tuberculosis* with a (genetically) impaired cholesterol uptake pathway, showed no difference in virulence and survival in the early stages of infection. However at later time points (4 weeks), these bacteria showed significant growth inhibition compared to wild types, implicating a requirement for cholesterol in long term persistence and pathogenesis (Pandey and Sassetti, 2008). In addition, *M. tuberculosis* is thought to induce the differentiation of macrophages into foamy macrophages, characterised by their high lipid content. The increased concentration of lipids (including cholesterol) is thought to augment their persistence in granulomas (Peyron et al., 2008).

Cholesterol manipulation has been proposed as a novel therapy for chronic infection with organisms that use it to augment their pathogenesis (Pucadyil et al., 2004; Rosch et al., 2010). Reducing cholesterol-dependent entry of microbes into cells has also been shown to reduce survival of pathogens in several systems (including *Brucella suis* (Naroeni and Porte, 2002) and *Bordetella pertussis* (Lamberti et al., 2008). The uptake and persistence of Map in THP-1 cells is mediated, at least in part, by cholesterol dependent mechanisms. Cholesterol depletion using statins or cyclodextrins may be a good candidate for research into Map infection of animals.

### 6.2 Spheroplasts

Many cases of clinically active TB are thought to be the result of reactivation of a latent infection, where actively growing organisms emerge from what was an apparently non-replicative state (Primm et al., 2000). The development of an intracellular phenotype is well documented for many species of mycobacteria (Bermudez et al., 2004). The culturability of Map bacteria decreases after intracellular passage (Bull et al., 2009), suggesting the induction of an non-culturable intracellular phenotype.

Spheroplast forms of mycobacteria have been isolated after prolonged passage through host phagocytes (Chiodini et al., 1986; Hines and Styer, 2003; Markova et al., 2008a; Markova et al., 2008b). In addition, several studies have isolated spheroplast–like forms from CD patient tissue (Chiodini et al., 1986; Hulten et al., 2000). Several theories exist as to how these forms could augment persistence. The loss of cell wall antigens is thought to allow the bacterium to escape immune detection, and reduce energy requirements, both of which would augment intracellular persistence.

An ability to chemically generate spheroplast forms of Map strain Dominic, as demonstrated here, now provides a tool to investigate a role for cell wall deficient forms in the pathogenesis and persistence of mycobacterial infections. Specifically, these forms may be useful for investigating the potential for pathogenic interactions between cell wall deficient forms and human or animal cells.

## 6.3 Map and CD

The involvement of Map in Crohn's disease has been debated since Dalziell first reported pathological similarities to Johne's disease in 1913 (Harris and Barletta, 2001). The isolation of Map bacteria, as well as Map reactive T cells from a significant proportion of CD patients (Naser et al., 2004; Naser et al., 2000; Olsen et al., 2009), supports a role for Map in this disease.

Several genes linked to CD are also involved with susceptibility to mycobacterial disease. Nramp-1 impairment has been linked to leprosy (Worobec, 2009), and Card15 is associated with increased susceptibility to Map infection in cattle (Pinedo et al., 2009). Functional studies of NOD-2, the first genetic element to be implicated in susceptibility to CD (Travassos et al., 2009), show that the CD associated NOD-2 polymorphism impairs killing of bacteria (Perez et al., 2010). NOD-2 is involved in the recognition of Map bacteria by the innate immune system (Ferwerda et al., 2007), specifically, the CD associated polymorphism results in increased susceptibility to mycobacterial infection in mice (Divangahi et al., 2008).

Isolating Map DNA from tissue requires specific extraction conditions. Several studies which showed no association between Map and CD (Cho et al., 1986; Heatley et al., 1975; Sasikala et al., 2009) have been criticised for using inadequate techniques and conditions for extracting mycobacterial DNA (Feller et al., 2008). In addition, many of the drugs commonly used to treat the symptoms of CD (asothioprine, 6-mercaptopurine and methotrexate) have significant, and specific effects on Map growth *in vitro* (Shin and Collins, 2008). Some hypothesise that these drugs are reducing the Map bacterial load, making detection of Map more difficult (Greenstein et al., 2007a; Greenstein et al., 2007b; Shin and Collins, 2008).

Despite the substantial efforts to elucidate a possible pathogenic mechanism by which Map bacteria are able to participate in the aetiology of Crohn's disease, the debate continues as to how this is able to occur without the overwhelming occurrence of bacilli that characterise bovine Johne's and other MAP infections in animals. Many hypotheses exist to try and explain this discrepancy. Some researchers have theorised that Map bacilli could be "hiding out" in gut-associated lymphoid tissue or the lymph system (Pierce, 2009). Others have suggested that the

infective form of Map in humans is cell wall deficient, and therefore is unable to be stained using conventional mycobacterial staining techniques (Chiodini et al., 1986). Interestingly, ovine Johne's disease is classified into two different forms. The first is a multibacillary disease with many ZN-positive Map in tissues and the characteristic widespread inflammation. The second form however, exhibits the same inflammatory symptoms, but few or no ZN positive bacilli can be found in the tissues (Smeed et al., 2007). Research into the aetiology of the differing forms of ovine Johne's is limited at this stage, but the lack of ZN positive bacilli coupled with inflammatory symptoms suggests an interesting area of future research.

### 6.4 Conclusions and future directions

The inactivation of Rab 7 by pathogenic mycobacteria, leading to a failure to bind Rab 7-interacting lysosomal protein (RILP) is well characterised. Experiments to determine the activity of Rab 7 present on the phagosomes of live and killed Map are currently being prepared.

Cholesterol has been shown to augment the persistence of many pathogenic species. However, many of its interactions with bacteria and host cells remain largely uncharacterised. In particular, its role in the short and long term survival of Map in human cells is far from understood. Much more research is needed to fully elucidate the role of cholesterol in Map infection. Given the precedence of cholesterol involvement in other pathogenic species, many techniques required to unravel its involvement are well developed and characterised. Given the growing awareness that cellular cholesterol is a major contributor to bacterial pathogenesis, it is likely that the inter-relationship between Map and cholesterol will be explored more fully in the near future.

The role of spheroplasts in mycobacterial infection is still unknown. The use of a Map specific probe to determine whether the coccoid forms seen in THP-1 cells are in fact Map bacteria will determine whether this avenue of research is viable.

Results presented in this thesis support the hypothesis that Map is able to persist in human cells, in compartments enriched with cholesterol, and positive for Rab 7 and TACO staining. These elements are seen on phagosomes of related pathogenic

mycobacteria. The role of Map in CD continues to be debated. The heterogeneity of Crohn's disease symptoms and pathology suggests that there may be several interacting causes, and even several diseases grouped under the CD umbrella. These results support the hypothesis that Map may be involved in the aetiology of at least a subset of CD cases.

# References


Abubakar, I., D. Myhill, S.H. Aliyu, and P.R. Hunter. 2008. Detection of *Mycobacterium avium* subspecies *paratuberculosis* from patients with Crohn's disease using nucleic acid-based techniques: a systematic review and meta-analysis. *Inflammatory Bowel Disease*. 14:401-410.

Aderem, A., and D. Underhill. 1999. Mechanisms of phagocytosis in macrophages. *Annual Review of Immunology*. 17:593-623.

Almog, Y., E. Shefer, V. Novack, N. Maimon, L. Barski, M. Eizinger, M. Friger, L. Zeller, and A. Danon. 2004. Proir statin therapy is associated with a decreased rate of severe sepsis. *Circulation*:880-885.

Anand, P.K., and D. Kaul. 2005. Downregulation of TACO gene transcription restricts mycobacterial entry/survival within human macrophages. *FEMS Microbiology Letters*. 250:137-144.

Anes, E., P. Peyron, L. Staali, L. Jordao, M. Gutierrez, H. Kress, M. Hagedorn, I. Maridonneau-Parini, M. Skinner, A. Wildeman, S. Kalamidas, M. Kuehnel, and G. Griffiths. 2006. Dynamic life and death interactions between *Mycobacterium smegmatis* and J774 macrophages. *Cellular Microbiology*. 8:939–960.

Bannatine, J., J. Huntley, E. Miltner, J. Stabel, and L. Bermudez. 2003. The *Mycobacterium avium* subsp. *paratuberculosis* 35kDa protein plays a role in invasion of bovine epithelial cells. *Microbiology*. 149:2061-2069.

Baorto, D., Z. Gao, R. Malaviya, M. Dustin, A. van der Merwe, D. Lublin, and S. Abraham. 1997. Survival of FimH-expressing enterobacteria in macrophages relies on glycolipid traffic. *Nature*. 389:636-639.

Baumgart, D.C., and W.J. Sandborn. 2007. Inflammatory bowel disease: clinical aspects and established and evolving therapies. *Lancet*. 369:1641-1657.

Bentley, R.W., J.I. Keenan, R.B. Gearry, M.A. Kennedy, M.L. Barclay, and R.L. Roberts. 2008. Incidence of *Mycobacterium avium* subspecies *paratuberculosis* in a population-based cohort of patients with Crohn's disease and control subjects. *American Journal of Gastroenterology*. 103:1168-1172.

Beran, V., M. Havelkova, J. Kaustove, L. Dvorska, and I. Pavlik. 2006. Cell wall deficient forms of mycobacteria: a review. *Veterinarni Medicina*. 51:365–389.

Berger, S.T., and F.T. Griffin. 2006. A comparison of ovine monocyte-derived macrophage function following infection with *Mycobacterium avium* ssp. *avium* and *Mycobacterium avium* ssp. *paratuberculosis*. *Immunology and Cell Biology*. 84:349-356.

Bermudez, L., M. Petrofsky, and F. Sangari. 2004. Intracellular phenotype of *M. avium* enters macrophages primarily by a macropinocytosis-like mechanism and survives in a compartment that differs from that with extracellular phenotype. *Cell Biology international* 28:411-419.

Bermudez, L., and F. Sangari. 2001. Cellular and molecular mechanisms of internalization of mycobacteria by host cells. *Microbes and Infection*. 3:37-42.

Beron, W., M.G. Gutierrez, M. Rabinovitch, and M.I. Colombo. 2002. *Coxiella burnetii* localizes in a Rab7-labeled compartment with autophagic characteristics. *Infection and Immunity*. 70:5816-5821.

Blowey, R., A. Weaver, and D. Blood. 1997. Diseases and disorders of cattle. Mosby-Wolfe. 219 pp.

Britton, W.J., P.W. Roche, and N. Winter. 1994. Mechanisms of persistence of mycobacteria. *Trends in Microbiology*. 2:284-288.

Bruckert, F., O. Laurent, and M. Satre. 2000. Rab7, a muitifaceted GTP-binding protein regulating access to degradative compartments in eukaryotic cells. *Protoplasma*. 210:108-116.

Brzostek, A., J. Pawelczyk, A. Rumijowska-Galewicz, B. Dziadek, and J. Dziadek. 2009. *Mycobacterium tuberculosis* is able to accumulate and utilize cholesterol. *Journal of Bacteriology*. 191:6584-6591.

Bull, T.J., R. Linedale, J. Hinds, and J. Hermon-Taylor. 2009. A rhodanine agent active against non-replicating intracellular Mycobacterium avium subspecies paratuberculosis. *Gut Pathogens*. 1:1-25.

Carvalho, F.A., N. Barnich, A. Sivignon, C. Darcha, C.H. Chan, C.P. Stanners, and A. Darfeuille-Michaud. 2009. Crohn's disease adherent-invasive *Escherichia coli* colonize and induce strong gut inflammation in transgenic mice expressing human CEACAM. *Journal of Experimental Medicine*. 206:2179-2189.

Catron, D., Y. Lange, J. Borensztajn, M. Sylvester, B. Jones, and K. Haldar. 2004. *Salmonella enterica* serovar *Typhimurium* requires nonsterol precursers of the cholesterol biosynthetic pathway for intracellular proliferation. *Infection and Immunity*. 72:1036-1042.

Chacon, O., L. Bermudez, and R. Barletta. 2004. Johne's Disease, Inflammatory bowel disease, and *Mycobacterium paratuberculosis*. *Annual Review of Microbiology*. 58:329-363.

Chamberlin, W., D.Y. Graham, K. Hulten, H.M. El-Zimaity, M.R. Schwartz, S. Naser, I. Shafran, and F.A. El-Zaatari. 2001. Review article: *Mycobacterium avium* subsp. *paratuberculosis* as one cause of Crohn's disease. *Alimentary Pharmacolological Therapy*. 15:337-346.

Chan, E.D., K.R. Morris, J.T. Belisle, P. Hill, L.K. Remigio, P.J. Brennan, and D.W. Riches. 2001. Induction of inducible nitric oxide synthase-NO* by lipoarabinomannan of *Mycobacterium tuberculosis* is mediated by MEK1-ERK, MKK7-JNK, and NF-kappaB signaling pathways. *Infection and Immunity*. 69:2001-2010.

Chandler, H.M., and R.C. Hamilton. 1975. The protective antigenicity of protoplasts and spheroplasts of a highly protective strain of *Clostridium chauvoei*. *Journal of General Microbiology*. 88:179-183.

Chiodini, R. 1989. Crohns disease and the mycobacterioses: a review and comparison of two disease entities. *Clinical Microbiology Reviews*. 1:90-117.

Chiodini, R., H. van Kruiningen, R. Merkal, W. Thayer, and J. Coutu. 1984. Characteristics of an unclassified mycobacterium species isolated from patients with Crohn's disease. *Journal of Clinical Microbiology*. 20:966-971.

Chiodini, R.J., H.J. Van Kruiningen, W.R. Thayer, and J.A. Coutu. 1986. Spheroplastic phase of mycobacteria isolated from patients with Crohn's disease. *Journal of Clinical Microbiology*. 24:357-363.

Cho, S.N., P.J. Brennan, H.H. Yoshimura, B.I. Korelitz, and D.Y. Graham. 1986. Mycobacterial aetiology of Crohn's disease: serologic study using common mycobacterial antigens and a species-specific glycolipid antigen from *Mycobacterium paratuberculosis*. *Gut*. 27:1353-1356.

Choi, Y.A., B.R. Chin, D.H. Rhee, H.G. Choi, H.W. Chang, J.H. Kim, and S.H. Baek. 2004. Methyl-beta-cyclodextrin inhibits cell growth and cell cycle arrest via a prostaglandin $E_2$ independent pathway. *Experimental Molecular Medicine*. 36:78-84.

Christian, A.E., M.P. Haynes, M.C. Phillips, and G.H. Rothblat. 1997. Use of cyclodextrins for manipulating cellular cholesterol content. *Journal of Lipid Research*. 38:2264-2272.

Clemens, D.L., and M.A. Horwitz. 1995. Characterization of the *Mycobacterium tuberculosis* phagosome and evidence that phagosomal maturation is inhibited. *Journal of Experimental Medicine*. 181:257-270.

Clemens, D.L., B.Y. Lee, and M.A. Horwitz. 2000a. Deviant expression of Rab5 on phagosomes containing the intracellular pathogens *Mycobacterium tuberculosis* and *Legionella pneumophila* is associated with altered phagosomal fate. *Infection and Immunity*. 68:2671-84.

Clemens, D.L., B.Y. Lee, and M.A. Horwitz. 2000b. *Mycobacterium tuberculosis* and *Legionella pneumophila* phagosomes exhibit arrested maturation despite acquisition of Rab7. *Infection and Immunity*. 68:5154-5166.

Collins, D.M., M. De Zoete, and S.M. Cavaignac. 2002. *Mycobacterium avium* subsp. *paratuberculosis* strains from cattle and sheep can be distinguished by a PCR test based on a novel DNA sequence difference. *Journal of Clinical Microbiology*. 40:4760-4762.

Collins, M., D. Gabric, and G. Lisle. 1990. Identification of two groups of *Mycobacterium paratuberculosis* strains by restriction endonuclease analysis and DNA hybridization. *Journal of Clinical Microbiology*. 28:1591-1596.

Cougoule, C., P. Constant, G. Etienne, M. Daffe, and I. Maridonneau-Parini. 2002. Lack of fusion of azurophil granules with phagosomes during phagocytosis of *Mycobacterium smegmatis* by human neutrophils is not actively controlled by the bacterium. *Infection and Immunity*. 70:1591-1598.

Cryz, S.J., Jr., E. Furer, and R. Germanier. 1982. Effect of chemical and heat inactivation on the antigenicity and immunogenicity of *Vibrio cholerae*. *Infection and Immunity*. 38:21-26.

Darnelishvilli, L., S. Cirillo, J. Cirillo, and L. Bermudez. 2007. Virulent mycobacteria and the many aspects of macrophage uptake. *Future Microbiology*. 2:451-464.

Day, A. 1995. Electron microscopy laboratory manual. 61.

de Chastellier, C. 2009. The many niches and strategies used by pathogenic mycobacteria for survival within host macrophages. *Immunobiology*. 214:526-542.

de Chastellier, C., and L. Thilo. 2006. Cholesterol depletion in *Mycobacterium avium* infected macrophages overcomes the block in phagosome maturation and leads to the reversible sequestration of viable mycobacteria in phagolysosome-derived autophagic vacuoles. *Cellular Microbiology*. 8:242–256.

Deghmane, A., H. Soulhine, H. Bach, K. Sendide, S. Itoh, A. Tam, S. Noubir, A. Taiai, R. Lo, S. Toyoshima, Y. Av-Gay, and Z. Hmama. 2007. Lipoamide dehydrogenase mediates retention of coronin-1 on BCG vacuoles, leading to arrest in phagosome maturation. *Journal of Cell Science*. 120:2796-2806.

Dequcker, C., E. N'Diaye, N. Cabec, M. Rittig, J. Prandi, and I. Parini. 1999. The mannose receptor mediates uptake of pathogenic and nonpathogenic mycobacteria and bypass bactericidal response in human macrophages. *Infection and Immunology*. 67:469-477.

Desjardins, M., J.E. Celis, G. van Meer, H. Dieplinger, A. Jahraus, G. Griffiths, and L.A. Huber. 1994a. Molecular characterization of phagosomes. *Journal of Biological Chemistry*. 269:32194-32200.

Desjardins, M., L.A. Huber, R.G. Parton, and G. Griffiths. 1994b. Biogenesis of phagolysosomes proceeds through a sequential series of interactions with the endocytic apparatus. *Journal of Cell Biology*. 124:677-688.

Divangahi, M., S. Mostowy, F. Coulombe, R. Kozak, L. Guillot, F. Veyrier, K.S. Kobayashi, R.A. Flavell, P. Gros, and M.A. Behr. 2008. NOD2-deficient mice

have impaired resistance to *Mycobacterium tuberculosis* infection through defective innate and adaptive immunity. *Journal of Immunology*. 181:7157-7165.

Drabikowski, W., E. Lagwinska, and M.G. Sarzala. 1973. Filipin as a fluorescent probe for the location of cholesterol in the membranes of fragmented sarcoplasmic reticulum. *Biochim Biophys Acta*. 291:61-70.

El-Zaatari, F., M. Osato, and D. Graham. 2001. Etiology of Crohn's disease: the role of *Mycobacterium avium paratuberculosis*. *Trends in Molecular Medicine*. 7:247-252.

Elsaghier, A., C. Prantera, C. Moreno, and J. Ivanyi. 1992. Antibodies to *Mycobacterium paratuberculosis*-specific protein antigens in Crohn's disease. *Clinical Experimental Immunology*. 90:503-508.

Emery, D., and R. Whittington. 2004. An evaluation of mycophage therapy, chemotherapy and vaccination for control of *Mycobacterium avium* subsp. *paratuberculosis* infection. *Veterinary Microbiology*. 104:143-155.

Favila-Humara, L., G. Chavez-Gris, E. Carrillo-Casas, and R. Hernandez-Castro. 2010. *Mycobacterium avium* subsp. *paratuberculosis* Detection in Individual and Bulk Tank Milk Samples from Bovine Herds and Caprine Flocks. *Foodborne Pathogens and Disease*. 7:1-5.

Feller, M., K. Huwiler, R. Stephan, E. Altpeter, A. Shang, H. Furrer, G. Pfyffer, T. Jemmi, A. Baumgartner, and M. Egger. 2008. *Mycobacterium avium* subspecies *paratuberculosis* and Crohn's disease: a systematic review and meta-analysis. *Lancet Infectious diseases*. 7:607-613.

Feola, R., M. Collins, and C. Czuprynski. 1999. Hormonal modulation of phagocytosis and intracellular growth of *Mycobacterium avium* subsp. *paratuberculosis* in bovine peripheral blood monocytes. *Microbial Pathogenesis*. 26:1-11.

Ferrari, G., H. Langen, M. Naito, and J. Pieters. 1999. A coat protein on phagosomes involved in the intracellular survival of mycobacteria. *Cell*. 97:435-447.

Ferwerda, G., B.J. Kullberg, D.J. de Jong, S.E. Girardin, D.M. Langenberg, R. van Crevel, T.H. Ottenhoff, J.W. Van der Meer, and M.G. Netea. 2007. *Mycobacterium paratuberculosis* is recognized by Toll-like receptors and NOD2. *Journal of Leukocyte Biology*. 82:1011-1018.

Flaminio, M.J., B.R. Rush, E.G. Davis, K. Hennessy, W. Shuman, and M.J. Wilkerson. 2002. Simultaneous flow cytometric analysis of phagocytosis and oxidative burst activity in equine leukocytes. *Veterinary Research Communications*. 26:85-92.

Frehel, C., C. de Chastellier, C. Offredo, and P. Berche. 1991. Intramacrophage growth of *Mycobacterium avium* during infection of mice. *Infection and Immunity*. 59:2207-2214.

Fujino, M., S. Miura, H. Tanigawa, Y. Matsuo, and K. Saku. 2005. Counteracting effects of high density lipoprotein-cholesterol subfractions on statin-induced growth arrest. *Cardiovascular Drugs and Therapy*. 19:113–118.

Gatfield, J., and J. Pieters. 2000. Essential role for cholesterol in entry of mycobacteria into macrophages. *Science*. 288:1647-1650.

Gearry, R., A. Richardson, C. Frampton, J. Collett, M. Burt, B. Chapman, and M. Barclay. 2006. High Incidence of Crohn's Disease in Canterbury, New Zealand: Results of an Epidemiologic Study. *Inflammatory Bowel Disorders*. 12:936-943.

Ghigo, E., C. Capo, C.H. Tung, D. Raoult, J.P. Gorvel, and J.L. Mege. 2002. Coxiella burnetii survival in THP-1 monocytes involves the impairment of phagosome maturation: IFN-gamma mediates its restoration and bacterial killing. *J Immunol*. 169:4488-95.

Gimpl, G., K. Burger, and F. Farenholz. 1997. Cholesterol as a modulator of receptor function. *Biochemistry*. 36:10959-10974.

Goluszko, P., and B. Nowicki. 2005. Membrane cholesterol: a crucial molecule affecting interactions of microbial pathogens with mammalian cells. *Infection and Immunity*. 73:7791-7796.

Gomes, M., S. Paul, A. Moreira, R. Appelberg, M. Rabinovich, and G. Kaplan. 1999. Survival of *Mycobacterium avium* and *Mycobacterium tuberculosis* in acidified vacuoles of murine macrophages. *Infection and Immunity*. 67:3199-3206.

Goswami, T., S. Joardar, G. Ram, R. Banerjee, and D. Singh. 2000. Association of *Mycobacterium paratuberculosis* in Crohn's disease and Johne's disease: A possible zoonotic threat. *Current Science*. 79:1076-1081.

Goyette, P., C. Labbé, T. Trinh, R. Xavier, and J. Rioux. 2007. Molecular pathogenesis of inflammatory bowel disease: genotypes, phenotypes and personalized medicine. *Annals of Medicine*. 39:177-199.

Greenstein, R. 2003. Is Crohn's disease caused by a mycobacterium? Comparisons with Leprosy, Tuberculosis, and Johnes disease. *The Lancet- Infectious Diseases*. 3:507-514.

Greenstein, R.J., L. Su, V. Haroutunian, A. Shahidi, and S.T. Brown. 2007a. On the action of methotrexate and 6-mercaptopurine on *M. avium* subspecies *paratuberculosis*. *PLoS One*. 2:e161.

Greenstein, R.J., L. Su, A. Shahidi, and S.T. Brown. 2007b. On the action of 5-amino-salicylic acid and sulfapyridine on *M. avium* including subspecies *paratuberculosis*. *PLoS One*. 2:e516.

Guenin-Mace, L., R. Simeone, and C. Demangel. 2009. Lipids of Pathogenic Mycobacteria: Contributions to Virulence and Host Immune Suppression. *Transboundary and Emerging Diseases*. 56:255–268.

Gui, G., P. Thomas, M. Tizard, J. Lake, J. Sanderson, and J. Hermon-Taylor. 1997. Two-year outcomes analysis of Crohn's Disease treated with rifabutin and macrolide antibiotics. *Journal of Antimicrobial Chemotherapy*. 39:393-400.

Harris, N.B., and R.G. Barletta. 2001. *Mycobacterium avium* subsp. *paratuberculosis* in Veterinary Medicine. *Clinical Microbiological Reviews*. 14:489-512.

Harrison, R.E., J.H. Brumell, A. Khandani, C. Bucci, C.C. Scott, X. Jiang, B.B. Finlay, and S. Grinstein. 2004. Salmonella impairs RILP recruitment to Rab7 during maturation of invasion vacuoles. *Molecular Biology of the Cell*. 15:3146-3154.

Harrison, R.E., C. Bucci, O.V. Vieira, T.A. Schroer, and S. Grinstein. 2003. Phagosomes fuse with late endosomes and/or lysosomes by extension of membrane protrusions along microtubules: role of Rab7 and RILP. *Molecular and Cellular Biology*. 23:6494-6506.

Hart, P., M. Young, A. Gordon, and K. Sullivan. 1987. Inhibition of phagosome-lysosome fusion in macrophages by certain mycobacteria can be explained by inhibition of lysosomal movements observed after phagocytosis. *Journal of Experimental Medicine*. 166:933-946.

Hasan, Z., M. Ashraf, A. Tayyebi, and R. Hussain. 2006. *M. leprae* inhibits apoptosis in THP-1 cells by downregulation of Bad and Bak and upregulation of Mcl-1 gene expression. *BMC Microbiology*. 6:78.

Haugland, R. 2005. The Handbook: A guide to fluorescent probes and labeling technologies. Invitrogen, Calsbad, CA USA. 421 pp.

Heatley, R.V., P.M. Bolton, E. Owen, W.J. Williams, and L.E. Hughes. 1975. A search for a transmissible agent in Crohn's disease. *Gut*. 16:528-532.

Hermanson, G. 2008. Bioconjugate techniques 2e. Academic Press. 1202 pp.

Hett, E.C., and E.J. Rubin. 2008. Bacterial growth and cell division: a mycobacterial perspective. *Microbiology and Molecular Biology Reviews*. 72:126-156.

Hines, M., and E. Styer. 2003. Preliminary characterization of chemically generated *Mycobacterium avium* subsp. *paratuberculosis* cell wall deficient forms (Spheroplasts). *Veterinary Microbiology* 95:247–258.

Hostetter, J., R. Kagan, and E. Steadham. 2005. Opsonization effects on *Mycobacterium avium* subsp. *paratuberculosis*- macrophage interactions. *Clinical and Diagnostic Laboratory Immunology*. 12:793-796.

Hulten, K., T.J. Karttunen, H.M. El-Zimaity, S.A. Naser, A. Almashhrawi, D.Y. Graham, and F.A. El-Zaatari. 2000. In situ hybridization method for studies of cell wall deficient *M. paratuberculosis* in tissue samples. *Veterinary Microbiology*. 77:513-518.

Huynh, K., E. Gershenzon, and S. Grinstein. 2008. Cholesterol accumulation by macrophages impairs phagosome maturation. *Journal of Biological Chemistry*. 283:35745-35755.

Ibrahim-Granet, O., B. Philippe, H. Boleti, E. Boisvieux-Ulrich, D. Grenet, M. Stern, and J.P. Latge. 2003. Phagocytosis and intracellular fate of *Aspergillus fumigatus* conidia in alveolar macrophages. *Infection and Immunity*. 71:891-903.

Jaravata, C.V., W.L. Smith, G.J. Rensen, J. Ruzante, and J.S. Cullor. 2007. Survey of ground beef for the detection of *Mycobacterium avium paratuberculosis*. *Foodborne Pathogenic Disease*. 4:103-106.

Jayachandran, R., J. Gatfield, J. Massner, I. Albrecht, B. Zanolari, and J. Pieters. 2008. RNA interference in J774 macrophages reveals a role for coronin 1 in mycobacterial trafficking but not in actin-dependent processes. *Molecular Biology of the Cell*. 19:1241-1251.

Jayachandran, R., V. Sundaramurthy, B. Combaluzier, P. Mueller, H. Korf, K. Huygen, T. Miyazaki, I. Albrecht, J. Massner, and J. Pieters. 2007. Survival of mycobacteria in macrophages is mediated by coronin 1-dependent activation of calcineurin. *Cell*. 130:37-50.

Jozefowski, S., A. Sobota, and K. Kwiatkowska. 2008. How *Mycobacterium tuberculosis* subverts host immune responses. *Bioessays*. 30:943-954.

Juste, R.A., N. Elguezabal, J.M. Garrido, A. Pavon, M.V. Geijo, I. Sevilla, J.L. Cabriada, A. Tejada, F. Garcia-Campos, R. Casado, I. Ochotorena, A. Izeta, and R.J. Greenstein. 2008. On the prevalence of *M. avium* subspecies *paratuberculosis* DNA in the blood of healthy individuals and patients with inflammatory bowel disease. *PLoS One*. 3:e2537.

Kang, P.B., A.K. Azad, J.B. Torrelles, T.M. Kaufman, A. Beharka, E. Tibesar, L.E. DesJardin, and L.S. Schlesinger. 2005. The human macrophage mannose receptor directs *Mycobacterium tuberculosis* lipoarabinomannan-mediated phagosome biogenesis. *Journal of Experimental Medicine*. 202:987-999.

Kaul, D. 2008. Coronin-1A epigenomics governs mycobacterial persistence in tuberculosis. *FEMS Microbiology Letters*. 278:4-10.

Kaul, D., P. Anand, and I. Verma. 2004. Cholesterol-sensor initiates *M. tuberculosis* entry into human macrophages. *Molecular and Cellular Biochemistry*. 258:219–222.

Kelley, V.A., and J.S. Schorey. 2003. Mycobacterium's arrest of phagosome maturation in macrophages requires Rab5 activity and accessibility to iron. *Molecular Biology of the Cell*. 14:3366-3377.

Kitano, M., M. Nakaya, T. Nakamura, S. Nagata, and M. Matsuda. 2008. Imaging of Rab5 activity identifies essential regulators for phagosome maturation. *Nature*. 453:241-245.

Knosel, T., C. Schewe, N. Petersen, M. Dietel, and I. Petersen. 2009. Prevalence of infectious pathogens in Crohn's disease. *Pathological Research and Practice*. 205:223-230.

Kudo, K., H. Sano, H. Takahashi, K. Kuronuma, S. Yokota, N. Fujii, K. Shimada, I. Yano, Y. Kumazawa, D. Voelker, S. Abe, and Y. Kuroki. 2004. Pulmonary collectins enhance phagocytosis of *Mycobacterium avium* through Increased Activity of Mannose Receptor *The Journal of Immunology*. 172:7592-7602.

Kurosu, H., and T. Katada. 2001. Association of phosphatidylinositol 3-kinase composed of p110beta-catalytic and p85-regulatory subunits with the small GTPase Rab5. *Journal of Biochemistry*. 130:73-78.

Kurup, I., and P. Mahadevan. 1982. Cholesterol metobolism of macrophages in relation to the presence of *Mycobacterium leprae*. *Journal of Bioscience*. 4:307–316.

Lamberti, Y., M.L. Perez Vidakovics, L.W. van der Pol, and M.E. Rodriguez. 2008. Cholesterol-rich domains are involved in *Bordetella pertussis* phagocytosis and intracellular survival in neutrophils. *Microbial Pathogenesis*. 44:501-511.

Lang, D., F. Dohle, M. Terstesse, P. Bangen, C. August, H.G. Pauels, and S. Heidenreich. 2002. Down-regulation of monocyte apoptosis by phagocytosis of platelets: involvement of a caspase-9, caspase-3, and heat shock protein 70-dependent pathway. *Journal of Immunology*. 168:6152-6158.

Lapaquette, P., A.L. Glasser, A. Huett, R.J. Xavier, and A. Darfeuille-Michaud. 2009. Crohn's disease-associated adherent-invasive *E. coli* are selectively favoured by impaired autophagy to replicate intracellularly. *Cellular Microbiology*. 12:99-113.

Lawrence, J., D. Saslowsky, J. Edwardson, and R. Henderson. 2003. Real-time analysis of the effects of cholesterol on lipid raft behaviour using atomic force microscopy. *Biophysical Journal*. 84:1827-1832.

Le Cabec, V., C. Cols, and I. Maridonneau-Parini. 2000. Nonopsonic phagocytosis of zymosan and *Mycobacterium kansasii* by CR3 (CD11b/CD18) involves distinct molecular determinants and is or is not coupled with NADPH oxidase activation. *Infection and Immunity*. 68:4736-4745.

Lewin, A., D. Baus, E. Kamal, F. Bon, R. Kunisch, S. Maurischat, M. Adonopoulou, and K. Eich. 2008. The mycobacterial DNA-binding protein 1 (MDP1) from *Mycobacterium bovis* BCG influences various growth characteristics. *Biomed Central Microbiology*. 8:1-12.

Lilenbaum, W., C. Marassi, and W. Oelemann. 2007. Paratuberculosis: an update. *Brazilian Journal of Microbiology* 38:580-590.

Lioke, J., D. Shabti, R. Neuhut, S. Malizky, E. Lu, J. Husemann, I. Goldberg, and S. Silverstein. 2004. Statin inhibition of Fc-mediated phagocytosis by macrophages is modulated by cell activation and cholesterol *Arteriosclerosis, Thrombosis, and Vascular Biology*:2051-2056.

Malik, Z., G. Denning, and D. Kusner. 2000. Inhibition of Ca signalling by *Mycobacterium tuberculosis* is associated with reduced phagosome-lysosome fusion and increased survival within human macrophages. *Journal of Experimental Medicine*. 191:287-302.

Markesich, D.C., D.Y. Graham, and H.H. Yoshimura. 1988. Progress in culture and subculture of spheroplasts and fastidious acid-fast bacilli isolated from intestinal tissues. *Journal of Clinical Microbiology*. 26:1600-1603.

Markova, N., Michailova L, M. Jourdanova, V. Kussovski, V. Valcheva, I. Mokrousov, and T. Radoucheva. 2008a. Exhibition of persistent and drug-tolerant L-form habit of *Mycobacterium tuberculosis* during infection in rats. *Central European Journal of Biology*. 3:407–416.

Markova, N., L. Michailova, V. Kussovski, and M. Jourdanova. 2008b. Formation of Persisting Cell Wall Deficient Forms of *Mycobacterium bovis* BCG during Interaction with Peritoneal Macrophages in Guinea Pigs. *Electronic Journal of Biology*:1-10.

Marques, M., V. Antonio, E. Sarno, P. Brennan, and M. Pessolani. 2001. Binding of alpha-2 laminins by pathogenic and non-pathogenic mycobacteria and adherence to schwann cells. *Journal of Medical Microbiology*. 50:23-28.

Martens, G., M. Arikan, J. Lee, F. Ren, T. Vallerskog, and H. Kornfeld. 2008. Hypercholesterolemia impairs immunity to tuberculosis. *Infectious Immunology*. 76:3464–3472.

Mattman, L. 2001. Cell wall deficient forms: stealth pathogens. CRC Press. 416 pp.

Miner, M.D., J.C. Chang, A.K. Pandey, C.M. Sassetti, and D.R. Sherman. 2009. Role of cholesterol in *Mycobacterium tuberculosis* infection. *Indian Journal of Experimental Biology*. 47:407-411.

Moss, M.T., J.D. Sanderson, M.L. Tizard, J. Hermon-Taylor, F.A. el-Zaatari, D.C. Markesich, and D.Y. Graham. 1992. Polymerase chain reaction detection of *Mycobacterium paratuberculosis* and *Mycobacterium avium* subsp *silvaticum* in long term cultures from Crohn's disease and control tissues. *Gut*. 33:1209-1213.

Motiwala, A.S., M. Strother, A. Amonsin, B. Byrum, S.A. Naser, J.R. Stabel, W.P. Shulaw, J.P. Bannantine, V. Kapur, and S. Sreevatsan. 2003. Molecular epidemiology of *Mycobacterium avium* subsp. *paratuberculosis*: evidence for limited strain diversity, strain sharing, and identification of unique targets for diagnosis. *Journal of Clinical Microbiology*. 41:2015-2026.

Naroeni, A., and F. Porte. 2002. Role of cholesterol and the ganglioside GM1 in entry and short-term survival of *Brucella suis* in murine macrophages. *Infection and Immunity*. 70:1640-1644.

Naser, S.A., G. Ghobrial, C. Romero, and J.F. Valentine. 2004. Culture of *Mycobacterium avium* subspecies *paratuberculosis* from the blood of patients with Crohn's disease. *Lancet*. 364:1039-1044.

Naser, S.A., D. Schwartz, and I. Shafran. 2000. Isolation of *Mycobacterium avium* subsp *paratuberculosis* from breast milk of Crohn's disease patients. *American Journal of Gastroenterology*. 95:1094-1095.

Neyrolles, O., R. Hernandez-Pando, F. Pietri-Rouxel, P. Fornes, L. Tailleux, J.A. Barrios Payan, E. Pivert, Y. Bordat, D. Aguilar, M.C. Prevost, C. Petit, and B. Gicquel. 2006. Is adipose tissue a place for *Mycobacterium tuberculosis* persistence? *PLoS One*. 1:e43.

Nguyen, L., and J. Pieters. 2005. The Trojan horse: survival tactics of pathogenic mycobacteria in macrophages. *Trends Cell Biol*. 15:269-76.

O'Reilly, L.M., and C.J. Daborn. 1995. The epidemiology of *Mycobacterium bovis* infections in animals and man: a review. *Tuberule Lung Disease*. 76 Suppl 1:1-46.

Olsen, I., S. Tollefsen, C. Aagaard, L.J. Reitan, J.P. Bannantine, P. Andersen, L.M. Sollid, and K.E. Lundin. 2009. Isolation of *Mycobacterium avium* subspecies *paratuberculosis* reactive CD4 T cells from intestinal biopsies of Crohn's disease patients. *PLoS One*. 4:Epub ahead of print.

Ott, S., S. Wells, and B. Wagner. 1999. Herd-level economic losses associated with Johne's disease on US dairy operations. *Preventative Veterinary Medicine*. 40:179-192.

Pandey, A., and C. Sassetti. 2008. Mycobacterial persistence requires the utilization of host cholesterol. *Proceedings of the National Acadamy of Science*. 105:4376–4380.

Parish, T., and N. Stoker. 1998. Mycobacteria protocols. Humana Press. 472 pp.

Patel, D., L. Danelishvili, Y. Yamazaki, M. Alonso, M.L. Paustian, J.P. Bannantine, L. Meunier-Goddik, and L.E. Bermudez. 2006. The ability of *Mycobacterium avium* subsp. *paratuberculosis* to enter bovine epithelial cells is influenced by preexposure to a hyperosmolar environment and intracellular passage in bovine mammary epithelial cells. *Infection and Immunity*. 74:2849-2855.

Perez, L.H., M. Butler, T. Creasey, J. Dzink-Fox, J. Gounarides, S. Petit, A. Ropenga, N. Ryder, K. Smith, P. Smith, and S.J. Parkinson. 2010. Direct bacterial killing in vitro by recombinant Nod2 is compromised by Crohn's disease-associated mutations. *PLoS One*. 5:e10915.

Perskvist, N., K. Roberg, A. Kulyte, and O. Stendahl. 2002. Rab5a GTPase regulates fusion between pathogen-containing phagosomes and cytoplasmic organelles in human neutrophils. *Journal of Cell Science*. 115:1321-1330.

Peyron, P., C. Bordier, E. Diaye, and I. Maridonneau-Parini. 2000. Nonopsonic phagocytosis of *Mycobacterium kansasii* by human neutrophils depends on cholesterol and Is mediated by CR3 associated with glycosylphosphatidylinositol-anchored proteins. *The Journal of Immunology*. 165:5186–5191.

Peyron, P., J. Vaubourgeix, Y. Poquet, F. Levillain, C. Botanch, F. Bardou, M. Daffe, J.F. Emile, B. Marchou, P.J. Cardona, C. de Chastellier, and F. Altare. 2008. Foamy macrophages from tuberculous patients' granulomas constitute a nutrient-rich reservoir for *M. tuberculosis* persistence. *PLoS Pathogens*. 4:e1000204.

Pierce, E.S. 2009. Where are all the *Mycobacterium avium* subspecies *paratuberculosis* in patients with Crohn's disease? *PLoS Pathogens*. 5:e1000234.

Pikaar, J., W. Voorhout, L. van Golde, J. Verhoef, J. van Strijp, and J. van Iwaarden. 1995. Opsonic activities of surfactant proteins A and D n phagocytosis of gram nagative bacteria by alveolar macrophages. *The Journal of Infectious Diseases*. 172:481-489

Pinedo, P.J., C.D. Buergelt, G.A. Donovan, P. Melendez, L. Morel, R. Wu, T.Y. Langaee, and D.O. Rae. 2009. Association between CARD15/NOD2 gene polymorphisms and paratuberculosis infection in cattle. *Veterinary Microbiology*. 134:346-352.

Polito, J.M., 2nd, B. Childs, E.D. Mellits, A.Z. Tokayer, M.L. Harris, and T.M. Bayless. 1996. Crohn's disease: influence of age at diagnosis on site and clinical type of disease. *Gastroenterology*. 111:580-586.

Pottosin, I., G. Valencia-Cruz, E. Bonales-Alatorre, S. Shabala, and O. Dobrovinskaya. 2007. Methyl-beta-cyclodextrin reversibly alters the gating of lipid rafts-associated Kv1.3 channels in Jurkat T lymphocytes. *Pflugers archive: European Journal of Physiology* 454:235-244.

Primm, T.P., S.J. Andersen, V. Mizrahi, D. Avarbock, H. Rubin, and C.E. Barry, 3rd. 2000. The stringent response of *Mycobacterium tuberculosis* is required for long-term survival. *Journal of Bacteriology*. 182:4889-4898.

Pucadyil, T.J., P. Tewary, R. Madhubala, and A. Chattopadhyay. 2004. Cholesterol is required for *Leishmania donovani* infection: implications in leishmaniasis. *Molecular Biochemistry and Parasitology*. 133:145-152.

Rinno, J., J. Gmeiner, J.R. Golecki, and H. Mayer. 1980. Localization of enterobacterial common antigen: *Proteus mirabilis* and its various L-forms. *Journal of Bacteriology*. 141:822-827.

Rise, P., C. Colombo, and C. Galli. 1997. Effects of simvastatin on the metabolism of polyunsaturated fatty acids and on glycerolipid, cholesterol, and de novo lipid synthesis in THP-1 cells. *Journal of Lipid Research*. 38:1299-1307.

Rodriguez, M.E., S.M. Hellwig, D.F. Hozbor, J. Leusen, W.L. van der Pol, and J.G. van de Winkel. 2001. Fc receptor-mediated immunity against *Bordetella pertussis*. *Journal of Immunology*. 167:6545-6551.

Rojas, M., L.F. Garcia, J. Nigou, G. Puzo, and M. Olivier. 2000. Mannosylated lipoarabinomannan antagonizes *Mycobacterium tuberculosis*-induced macrophage apoptosis by altering Ca+2-dependent cell signaling. *Journal of Infectious Disease*. 182:240-251.

Root, R.K., A.S. Rosenthal, and D.J. Balestra. 1972. Abnormal bactericidal, metabolic, and lysosomal functions of Chediak-Higashi Syndrome leukocytes. *Journal of Clinical Investigation*. 51:649-665.

Rosai, J. 2004. Rosai and Ackerman's Surgical Pathology. Mosby. 3000 pp.

Rosch, J.W., A.R. Boyd, E. Hinojosa, T. Pestina, Y. Hu, D.A. Persons, C.J. Orihuela, and E.I. Tuomanen. 2010. Statins protect against fulminant pneumococcal infection and cytolysin toxicity in a mouse model of sickle cell disease. *Journal of Clinical Investigation*. 120:627-635.

Rosenberger, C., J. Burumell, and B. Finlay. 2000. Microbial pathogenesis: Lipid rafts as pathogen portals. *Current Biology*. 10:823-825.

Rowe, M., I. Grant, L. Dundee, and H. Ball. 2000. Heat resistance of *Mycobacterium avium* subsp. *paratuberculosis* in milk. *Irish Journal of Agricultural and Food Research*. 39:203-208.

Rumsey, J., J. Valentine, and S. Naser. 2006. Inhibition of phagosome maturation and survival of *Mycobacterium avium* subspecies *paratuberculosis* in polymorphonuclear leukocytes from Crohn's disease patients. *Medical Science Monitor*. 12:130-139.

Sandermann, H., Jr., and J.L. Strominger. 1972. Purification and properties of C 55 - isoprenoid alcohol phosphokinase from *Staphylococcus aureus*. *Journal of Biological Chemistry*. 247:5123-5131.

Sasikala, M., D.N. Reddy, N. Pratap, S.K. Sharma, P.R. Balkumar, A. Sekaran, R. Banerjee, and D.B. Reddy. 2009. Absence of *Mycobacterium avium* subspecies *paratuberculosis*-specific IS900 sequence in intestinal biopsy tissues of Indian patients with Crohn's disease. *Indian Journal of Gastroenterology*. 28:169-174.

Schaffler, A., J. Scholmerich, and C. Buchler. 2005. Mechanisms of disease: adipocytokines and visceral adipose tissue--emerging role in nonalcoholic fatty liver disease. *National Clinical Practice of Gastroenterology and Hepatology*. 2:273-280.

Schuller, S., J. Neefjes, T. Ottenhoff, J. Thole, and D. Young. 2001. Coronin is involved in uptake of *Mycobacterium bovis* BCG in human macrophages but not in phagosome maintenance. *Cellular Microbiology*. 3:785-793.

Sechi, L.A., M. Mura, E. Tanda, A. Lissia, G. Fadda, and S. Zanetti. 2004. *Mycobacterium avium* sub. *paratuberculosis* in tissue samples of Crohn's disease patients. *New Microbiology*. 27:75-77.

Shanahan, F. 2002. Crohn's Disease. *The Lancet*. 359:62-69.

Shin, J., and S. Abraham. 2001. Caveolae as portals of entry for microbes. *Microbes and Infection*. 3:755-761.

Shin, S., and M. Collins. 2008. Thiopurine Drugs Azathioprine and 6-Mercaptopurine Inhibit *Mycobacterium paratuberculosis* Growth In Vitro. *Antimicrobial Agents and Chemotherapy*. 52:418–426.

Sibley, L.D., L.B. Adams, and J.L. Krahenbuhl. 1990. Inhibition of interferon-gamma-mediated activation in mouse macrophages treated with lipoarabinomannan. *Clinical Experimental Immunology*. 80:141-148.

Smeed, J.A., C.A. Watkins, S.M. Rhind, and J. Hopkins. 2007. Differential cytokine gene expression profiles in the three pathological forms of sheep paratuberculosis. *BMC Veterinary Research*. 3:18.

Smit, J., C. Meijer, F. Decary, and T. Feltkamp-Vroom. 1974. Paraformaldehyde fixation in immunofluorescence and immunoelectron microscopy. Preservation of tissue and cell surface membrane antigens. *Journal of Immunological methods*. 6:93-98.

Soccio, R.E., and J.L. Breslow. 2004. Intracellular cholesterol transport. *Arteriosclerotic Thrombic Vascular Biology*. 24:1150-1160.

Sturgill-Koszycki, S., P.H. Schlesinger, P. Chakraborty, P.L. Haddix, H.L. Collins, A.K. Fok, R.D. Allen, S.L. Gluck, J. Heuser, and D.G. Russell. 1994. Lack of acidification in Mycobacterium phagosomes produced by exclusion of the vesicular proton-ATPase. *Science*. 263:678-81.

Sun, J., A. Deghmane, H. Soualhine, T. Hong, C. Bucci, A. Solodkin, and Z. Hmama. 2007. *Mycobacterium Bovis* BCG disrupts the interaction of Rab7 with RILP contributing to inhibition of phagosome maturation. *Journal of Leukocyte Biology*. 82:1-9.

Sung, N., and M.T. Collins. 1998. Thermal tolerance of Mycobacterium paratuberculosis. *Appl Environ Microbiol*. 64:999-1005.

Thacore, H., and H.P. Willett. 1966. The formation of spheroplasts of *Mycobacterium tuberculosis* in tissue culture cells. *American Reveue of Respiratory Disease*. 93:786-796.

Toba, K., E.F. Winton, and R.A. Bray. 1992. Improved Staining Method for the Simultaneous Flow Cytofluorometric Analysis of DNA Content, S-Phase Fraction, and Surface Phenotype Using Single Laser Instrumentation. *Cytometry*. 13:60-67.

Torrado, E., A. Fraga, A. Castro, P. Stragier, W. Meyers, F. Portaels, M. Silva, and J. Pedrosa. 2007. Evidence for an intramacrophage growth phase of *Mycobacterium ulcerans*. *Infection and Immunity*. 75:977-987.

Travassos, L.H., L.A. Carneiro, M. Ramjeet, S. Hussey, Y.G. Kim, J.G. Magalhaes, L. Yuan, F. Soares, E. Chea, L. Le Bourhis, I.G. Boneca, A. Allaoui, N.L. Jones, G. Nunez, S.E. Girardin, and D.J. Philpott. 2009. Nod1 and Nod2 direct autophagy by recruiting ATG16L1 to the plasma membrane at the site of bacterial entry. *Nature Immunology*. 11:55-62.

Tsuchiya, S., M. Yamabe, Y. Yamaguchi, Y. Kobayashi, T. Konno, and K. Tada. 1980. Establishment and characterization of a human acute monocytic leukemia cell line (THP-1). *International Journal of Cancer*. 26:171-176.

Udou, T., M. Ogawa, and Y. Mizuguchi. 1982. Spheroplast formation of *Mycobacterium smegmatis* and morphological aspects of their reversion to the bacillary form. *Journal of Bacteriology*. 151:1035-1039.

Valentin-Weigand, P., and R. Goethe. 1999. Pathogenesis of *Mycobacterium avium* subspecies *paratuberculosis* infections in ruminants: still more questions than answers. *Microbes and infection*. 1:1121−1127.

van der Giessen, J., R. Haring, and B. van der Zeijst. 1994. Comparison of the 23s ribosomal RNA genes and the spacer region between the 16s and 23s rRNA genes of the closely related *Mycobacterium avium* and *Mycobacterium paratuberculosis* and the fast-growing *Mycobacterium phlei*. *Microbiology*. 140:1103-1108.

Via, L.E., D. Deretic, R.J. Ulmer, N.S. Hibler, L.A. Huber, and V. Deretic. 1997. Arrest of mycobacterial phagosome maturation is caused by a block in vesicle fusion between stages controlled by rab5 and rab7. *Journal of Biological Chemistry*. 272:13326-13331.

Vieira, O.V., R.J. Botelho, and S. Grinstein. 2002. Phagosome maturation: aging gracefully. *Biochemistry Journal*. 366:689-704.

Watt, B. 1995. Lesser known mycobacteria. *Journal of Clinical Pathology*. 48:701-705.

Willet, H., and H. Thacore. 1967. Formation of spheroplasts of *Mycobacterium tuberculosis* by lysozyme in combination with certain enzymes of rabbit peritoneal monocytes. *Canadian Journal of Microbiology*. 13:481-488.

Woo, R., J. Heintz, R. Albrecht, R. Barletta, and C. Czuprynski. 2007. Life and death in bovine monocytes: the fate of *Mycobacterium avium* subsp. *paratuberculosis*. *Microbial Pathogenesis*. 43:106-113.

Wooldridge, K.G., P.H. Williams, and J.M. Ketley. 1996. Host signal transduction and endocytosis of *Campylobacter jejuni*. *Microbial Pathogenesis*. 21:299-305.

Worobec, S.M. 2009. Treatment of leprosy/Hansen's disease in the early 21st century. *Dermatological Therapy*. 22:518-537.

Yabu, K., and S. Takahashi. 1977. Protoplast formation of selected Mycobacterium smegmatis mutants by lysozyme in combination with methionine. *Journal of Bacteriology*. 129:1628-1631.

Yakes, B.J., R.J. Lipert, J.P. Bannantine, and M.D. Porter. 2008. Detection of *Mycobacterium avium* subsp. *paratuberculosis* by a sonicate immunoassay based on surface-enhanced Raman scattering. *Clinical Vaccine Immunology*. 15:227-234.

Yamazaki, Y., L. Danelishvili, M. Wu, E. Hidaka, T. Katsuyama, B. Stang, M. Petrofsky, R. Bildfell, and L.E. Bermudez. 2006. The ability to form biofilm influences *Mycobacterium avium* invasion and translocation of bronchial epithelial cells. *Cellular Microbiology*. 8:806-814.

Zass, D., M. Duncan, J. Wright, and S. Abraham. 2005. The role of lipid rafts in the pathogenesis of bacterial infections. *Biochimica et Biophysica Acta*. 1746:305-313.

Zheng, P.Y., and N.L. Jones. 2003. *Helicobacter pylori* strains expressing the vacuolating cytotoxin interrupt phagosome maturation in macrophages by recruiting and retaining TACO (coronin 1) protein. *Cellular Microbiology*. 5:25-40.

**Appendix 1 - Ziehl-Neelson (acid fast) stain for mycobacterial visualisation.**

1.) Bacteria were heat fixed to a microscope slide
2.) Slide was flooded with carbolfuchsin (containing 1% basic fuschin (w/v), 10% ethanol and 5% phenol) for 2 min.
3.) Slide was decolourised with acid alcohol (1% HCl in ethanol)
4.) Slide was counterstained with methylene blue (containing 0.14% methylene blue) for 30 seconds.

**Appendix 2 - Cholesterol standard curve**

Substrate was control sera from cholesterol quantitation kit (Roche, Mannheim, Germany). The trendline was generated from three representative experiments measuring absorbance at 490 nm.

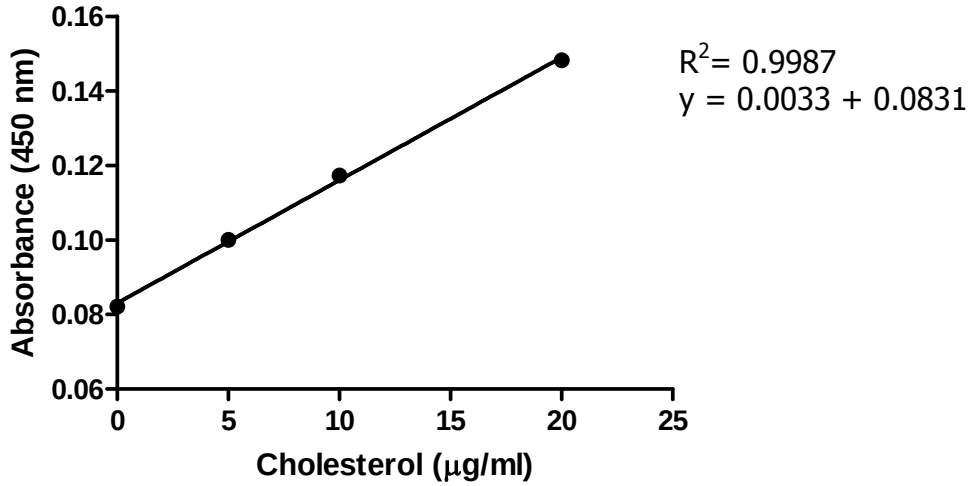

## Appendix 3 - Whole cell lysis buffer for cholesterol extraction

HEPES 20 mM, pH 7.5

NaCl 0.35 M

20% glycerol

1% NP-40

1 mM MgCl2

0.5 mM EDTA

0.1 mM EGTA

1x protease inhibition tablet (Roche)/50ml solution

## Appendix 4 - Protein assay

Protein assays were conducted using a published method (Sandermann and Stromiger 1972). 1 ml of Solution A, was added to eppendorf tubes, and increasing concentrations of BSA (up to 25 mg/ml) were added to duplicate standard curve tubes. 10 µl of bacterial or cellular lysate from each experimental treatment was added to duplicate tubes. Tubes were left for 15 min at room temperature. Then, 100 µl Folins reagent (Merck, Darmstadt, Germany) was added, tubes were then vortexed and incubated at room temperature for 30 mins. For analysis, 250 µl of sample from each tube was aliquoted into wells of a 96 well plate, then read at 660 nm using a spectrophotometer. Sample protein was quantitated using a standard curve.

Solution A: Made up in distilled water.
2 % sodium carbonate
0.4 % sodium hydroxide
0.16 % potassium sodium tartrate
1 % sodium dodecyl sulfate

## Appendix 5 - Electron microscopy

### Sample plugs

Samples were fixed in 2.5 % gluteraldehyde for 1 h at room temperature, washed twice in low salt phosphate buffer, then resuspended in 50 µl 3 % agarose solution (warm/liquid). The suspension was mixed and aliquoted onto a microscope to set. Bacteria/cell rich areas of agarose were cut into 1 mm cubes and transferred to an eppendorf tube.

### Staining

Plugs were resuspended in 1 % osmium tetroxide solution for 1 h (with gentle spinning), then washed three times with low salt phosphate buffer. They were then resuspended in urinal acetate solution and incubated at RT for 20 minutes with gentle spinning.

### Processing

Plugs were sequentially dehydrated by 5 min washes with increasing concentrations of EtOH (50 %, 75 %, 95 %, 100 %, 100%). After the final wash, the plugs were resuspended in a mixture of 50 % Spurrs resin and 50 % EtOH (100 %). After 1 h of incubation at RT, the resin EtOH mix was replaced with Spurrs resin, and tubes were incubated for 1 h at RT. After a further incubation with resin, plug pieces were placed in block moulds, which were filled with resin and incubated overnight at 65$^{o}$C.

### Low salt phosphate buffer solution

0.0089 g/ml $Na_2HPO4.2H_20$ (pH 7.2 in $H_2O$)